2
Photosynthesis, Respiration, and Long-Distance Transport

2A. Photosynthesis

1. Introduction

Approximately 40% of a plant's dry mass consists of carbon, fixed in photosynthesis. This process is vital for growth and survival of virtually all plants during the major part of their growth cycle. In fact, life on Earth in general, not just that of plants, totally depends on current and/or past photosynthetic activity. Leaves are beautifully specialized organs that enable plants to intercept light necessary for photosynthesis. The light is captured by a large array of chloroplasts that are in close proximity to air and not too far away from vascular tissue, which supplies water and exports the products of photosynthesis. In most plants, CO_2 uptake occurs through leaf pores, the stomata, which are able to rapidly change their aperture (Sect. 5.4 of Chapter 3 on plant water relations). Once inside the leaf, CO_2 diffuses from the intercellular air spaces to the sites of carboxylation in the chloroplast (C_3 species) or in the cytosol (C_4 and CAM species).

Ideal conditions for photosynthesis include an ample supply of water and nutrients to the plant, and optimal temperature and light conditions. Even when the environmental conditions are less favorable, however, such as in a desert, alpine environments, or the understory of a forest, photosynthesis, at least of the adapted and acclimated plants, continues (for a discussion of the concepts of **acclimation** and **adaptation**, see Fig. 3 and Sect. 4 in Chapter 1 on assumptions and approaches). This chapter addresses how such plants manage to photosynthesize and/or protect their photosynthetic machinery in adverse environments, what goes wrong in plants that are not adapted and fail to acclimate, and how photosynthesis depends on a range of other physiological activities in the plant.

2. General Characteristics of the Photosynthetic Apparatus

2.1 The "Light" and "Dark" Reactions of Photosynthesis

To orient ourselves, we imagine zooming in on a chloroplast: from a tree, to a leaf, to a cell in a leaf, and then to the many chloroplasts in a single cell, where the primary processes of photosynthesis occur. In C_3 plants most of the chloroplasts are located in the mesophyll cells of the leaves (Fig. 1). Three main processes are distinguished:

1. Absorption of photons by pigments, mainly chlorophylls, associated with two photosystems. The pigments are embedded in internal membrane structures (**thylakoids**) and absorb a major part of the energy of the photosynthetically

H. Lambers et al., *Plant Physiological Ecology*, Second edition, DOI: 10.1007/978-0-387-78341-3_2,

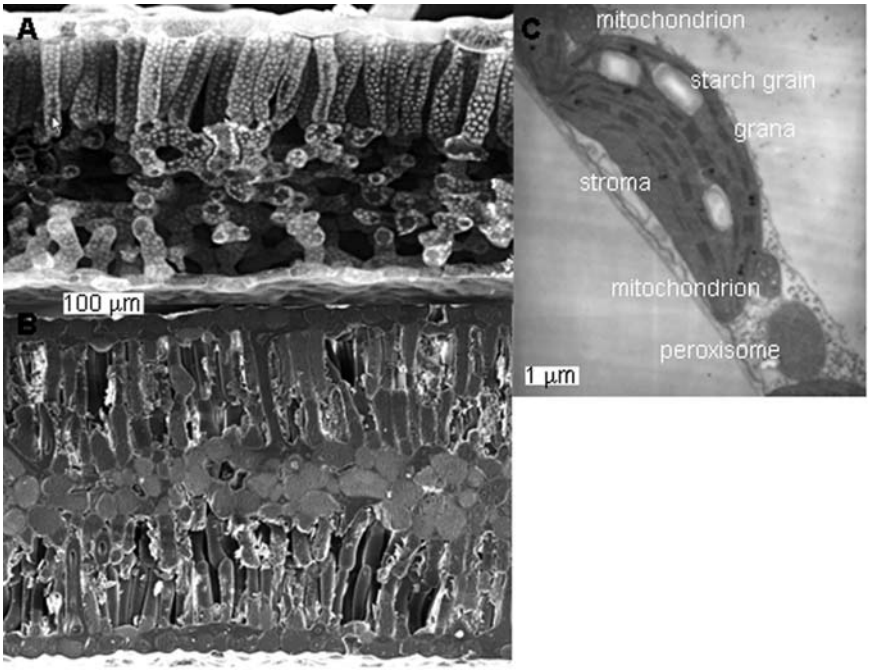

FIGURE 1. (A) Scanning electron microscope cross-sectional view of a dorsiventral leaf of *Nicotiana tabacum* (tobacco), showing palisade tissue beneath the upper (adaxial) epidermis, and spongy tissue adjacent to the (lower) abaxial epidermis. (B) Scanning electron microscope cross-sectional view of an isobilateral leaf of *Hakea prostrata* (harsh hakea). (C) Transmission electron microscope micrograph of a tobacco chloroplast, showing appressed (grana) and unappressed regions of the thylakoids, stroma, and starch granules. Note the close proximity of two mitochondria (top and bottom) and one peroxisome (scale bar is 1 µm) (*Nicotiana tabacum:* courtesy J.R. Evans, Research School of Biological Sciences, Australian National University, Canberra, Australia; *Hakea prostrata:* courtesy M.W Shane, School of Plant Biology, The University of Western Australia, Australia).

active radiation (PAR; 400–700 nm). They transfer the excitation energy to the reaction centers of the photosystems where the second process starts.

2. Electrons derived from the splitting of water with the simultaneous production of O_2 are transported along an electron-transport chain embedded in the thylakoid membrane. NADPH and ATP produced in this process are used in the third process. Since these two reactions depend on light energy, they are called the "**light reactions"** of photosynthesis.
3. The NADPH and ATP are used in the photosynthetic carbon-reduction cycle (Calvin cycle), in which CO_2 is assimilated leading to the synthesis of C_3 compounds (triose-phosphates). These processes can proceed in the absence of light and are referred to as the "**dark reactions"** of photosynthesis. As discussed in Sect. 3.4.2, however, some of the enzymes involved in the "dark" reactions require light for their activation, and hence the difference between "light" and "dark" reaction is somewhat blurred.

2.1.1 Absorption of Photons

The **reaction center** of **photosystem I** (PS I) is a chlorophyll dimer with an absorption peak at 700 nm, hence called P_{700}. There are about 110 "ordinary" chlorophyll *a* (chl *a*) molecules per P_{700} as well as several different protein molecules, to keep the chlorophyll molecules in the required position in the thylakoid membranes (Lichtenthaler & Babani 2004). The number of PS I units can be quantified by determining the amount of P_{700} molecules, which can be assessed by measuring absorption changes at 830 nm.

The **reaction center** of **photosystem II** (PS II) contains redox components, including a chlorophyll *a* molecule with an absorption peak at 680 nm, called

P_{680}, pheophytin, which is like a chlorophyll molecule but without the Mg atom, and the first quinone acceptor of an electron (Q_A) (Chow 2003). Redox cofactors in PS II are bound to the structure of the so-called **D1/D2 proteins** in PS II. PS I and PS II units do not contain chl *b* (Lichtenthaler & Babani 2004). Several protein molecules keep the chlorophyll molecules in the required position in the thylakoid membranes. In vitro, P_{680} is too unstable to be used to quantify the amount of PS II. The **herbicide** atrazine binds specifically to one of the complexing protein molecules of PS II, however; when using ^{14}C-labeled atrazine, this binding can be quantified and used to determine the total amount of PS II. Alternatively, the quantity of functional PS II centers can be determined, in vivo, by the O_2 yield from leaf disks, exposed to 1% CO_2 and repetitive light flashes. A good correlation exists between the two assays. The O_2 yield per flash provides a convenient, direct assay of PS II in vivo when conditions are selected to avoid limitation by PS I (Chow et al. 1989).

A large part of the chlorophyll is located in the **light-harvesting complex** (LHC). These chlorophyll molecules act as antennae to trap light and transfer its excitation energy to the reaction centers of one of the photosystems. The reaction centers are strategically located to transfer electrons along the electron-transport chains. The ratio of chl *a*/chl *b* is about 1.1–1.3 for LHC (Lichtenthaler & Babani 2004).

Leaves appear green in white light, because chlorophyll absorbs more efficiently in the blue and red than in the green portions of the spectrum; beyond approximately 720 nm, there is no absorption by chlorophyll at all. The **absorption spectrum** of intact leaves differs from that of free chlorophyll in solution, and leaves absorb a significant portion of the radiation in regions where chlorophyll absorbs very little in vitro (Fig. 2). This is due to (1) the modification of the absorption spectra of the chlorophyll molecules bound in protein complexes in vivo, (2) the presence of accessory pigments, such as carotenoids, in the chloroplast, and, most importantly, (3) light scattering within the leaf (Sect. 3.2.2).

2.1.2 Fate of the Excited Chlorophyll

Each quantum of red light absorbed by a chlorophyll molecule raises an electron from a ground state to an excited state. Absorption of light of shorter wavelengths (e.g., blue light) excites the chlorophyll to an even higher energy state. In the

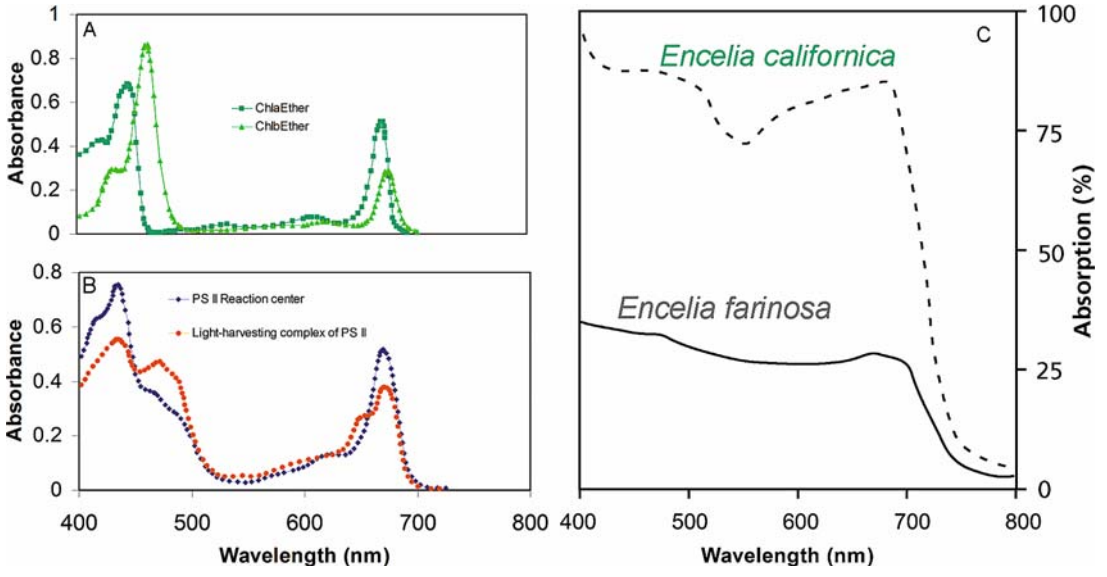

FIGURE 2. (A) The relative absorbance spectrum of chlorophyll *a* and chlorophyll *b*; absorbance = –log (transmitted light/incident light); (B) The relative absorbance spectrum of pigment-protein complexes: PS II reaction centre and PS II light-harvesting complex; (courtesy J.R. Evans, Research School of Biological Sciences, Australian National University, Canberra, Australia. (C) Light absorption of an intact green leaf of *Encelia californica*; for comparison the absorption spectrum of an intact white (pubescent) leaf of *Encelia farinosa* (brittlebush) is also given. From Ehleringer et al. (1976), *Science* 227: 1479–1481. Reprinted with kind permission from AAS.

higher energy state after absorption of blue light, however, chlorophyll is unstable and rapidly gives up some of its energy to the surroundings as heat, so that the elevated electron immediately falls back into the orbit of the electron excited by red light. Thus, whatever the wavelength of the light absorbed, chlorophyll reaches the same excitation state upon photon capture. In this excitation state, chlorophyll is stable for 10^{-9} seconds, after which it disposes of its available energy in one of three ways (Krause & Weis 1991):

1. The primary pathway of excitation energy is its highly efficient transfer to other chlorophyll molecules, and ultimately to the reaction center where it is used in **photochemistry**, driving biochemical reactions.
2. The excited chlorophyll can also return to its ground state by converting its excitation energy into **heat**. In this process no photon is emitted.
3. The excited chlorophyll can emit a photon and thereby return to its ground state; this process is called **fluorescence**. Most fluorescence is emitted by chl *a* of PS II. The wavelength of fluorescence is slightly longer than that of the absorbed light, because a portion of the excitation energy is lost before the fluorescence photon is emitted. Chlorophylls usually fluoresce in the red; it is a deeper red (the wavelength is about 10 nm longer) than the red absorption peak of chlorophyll. Fluorescence increases when photochemistry and/or dissipation are low relative to photon absorption, but the process is not regulated as such. This can occur under conditions of excessive light, severely limiting CO_2 supply, or stresses that inhibit photochemistry.

The primary photochemical reactions of PS II and PS I occur at a much faster rate than subsequent electron transport (Sect. 2.1.3), which in turn occurs faster than carbon reduction processes (Sect. 2.1.4). Since the three compartments of the photosynthetic apparatus operate in series, they are each tightly regulated to coordinate their activity under changing conditions.

2.1.3 Membrane-Bound Photosynthetic Electron Transport and Bioenergetics

The excitation energy captured by the pigments is transferred to the reaction centers of PS I and PS II. PS I and PS II are associated with different regions of the thylakoid membrane. PS I is located in the stroma-exposed "**unappressed**" regions, and PS II is largely associated with the "**appressed**" regions where thylakoids border other thylakoids (grana) (Fig. 1). In PS II an electron, derived from the splitting of water into O_2 and protons, is transferred to pheophytin, and then to plastoquinone (Q_A, bound to D2 protein, a one-electron carrier), followed by transfer to Q_B (bound to D1 protein, a two-electron carrier), and then to free plastoquinone. Plastoquinone (PQ) is subsequently reduced and transported to the cytochrome b/f complex. In the process protons are transported across the membrane into the thylakoid lumen (Fig. 3). The two sources of protons acidify and charge the thylakoid lumen positively. The **electrochemical potential gradient** across the thylakoid membrane, representing a **proton-motive force**, is subsequently used to phosphorylate ADP, thus producing **ATP**. This reaction is catalyzed by an ATPase, or coupling factor, located in the stroma-exposed, unappressed regions of the thylakoids. In **linear electron transport**, electrons are transferred from the cytochrome b/f complex to PS I through plastocyanin (PC) that migrates through the thylakoid lumen. NADP is reduced by ferredoxin as the terminal acceptor of electrons from PS I which results in formation of NADPH. In **cyclic electron transport**, electrons are transferred from PS I back to cytochrome b/f through plastoquinone, thus contributing to proton extrusion in the lumen and subsequent ATP synthesis. NADPH and ATP are used in the carbon-reduction cycle that is located in the stroma. Linear electron transport is the principal pathway, whereas the engagement of cyclic electron transport is tuned to the demand for ATP relative to NADPH. Other components of the photosynthetic membrane are also regulated, particularly with respect to the prevailing light conditions.

2.1.4 Photosynthetic Carbon Reduction

Ribulose-1,5-bisphosphate (RuBP) and CO_2 are the substrates for the principal enzyme of the carbon-reduction or Calvin cycle: ribulose-1,5-bisphosphate carboxylase/oxygenase (**Rubisco**) (Fig. 4). The first product of carboxylation of RuBP by Rubisco is phosphoglyceric acid (PGA) a compound with three carbon atoms, hence, the name **C_3 photosynthesis**. With the consumption of the ATP and NADPH produced in the light reactions, PGA is reduced to a triose-phosphate (triose-P), some of which is exported to the cytosol in exchange for inorganic phosphate (P_i). In the cytosol, triose-P is used to produce sucrose and other metabolites that are exported via the phloem or used in the leaves. Most of the triose-P remaining in the chloroplast is used to regenerate RuBP through a series of

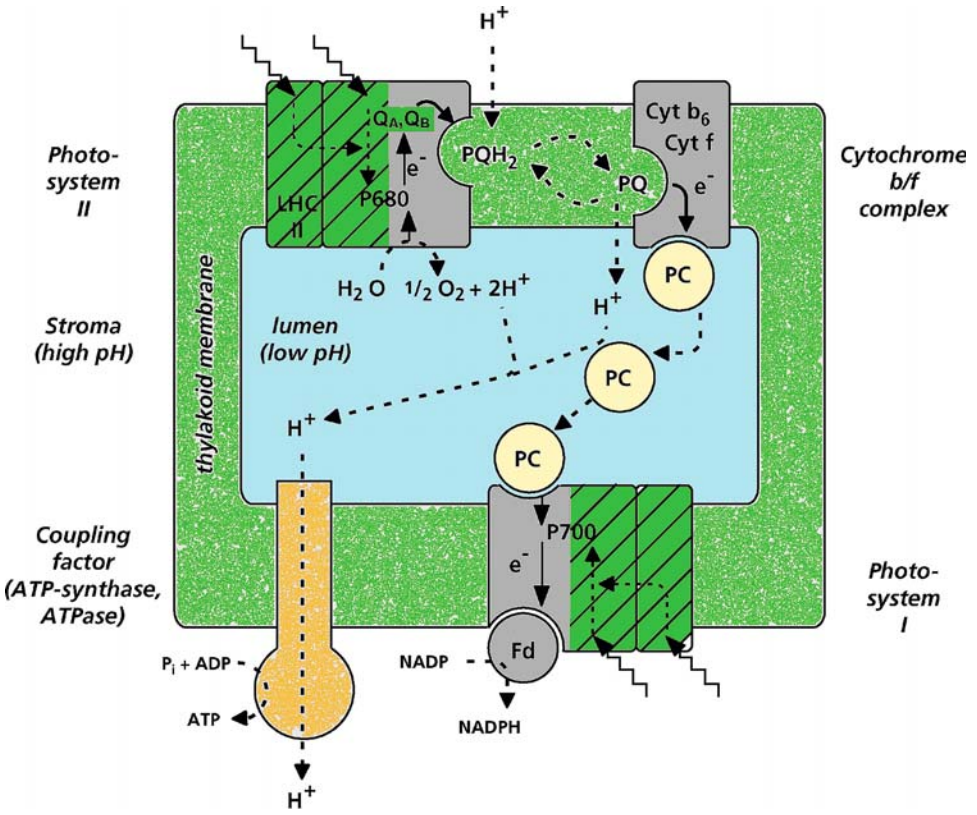

FIGURE 3. Schematic representation of the thylakoid membrane, enclosing the thylakoid lumen, showing the transfer of excitation energy and of electrons, migration of molecules and chemical reactions. P_{700}: reaction center of photosystem I; P_{680}: reaction center of photosystem II; LHC: light-harvesting complex; Q: quinones; PC, plastocyanin; Fd: ferredoxin; cyt: cytochromes.

reactions that are part of the **Calvin cycle** in which ATP and NADPH are consumed (Fig. 4). About 1/6 of the triose-P remaining in the chloroplast is used to produce **starch**, which is stored inside the chloroplast, or is **exported**. During the night, starch may be hydrolyzed, and the product of this reaction, triose-P, is exported to the cytosol. The photosynthetic carbon-reduction cycle has various control points and factors that function as stabilizing mechanisms under changing environmental conditions.

2.1.5 Oxygenation and Photorespiration

Rubisco catalyzes not only the **carboxylation** of RuBP, but also its **oxygenation** (Fig. 5). The ratio of the carboxylation and the oxygenation reaction strongly depends on the relative concentrations of CO_2 and O_2 and on leaf temperature. The products of the carboxylation reaction are two C_3 molecules (PGA), whereas the oxygenation reaction produces only one PGA and one C_2 molecule: phosphoglycolate. This C_2 molecule is first dephosphorylated in the chloroplast, producing glycolate (Fig. 5), which is exported to the peroxisomes, where it is metabolized to glyoxylate and then **glycine**. Glycine is exported to the mitochondria where two molecules are converted to produce one serine with the release of one molecule of CO_2 and one NH_3. Serine is exported back to the peroxisomes, where a transamination occurs, producing one molecule of hydroxypyruvate and then glycerate. Glycerate moves back to the chloroplast, to be converted into PGA. So, out of two phosphoglycolate molecules one glycerate is made and one C-atom is lost as CO_2. The entire process, starting with the oxygenation reaction, is called **photorespiration**, as it consumes O_2 and releases CO_2; it depends on light, or, more precisely, on photosynthetic activity. The process is distinct from "dark respiration" that largely consists of mitochondrial decarboxylation processes that proceed independent of light. Dark respiration is discussed in Chapter 2B on respiration.

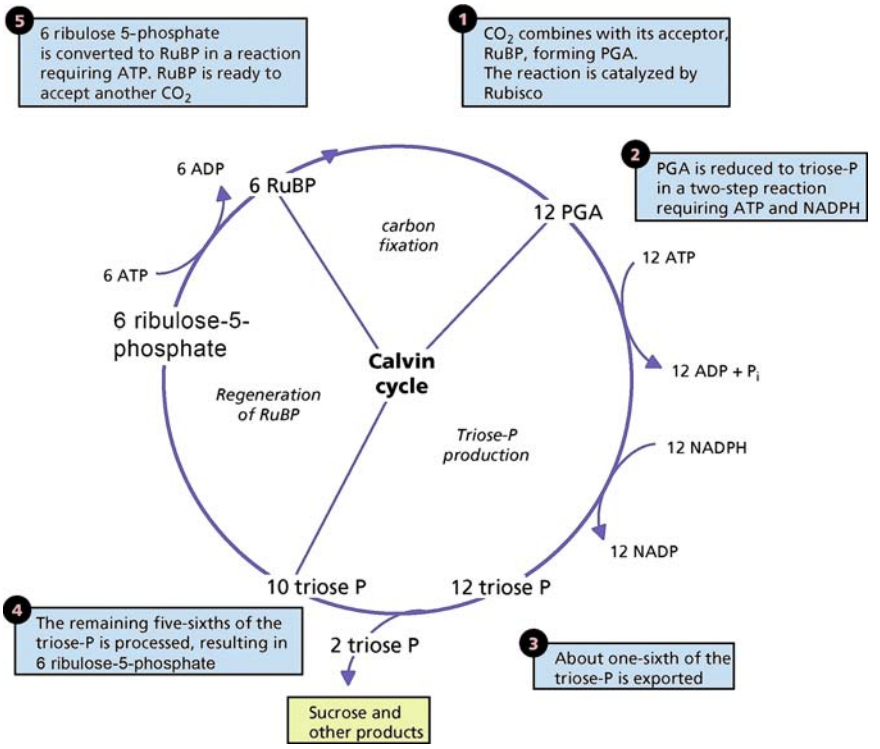

FIGURE 4. Schematic representation of the photosynthetic carbon reduction cycle (Calvin cycle) showing major steps: carbon fixation, triose-P production and regeneration of RuBP. 1: CO_2 combines with its substrate, ribulose-1,5-bisphosphate (RuBP), catalyzed by ribulose bisphosphate carboxylase/oxygenase (Rubisco), producing phosphoglyceric acid (PGA). 2: PGA is reduced to triose-phosphate (triose-P), in a two-step reaction; the reaction for which ATP is required is the conversion of PGA to 1,3-bisphosphoglycerate, catalyzed by phosphoglycerate kinase. 3 and 4: Part of the triose-P is exported to the cytosol, in exchange for P_i; the remainder is used to regenerate ribulose-1-monophosphate. 5: ribulose-1-monophosphate is phosphorylated, catalyzed by ribulose-5-phosphate kinase, producing RuBP.

2.2 Supply and Demand of CO_2 in the Photosynthetic Process

The rate of photosynthetic carbon assimilation is determined by both the supply and demand for CO_2. The **supply of CO_2** to the chloroplast is governed by diffusion in the gas and liquid phases and can be limited at several points in the pathway from the air surrounding the leaf to the site of carboxylation inside. The **demand for CO_2** is determined by the rate of processing the CO_2 in the chloroplast which is governed by the structure and biochemistry of the chloroplast (Sect. 2.1), by environmental factors such as irradiance, and factors that affect plant demand for carbohydrates (Sect. 4.2). Limitations imposed by either supply or demand can determine the overall rate of carbon assimilation, as explained below.

2.2.1 Demand for CO_2—the CO_2-Response Curve

The response of photosynthetic rate to CO_2 concentration is the principal tool to analyze the demand for CO_2 and partition the limitations imposed by demand and supply (Warren 2007, Flexas et al. 2008) (Fig. 6). The graph giving net CO_2 assimilation (A_n) as a function of CO_2 concentration at the site of Rubisco in the chloroplast (C_c) is referred to as the **A_n-C_c curve**. With rising CO_2, there is no net CO_2 assimilation, until the production of CO_2 in respiration (mainly photorespiration, but also some dark respiration occurring in the light) is fully compensated by the fixation of CO_2 in photosynthesis. The CO_2 concentration at which this is reached is the **CO_2-compensation point** (Γ). In C_3 plants this is largely determined by the kinetic properties of Rubisco,

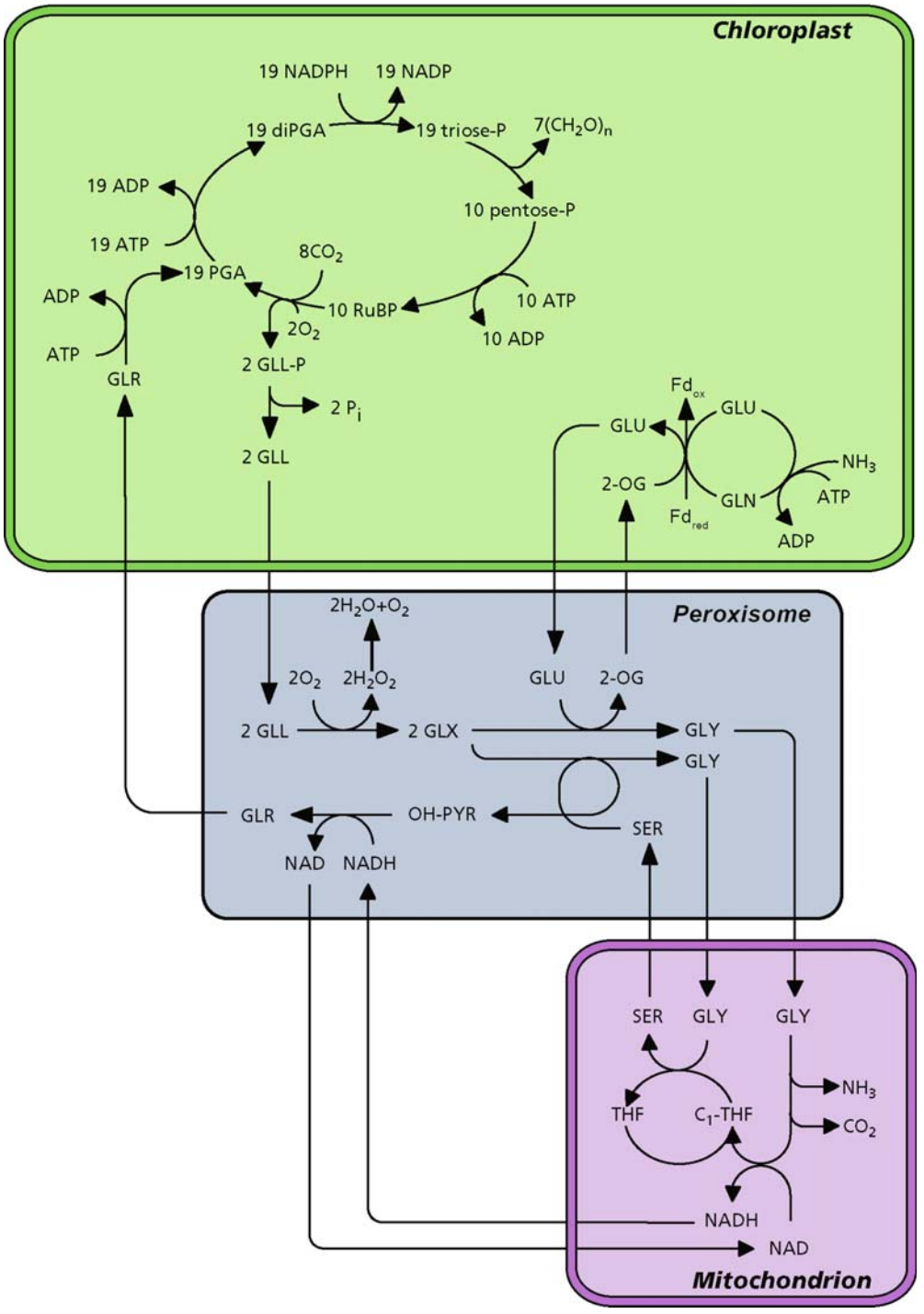

FIGURE 5. Reactions and organelles involved in photorespiration. In C_3 plants, at 20% O_2, 0.035% CO_2, and 20°C, two out of ten RuBP molecules are oxygenated, rather than carboxylated. The oxygenation reaction produces phosphoglycolate (GLL-P), which is dephosphorylated to glycolate (GLL). Glycolate is subsequently metabolized in peroxisomes and mitochondria, in which glyoxylate (GLX) and the amino acids glycine (GLY) and serine (SER) play a role. Serine is exported from the mitochondria and converted to hydroxypyruvate (OH-PYR) and then glycerate (GLR) in the peroxisomes, after which it returns to the chloroplast (after Ogren 1984). Reprinted with kind permission from the Annual Review of Plant Physiology, Vol. 35, copyright 1984, by Annual Reviews Inc.

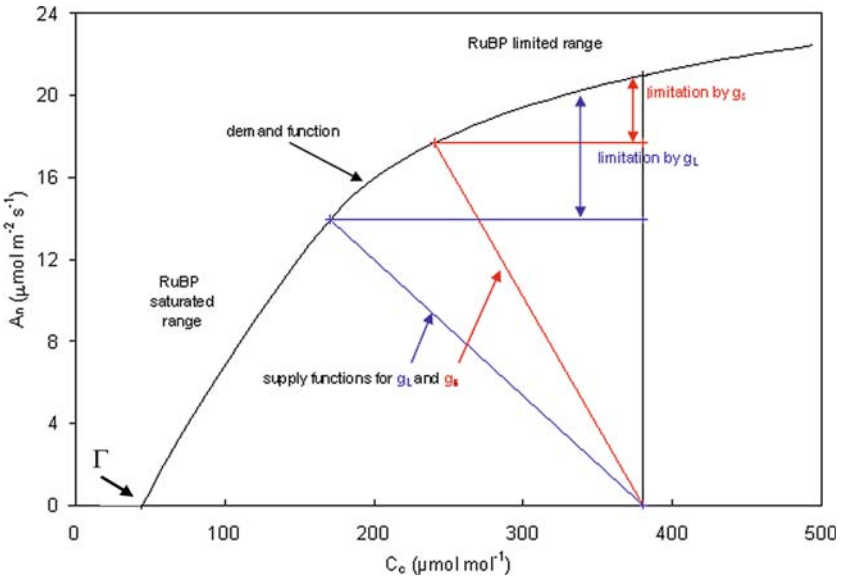

FIGURE 6. The relationship between the rate of net CO_2 assimilation (A_n) and the CO_2 concentration at the site of Rubisco in the chloroplasts (C_c) for a C_3 leaf: the "demand function". The concentration at which $A_n = 0$ is the CO_2-compensation point (Γ). The rate of diffusion of CO_2 from the atmosphere to the intercellular spaces and to Rubisco in the chloroplast is given by the "supply functions" (the red and blue lines). The slopes of these lines are the leaf conductance (g_L) and mesophyll conductance (g_m), respectively. The intersection of the "supply functions" with the "demand function" is the actual rate of net CO_2 assimilation at a value of C_i and C_c that occurs in the leaf intercellular spaces (C_i) and at the site of Rubisco (C_c) for C_a in normal air (indicated by the vertical line). The difference in A_n described by the demand function and the two horizontal lines depicts the degree of limitation imposed by the mesophyll resistance and leaf resistance.

with values for Γ in the range 40–50 μmol (CO_2) mol^{-1} (air) (at 25°C and atmospheric pressure).

Two regions of the CO_2-response curve above the compensation point can be distinguished. At low C_c, that is below values normally found in leaves (approximately 165 μmol mol^{-1}), photosynthesis increases steeply with increasing CO_2 concentration. This is the region where CO_2 limits the rate of functioning of Rubisco, whereas RuBP is present in saturating quantities (**RuBP-saturated** or **CO_2-limited region**). This part of the A_n–C_c relationship is also referred to as the **initial slope** or the **carboxylation efficiency**. At light saturation and with a fully activated enzyme (Sect. 3.4.2 for details on "activation"), the initial slope governs the carboxylation capacity of the leaf which in turn depends on the amount of active Rubisco.

In the region at high C_c, the increase in A_n with increasing C_c levels off. CO_2 no longer restricts the carboxylation reaction, but now the rate at which RuBP becomes available limits the activity of Rubisco (**RuBP-limited region**). This rate, in turn, depends on the activity of the Calvin cycle, which ultimately depends on the rate at which ATP and NADPH are produced in the light reactions; in this region, photosynthetic rates are limited by the rate of electron transport. This may be due to limitation by light or, at light saturation, by a limited capacity of electron transport (Box 2A.1). Even at a high C_c, in the region where the rate of electron transport, J, no longer increases with increasing C_c, the rate of net CO_2 assimilation continues to increase slightly, because the oxygenation reaction of Rubisco is increasingly suppressed with increasing CO_2 concentration, in favor of the carboxylation reaction. At a normal atmospheric concentration of CO_2 (C_a) and O_2 (ca. 380 and 210000 μmol mol^{-1}, respectively) and at a temperature of 20°C, the ratio between the carboxylation and oxygenation reaction is about 4:1. How exactly this ratio and various other parameters of the A_n–C_c curve can be assessed is further explained in Box 2A.1. Typically, plants operate at a C_c where **CO_2** and **electron transport co-limit** the rate of CO_2 assimilation (i.e., the point where the Rubisco-limited/RuBP-saturated and the RuBP-limited part of the CO_2-response curve intersect). This allows effective utilization of all components of the light and dark reactions.

Box 2A.1
Modeling C_3 Photosynthesisis

Based on known biochemical characteristics of Rubisco and the requirement of $NADPH_2$ and ATP for CO_2 assimilation, Farquhar et al. (1980) developed a model of photosynthesis in C_3 plants. This model was recently updated, based on the CO_2 concentration in the chloroplast (C_c) rather than the intercellular CO_2 concentration (C_i) (Sharkey et al. 2007). It is widely used in ecophysiological research and more recently also in global change modeling. The model elegantly demonstrates that basic principles of the biochemistry of photosynthesis explain physiological properties of photosynthesis of intact leaves.

Net CO_2 assimilation (A_n) is the result of the rate of carboxylation (V_c) minus photorespiration and other respiratory processes. In photorespiration, one CO_2 molecule is produced per two oxygenation reactions (V_o) (Fig. 5). The rate of dark respiration during photosynthesis may differ from dark respiration at night, and is called "day respiration" (R_{day}):

$$A_n = V_c - 0.5V_o - R_{day} \quad (1)$$

CO_2-limited and O_2-limited rates of carboxylation and oxygenation are described with standard Michaelis–Menten kinetics. When both substrates are present, however, they competitively inhibit each other. An effective Michaelis–Menten constant for the carboxylation reaction (K_m) that takes into account competitive inhibition by O_2 is described as

$$K_m = K_c(1 + O/K_o) \quad (2)$$

where K_c and K_o are the Michaelis–Menten constants for the carboxylation and oxygenation reaction, respectively, and O is the oxygen concentration.

The rate of carboxylation in the CO_2-limited part of the CO_2-response curve (Fig. 1) can then be described as

$$V_c = \frac{V_{cmax} \cdot C_c}{C_c + K_m} \quad (3)$$

where V_{cmax} is the rate of CO_2 assimilation at saturating C_c (note that the subscript "max" refers to the rate at saturating C_c).

The ratio of oxygenation and carboxylation depends on the specificity of Rubisco for CO_2 relative to O_2 ($S_{c/o}$) which varies widely among photosynthetic organisms (Von Caemmerer 2000), but much less so among C_3 higher plants (Galmés et al. 2005). Increasing temperature, however, decreases the specificity, because K_o decreases faster with increasing temperature than K_c does (Fig. 35).

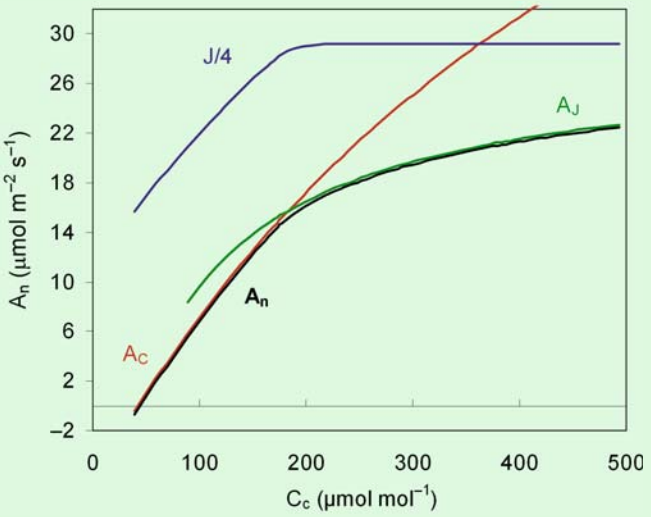

FIGURE 1. The response of net photosynthesis (A_n) to the CO_2 concentration in the chloroplast (C_c) at 25°C and light saturation (*solid black line*). Calculations were made as explained in the text, with values for V_{cmax}, J_{max}, and R_{day} of 90, 117, and 1 μmol m^{-2} s^{-1}, respectively. The lower part of the A_n-C_c relationship (A_c; *red line*) is limited by the carboxylation capacity (V_{cmax}) and the upper part (A_j; *green line*) by the electron-transport capacity (J_{max}; *blue line*). The rate of electron transport (J/4; *blue line*) is also shown.

continued

Box 2A.1 *Continued*

The CO_2-compensation point in the absence of R_{day} (Γ^*) depends on the specificity factor and the O_2 concentration (O):

$$\Gamma^* = 0.5 \quad O/(S_{c/o} \cdot S_c/S_o) \tag{4}$$

Γ^* increases more strongly with rising temperature than would be expected from the decrease in $S_{c/o}$ because the solubility in water for CO_2 (S_c) decreases more with increasing temperature than does that for O_2 (S_o). Γ^* shows little variation among C_3 angiosperms as follows from the similarity of $S_{c/o}$. Γ^* is determined experimentally and used to calculate the ratio of carboxylation and oxygenation as dependent on CO_2:

$$V_o/V_c = 2\Gamma^*/C_c \tag{5}$$

thus avoiding the need for incorporating the specificity factor and solubilities (Equation 4).

In the RuBP-limited part of the CO_2-response curve (Fig. 1.1), the rate of electron transport (J) is constant. Increasing C_c increases the rate of carboxylation at the expense of the rate of oxygenation. There is a minimum requirement of four electrons per carboxylation or oxygenation reaction. Hence, the minimum electron transport rate (J) required for particular rates of carboxylation and oxygenation is

$$J = 4(V_c + V_o) \tag{6}$$

At light saturation, J is limited by the capacity of electron transport and is called J_{max}.

Using Equations (5) and (6), the rate of carboxylation can then be expressed as

$$V_c = J/\{4(1 + 2\Gamma^*/C_c)\} \tag{7}$$

The CO_2-limited and RuBP-saturated rate of photosynthesis (A_c) can then be calculated using Equations (1), (3), and (5) as

$$A_c = \frac{V_{cmax}(C_c - \Gamma^*)}{C_c + K_m} - R_{day} \tag{8}$$

The RuBP-limited rate of photosynthesis (A_j) can be calculated using Equations (1), (5), and (7) as

$$A_j = \frac{J(C_c - \Gamma^*)}{4(C_c + 2\Gamma^*)} - R_{day} \tag{9}$$

The minimum of Equations (8) and (9) describes the full CO_2-response curve as shown in Fig. 1.

In the above equations, gas concentrations are expressed as molar fraction (mol mol^{-1}). If required, partial pressure can be converted to molar fraction by dividing it by total air pressure.

The CO_2 conductance for CO_2 diffusion in the mesophyll (g_m) can only be calculated when the concentration in the chloroplast (C_c) is known. g_m can then be calculated from C_i as

$$A_n/g_m = C_i - C_c \tag{10}$$

Information about g_m may not always be available. As an approximation, the same model can be used assuming that $C_c = C_i$. Parameter values specific for that scenario should then be used (see below).

Parameter values for the above equations are normally given for 25°C. Values for other temperatures can be calculated from their temperature dependencies, as described by the generic equation:

$$\text{parameter} = \exp(c - \Delta H_\alpha/R\,T_L) \tag{11}$$

Where T_L is leaf temperature (K), R is the molar gas constant, c is a dimensionless constant, and ΔH_α is the activation energy (kJ mol^{-1}). Parameter values estimated for *Nicotiana tabacum* (tobacco) for the CO_2 response at 25°C, an atmospheric pressure, of 99.1 kPa, and an infinite ($C_c = C_i$) and a finite g_m, together with the temperature dependencies for the latter scenario (Bernacchi et al. 2001, 2002) are

	$C_c = C_i$		finite g_m ($C_c < C_i$)	
CO_2 response parameter	**at 25°C**	**at 25°C**	**c**	**ΔH_α**
Γ^* (μmol mol^{-1})	**42.75**	**37.43**	**19.02**	**24.46**
K_c (μmol mol^{-1})	**404.9**	**272.4**	**38.28**	**80.99**
K_o (mmol mol^{-1})	**278.4**	**165.8**	**14.68**	**23.72**

Temperature dependencies of model parameters describing the rates of metabolic processes that are leaf specific (J_{max}, V_{max}, R_{day}) are calculated in a similar manner, but Equation (11) must then be multiplied by the rates at 25°C. For constants and activation energies, see Bernacchi et al. (2001, 2003).

continued

Box 2A.1 *Continued*

Values of C_c depend on the balance between supply and demand for CO_2. The demand function is described above; the supply function is described in Sect. 2.2.2. Electron-transport rates depend on irradiance (Sect. 3.2.1), where the equation describing net CO_2 assimilation as a function of irradiance can be used to calculate J by substituting J and J_{max} for A_n and A_{max}, respectively. A combination of these mathematical equations makes it possible to model C_3 photosynthesis over a wide range of environmental conditions.

2.2.2 Supply of CO_2—Stomatal and Boundary Layer Conductances

The supply of CO_2 by way of its diffusion from the surrounding atmosphere to the intercellular spaces (this CO_2 concentration is denoted as C_i) and to the site of carboxylation in the chloroplasts (this CO_2 concentration is described as C_c) represents a limitation for the rate of photosynthesis. The magnitude of the limitation can be read from the A_n–C_c curve as the difference in photosynthetic rate at C_a and C_i and C_c, respectively (Fig. 6). To analyze diffusion limitations it is convenient to use the term **resistance**, because resistances can be summed to arrive at the total resistance for the pathway. When considering fluxes, however, it is more convenient to use **conductance**, which is the reciprocal of resistance, because the flux varies in proportion to the conductance.

In a steady state, the rate of net CO_2 assimilation (A_n) equals the rate of CO_2 diffusion into the leaf. The rate of CO_2 diffusion can be described by **Fick's first law**. Hence:

$$A_n = g_c(C_a - C_c) = (C_a - C_c)/r_c \qquad (1)$$

where, g_c is the leaf conductance for CO_2 transport; C_a and C_c are the mole or volume fractions of CO_2 in air at the site of carboxylation and in air, respectively; r_c is the inverse of g_c (i.e., the leaf resistance for CO_2 transport).

The leaf conductance for CO_2 transport, g_c, can be derived from measurements on leaf transpiration, which can also be described by Fick's first law in a similar way:

$$E = g_w(w_i - w_a) = (w_i - w_a)r_w \qquad (2)$$

where g_w is the leaf conductance for water vapor transport; w_i and w_a are the mole or volume fractions of water vapor in air in the intercellular spaces and in air, respectively; r_w is the inverse of g_w (i.e., the leaf resistance for water vapor transport); and E is the rate of leaf transpiration. E can be measured directly. The water vapor concentration in the leaf can be calculated from measurements of the leaf's temperature, assuming a saturated water vapor pressure inside the leaf. Under most conditions this is a valid assumption. Therefore, the leaf conductance for water vapor transport can be determined.

The total leaf resistance for water vapor transfer, r_w, is largely composed of two components that are in series: the **boundary layer resistance**, r_a, and the **stomatal resistance**, r_s. The boundary layer is the thin layer of air adjacent to the leaf that is modified by the leaf (Fig. 6 in Chapter 4A on the plant's energy balance). Turbulence is greatly reduced there, and transport is largely via diffusion. Its limit is commonly defined as the point at which the properties of the air are 99% of the values in ambient air. The boundary layer resistance can be estimated by measuring the rate of evaporation from a water-saturated piece of filter paper of exactly the same shape and size as that of the leaf. Conditions that affect the boundary layer, such as wind speed, should be identical to those during measurements of the leaf resistance. The stomatal resistance for water vapor transfer (r_s) can now be calculated since r_w and r_a are known:

$$r_w = r_a + r_s \qquad (3)$$

The resistance for CO_2 transport (r_c) across boundary layer and stomata can be calculated from r_w, taking into account that the diffusion coefficients of the two molecules differ. The ratio H_2O diffusion/CO_2 diffusion in air is approximately 1.6, because water is smaller and diffuses more rapidly than CO_2. This value pertains only to the movement of CO_2 inside the leaf air spaces and through the stomata. For the boundary layer above the leaf, where both turbulence and diffusion influence flux, the ratio is approximately 1.37.

$$r_c = (r_a.1.37) + (r_s.1.6) = 1/g_c \qquad (4)$$

C_i can now be calculated from Equation (1), after substitution of C_i for C_c. If calculated according to this, C_i is the CO_2 concentration at the point where evaporation occurs inside the leaf (i.e., largely the mesophyll cell walls bordering the substomatal

cavity), but higher than C_c, the CO_2 concentration at the point where Rubisco assimilates CO_2 (Sect. 2.2.3).

In C_3 plants, C_i is generally maintained at around 250 μmol mol^{-1}, but may increase to higher values at a low irradiance and higher humidity of the air, and decrease to lower values at high irradiance, low water availability, and low air humidity. For C_4 plants, C_i is around 100 μmol mol^{-1} (Osmond et al. 1982).

Under most conditions, the stomatal conductance is considerably less than the boundary layer conductance (g_a is up to 10 mol m^{-2} s^{-1}, at wind speeds of up to 5 m s^{-1}; g_s has values of up to 1 mol m^{-2} s^{-1} at high stomatal density and widely open stomata), so that stomatal conductance strongly influences CO_2 diffusion into the leaf. For large leaves in still humid air, where the boundary layer is thick, however, the situation is opposite.

2.2.3 The Mesophyll Conductance

For the transport of CO_2 from the substomatal cavity to the chloroplast, a **mesophyll conductance** (also called **internal conductance**), g_m (or resistance, r_m) should be considered. Hence, we can describe the net rate of net CO_2 assimilation by

$$A_n = (C_a - C_c)/(r_a + r_s + r_m) \quad (5)$$

Until fairly recently, the mesophyll conductance has been assumed to be large and has often been ignored in analyses of gas-exchange measurements. However, recent evidence shows that this is not justified (Warren 2007, Flexas et al. 2008). In addition, we have come to realize that g_m changes with environmental conditions, and often quite rapidly, compared with changes in stomatal conductance (Flexas et al. 2007a, Warren 2007).

Two types of measurements are commonly employed for the estimation of C_c, which is subsequently used to calculate g_m. **Carbon-isotope fractionation** (Box 2A.2) during gas exchange, and simultaneous measurement of **chlorophyll fluorescence** and gas exchange. The two methods rely on a number of assumptions that are largely independent, but they yield similar results (Evans & Loreto 2000). From the estimates made so far, it appears that g_m is of similar magnitude as g_s; whilst g_m is generally somewhat higher, the opposite can also be observed (Galmés et al. 2007). Consequently, C_c is

Box 2A.2
Fractionation of Carbon Isotopes in Plants

CO_2 in the Earth's atmosphere is composed of different carbon isotopes. The majority is $^{12}CO_2$; approximately 1% of the total amount of CO_2 in the atmosphere is $^{13}CO_2$; a much smaller fraction is the radioactive species $^{14}CO_2$ (which will not be dealt with in the present context). Modern ecophysiological research makes abundant use of the fact that the isotope composition of plant biomass differs from that of the atmosphere. Carbon isotopes are a crucial tool in estimating time-integrated measures of photosynthetic performance of individual plants or plant communities, information that would be difficult or impossible to obtain from direct physiological measurements. It is of special interest that carbon-isotope composition differs among plants that differ in photosynthetic pathway or water-use efficiency. How can we account for that?

The molar abundance ratio, R, of the two carbon isotopes is the ratio between ^{13}C and ^{12}C. The constants K^{12} and K^{13} refer to the rate of processes and reactions in which ^{12}C and ^{13}C participate, respectively. The "isotope effect" is described as

$$R_{source}/R_{product} = k^{12}/k^{13} \quad (1)$$

For plants, the isotope effect is, to a small extent, due to the slower diffusion in air of $^{13}CO_2$, when compared with that of the lighter isotope $^{12}CO_2$ (1.0044 times slower; during diffusion in water, there is little fractionation) (Table 1). The isotope effect is largely due to the biochemical properties of Rubisco, which reacts more readily with $^{12}CO_2$ than it does with $^{13}CO_2$. As a result, Rubisco discriminates against the heavy isotope. For Rubisco from *Spinacia oleracea*(spinach), the discrimination is 30.3%, whereas smaller values are found for this enzyme from bacteria (Guy et al. 1993).

continued

Box 2A.2 *Continued*

Table 1. The magnitude of fractionation during CO_2 uptake.

Process or enzyme	Fractionation (‰)
Diffusion in air	4.4
Diffusion through the boundary layer	2.9
Dissolution of CO_2	1.1
Diffusion of aqueous CO_2	0.7
CO_2 and HCO_3^- in equilibrium	–8.5 at 30°C –9.0 at 25°C
CO_2 - HCO_3^- catalyzed by carbonic anhydrase	1.1 at 25°C
HCO_3^- - CO_2 in water, catalyzed by carbonic anhydrase	10.1 at 25°C
PEP carboxylase	2.2
Combined process	–5.2 at 30°C –5.7 at 25°C
Rubisco	30 at 25°C

***Source*: Henderson et al. 1992.**

On the path from intercellular spaces to Rubisco a number of additional steps take place, where some isotope fractionation can occur. Taken together, the isotope effect in C_3 plants is approximated by the empirical equation (Farquhar et al. 1982):

$$R_a/R_p = 1.0044\ [(C_a - C_i)/C_a] + 1.027\, C_i/C_a \quad (2)$$

where R_a and R_p are the molar abundance ratios of the atmospheric CO_2 and of the C fixed by the plant, respectively; the symbols C_a and C_i are the atmospheric and the intercellular partial pressure of CO_2, respectively. The value 1.027 is an empirical value, incorporating the major fractionation by Rubisco, as well as accounting for the internal diffusion resistance for CO_2 (g_m).

Since values for R_a/R_p appear rather "clumsy," data are commonly expressed as fractionation values, Δ ("capital delta"), defined as $(R_a/R_p - 1) \times 1000$, or:

$$\begin{aligned}\Delta &= [(1.0044\, C_a - 1.0044\, C_i + 1.027\, C_i)/C_a] - 1 \\ &= [(1.0044\, C_a + 0.0226\, C_i)/C_a] - 1 \\ &= (4.4 + 22.6\, C_i/C_a) \times 10^{-3}\end{aligned} \quad (3)$$

The isotope composition is described as $\delta^{13}C$ ("lower case delta"):

$$\delta^{13}C\ (‰) = (R_{sample}/R_{standard} - 1) \cdot 1000 \quad (4)$$

Values for $\Delta^{13}C$ and $\delta^{13}C$ are related as

$$\Delta = (\delta_{source} - \delta_{plant})/(1 + \delta_{plant}) \quad (5)$$

where $\delta_{source} \cong -8‰$ if the source is air (δ_{air}) (to be entered as -0.008 in Equation (5); a $\delta_{\pi\lambda\alpha\nu\tau}$ value of $-27‰$, therefore, converts to a Δ value of 19.5‰). The standard is a cretaceous limestone consisting mostly of the fossil carbonate skeletons of *Belemnitella americana* (referred to as PDB-belemnite). By definition, it has a $\delta^{13}C$ value equal to 0‰. Plant $\delta^{13}C$ values are negative, because they are depleted in ^{13}C compared with the fossil standard. Diffusion and carboxylation discriminate against $^{13}CO_2$; δ-values for C_3 plants are approx. $-27‰$, showing that Rubisco is the predominant factor accounting for the observed values and that diffusion is less important.

For C_4 plants, the following empirical equation has been derived:

$$\Delta = 4.4 + [-5.7 + (30 - 1.8)\phi - 4.4]\, C_i/C_a \quad (6)$$

where ϕ refers to the leakage of CO_2 from the bundle sheath to the mesophyll.

Where do these equations lead us? Within C_3 plants the $\delta^{13}C$ of whole-plant biomass gives a better indication of C_i over a longer time interval than can readily be obtained from gas-exchange measurements. The value of C_i in itself is a reflection of stomatal conductance (g_s), relative to photosynthetic activity (A). As such, $\delta^{13}C$ provides information on a plant's water-use efficiency (WUE) (Sect. 5.2). How do we arrive there? As can be derived from Equation (3), the extent of the fractionation of carbon isotopes depends on the intercellular partial pressures of CO_2, relative to that in the atmosphere. If C_i is high, g_s is large relative to A, and much of the $^{13}CO_2$ discriminated against by Rubisco diffuses back to the atmosphere; hence the fractionation is large. If C_i is low, then relatively more of the accumulated $^{13}CO_2$ is fixed by Rubisco, and therefore the fractionation of the overall photosynthesis process is less. Comparison of WUE calculated on the basis of $\delta^{13}C$ is only valid at constant vapor pressure difference (Δw) and is called intrinsic WUE (A/g_s).

continued

Box 2A.2 *Continued*

Under many situations $\delta^{13}C$ is a good proxy for WUE and it can be used for, e.g., paleoclimatic studies and genetic screening for drought-tolerant varieties. However, under conditions where Δw varies or g_s and g_m are not strongly correlated, $\delta^{13}C$ may not be a good predictor of WUE.

Carbon-isotope fractionation values differ between C_3, C_4, and CAM species (Sects. 9 and 10). In C_4 plants, little of the $^{13}CO_2$ that is discriminated against by Rubisco diffuses back to the atmosphere. This is prevented, first, by the diffusion barrier between the vascular bundle sheath and the mesophyll cells. Second, the mesophyll cells contain PEP carboxylase, which scavenges most of the CO_2 that escapes from the bundle sheath (Table 1). Fractionation during photosynthesis in C_4 plants is therefore dominated by fractionation during diffusion (4.4%). There is also little fractionation in CAM plants, where the heavy isotopes discriminated against cannot readily diffuse out of the leaves because the stomata are closed for most of the day. The actual $\delta^{13}C$ of CAM plant biomass depends on the fractions of the carbon fixed by CAM and C_3 photosynthesis.

Aquatic plants show relatively little fractionation, due to unstirred layers surrounding the leaf, rather than to a different photosynthetic pathway (Sect. 11.6). The unstirred boundary layers cause diffusion to be a major limitation for their photosynthesis, so that fractionation in these plants tends toward the value found for the diffusion process (Fig. 1).

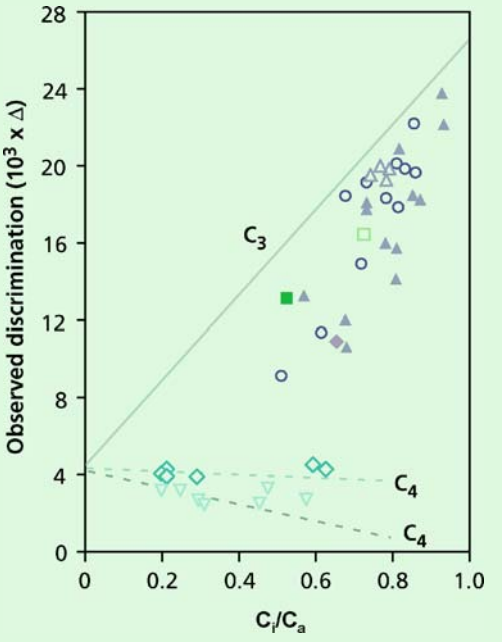

FIGURE 1. The relationship between the ratio of the internal and the atmospheric CO_2 concentration, at a constant C_a of 340 µmol mol^{-1}. Data for both C_3 and C_4 species are presented; the lines are drawn on the basis of a number of assumptions, relating to the extent of leakage of CO_2 from the bundle sheath back to the mesophyll (Evans et al. 1986, *Australian Journal of Plant Physiology* 13: 281–292). Copyright CSIRO, Australia.

substantially lower than C_i(the CO_2 concentration in the intercellular spaces); a difference of about 80 µmol mol^{-1}is common, as compared with C_a–C_i of about 100 µmol mol^{-1}. The mesophyll conductance varies widely among species and correlates with the photosynthetic capacity (A_{max}) of the leaf (Fig. 7). Interestingly, the relationship between mesophyll conductance and photosynthesis is rather similar for scleromorphic and mesophytic leaves, but scleromorphs tend to have a somewhat larger draw-down of CO_2 between intercellular space and chloroplast (C_i–C_c) (Warren & Adams 2006).

The mesophyll conductance is a complicated trait, involving diffusion of CO_2 in the intercellular spaces in the gas phase, dissolving of CO_2 in the liquid phase, conversion of CO_2 into HCO_3^- catalyzed by carbonic anhydrase, and diffusion in the liquid phase and across membranes. The resistance in the gas phase is low and is considered as normally not a limiting factor (Bernacchi et al. 2002). Diffusion in the liquid phase is much slower (10^4 times less), and the path length is minimized by chloroplast position against the cell wall opposite intercellular spaces (Fig. 1). This component likely represents a large fraction of total r_m, and **carbonic anhydrase** is important for minimizing it (Gillon & Yakir 2000). Evidence for an important role for the area of chloroplasts bordering intercellular spaces as a determinant of g_m stems from a positive relationship with this parameter per unit leaf area (Evans & Loreto 2000). Data about a similar parameter, chloroplast area per leaf area, are more widely available and vary by an order of magnitude among species (Table 1) which is likely associated with g_m. There

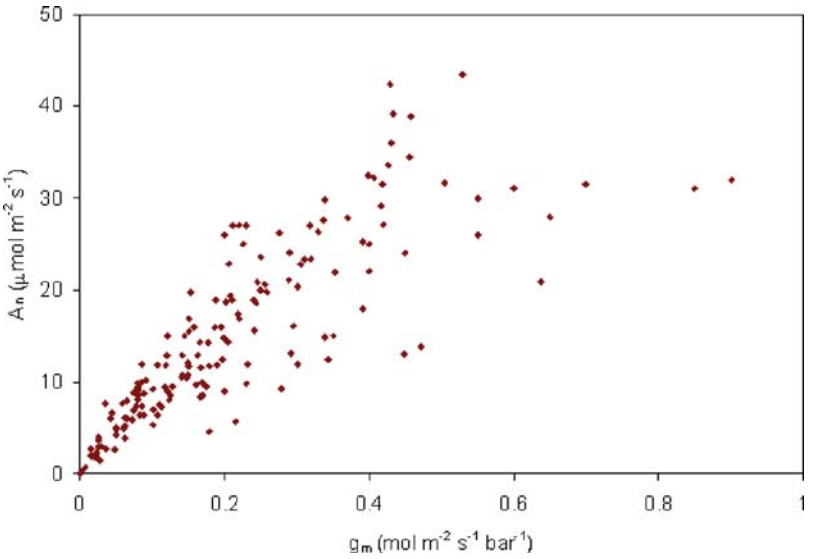

FIGURE 7. The relationship between the rate of photosynthesis (A_n) and maximum mesophyll conductance (g_m), determined for a wide range of species. Values for scleromorphic leaves are at most 0.21 mol m^{-2} s^{-1} bar^{-1} (g_m) and 22.9 μmol m^{-2} s^{-1} (A_n), whereas those for mesomorphic leaves span the entire range shown here. The units of conductance as used in this graph differ from those used elsewhere in this text. The reason is that when CO_2 is dissolving to reach the sites of carboxylation, the amount depends on the partial pressure of CO_2 and conductance has the units used in this graph. For air space conductance the units could be the same as used elsewhere: mol m^{-2} s^{-1}, if CO_2 is given as a mole fraction (based on data compiled in Flexas et al. 2008). Courtesy, J. Flexas, Universitat de les Illes Balears, Palma de Mallorca, Balears, Spain.

is evidence that specific **aquaporins** facilitate transport of CO_2 across membranes. Their role in the transport of CO_2 might account for rapid modulation of g_m in response to environmental factors such as temperature, CO_2, and desiccation (Flexas et al. 2006a). The mesophyll conductance is proportional to chloroplast surface area within a given functional group. The difference in g_m between functional groups is associated with mesophyll cell wall thickness, which varies from 0.1 μm in annuals, 0.2–0.3 μm in deciduous, broad-leaved species, and 0.3–0.5 μm in evergreen, broad-leaved species (Terashima et al. 2006).

When stomatal and mesophyll conductance are considered in conjunction with the assimilation of CO_2, the "supply function" (Equation 1) tends to intersect the "demand function" in the region where carboxylation and electron transport are co-limiting (Fig. 6).

TABLE 1. The area of the chloroplast in palisade (P) and spongy (S) mesophyll ($Area_{chlor}$) expressed per unit leaf area ($Area_{leaf}$) for species from the mountain range of the East Pamirs, Tadjikistan (3500–4500 m).*

	$(Area_{chlor})/Area_{leaf}$				
	P	S	P+S	Lowest (P+S)	Highest (P+S)
Perennial dicotyledonous herbs (54)	12	9	18	3	41
Cushion plants (4)	20	11	26	12	40
Dwarf semishrubs (12)	16	6	21	5	48
Subshrubs (8)	9	7	15	7	24

Source: Pyankov & Kondratchuk (1995, 1998).

* The number of investigated species is given in brackets. The sum P+S differs from P+S, because data pertain to both dorsiventral (P+S) and isopalisade (P) species.

3. Response of Photosynthesis to Light

The level of irradiance is an important ecological factor on which all photo-autotrophic plants depend. Only the photosynthetically active part of the spectrum (PAR; 400–700 nm) directly drives photosynthesis. Other effects of radiation pertain to the photoperiod, which triggers flowering and other developmental phenomena in many species, the direction of the light, and the spectral quality, characterized by the red/far-red ratio, which is of major importance for many aspects of morphogenesis. These effects are discussed in Chapter 7 on growth and allocation and Chapter 8 on life cycles; effects of infrared radiation are discussed in Chapter 4A on the plant's energy balance and its significance through temperature effects on photosynthesis in Sect. 7. Effects of ultraviolet radiation are treated briefly in Sect. 2.2 of Chapter 4B on effects of radiation and temperature.

Low light intensities pose stresses on plants because irradiance limits photosynthesis and thus net carbon gain and plant growth. Responses of the photosynthetic apparatus to shade can be at two levels: either at the structural level, or at the level of the biochemistry in chloroplasts. Leaf anatomy, and structure and biochemistry of the photosynthetic apparatus are treated in Sect. 3.2.2; aspects of morphology at the whole plant level are discussed in Sect. 5.1 of Chapter 7 on growth and allocation.

High light intensities may also be a stress for plants, causing damage to the photosynthetic apparatus, particularly if other factors are not optimal. The kind of damage to the photosynthetic apparatus that may occur and the mechanisms of plants to cope with excess irradiance are treated in Sect. 3.3.

To analyze the response of photosynthesis to irradiance, we distinguish between the dynamic response of photosynthesis to light (or any other environmental factor) and the steady-state response. A steady-state response is achieved after exposure of a leaf to constant irradiance for some time until a constant response is reached. Dynamic responses are the result of perturbations of steady-state conditions due to sudden changes in light conditions resulting in changes in photosynthetic rates.

Certain genotypes have characteristics that are adaptive in a shady environment (shade-adapted plants). In addition, all plants have the capability to acclimate to a shady environment, to a greater or lesser extent, and form a shade plant phenotype (shade form). The term **shade plant** may therefore refer to an "adapted" genotype or an "acclimated" phenotype. Similarly, the term **sun plant** normally refers to a plant grown in high-light conditions, but is also used to indicate a shade-avoiding species or ecotype. The terms sun leaf and shade leaf are used more consistently; they refer to leaves that have developed at high and low irradiance, respectively.

3.1 The Light Climate Under a Leaf Canopy

The average **irradiance** decreases exponentially through the plant canopy, with the extent of light attenuation depending on both the amount and arrangement of leaves (Monsi & Saeki 1953, 2005):

$$I = I_o e^{-kL} \quad (6)$$

where I is the irradiance beneath the canopy; I_o is the irradiance at the top of the canopy; k is the extinction coefficient; and L is the leaf area index (total leaf area per unit ground area). The extinction coefficient is low for vertically inclined leaves (for example 0.3–0.5 for grasses), higher for a more horizontal leaf arrangement, and approaching 1.0 for randomly distributed, small, perfectly horizontal leaves. A clumped leaf arrangement and deviating leaf angles result in intermediary values for k. A low extinction coefficient allows more effective light transfer through canopies dominated by these plants. Leaves are more vertically inclined in high-light than in cloudy or shaded environments. This minimizes the probability of photoinhibition and increases light penetration to lower leaves in high-light environments, thereby maximizing whole-canopy photosynthesis (Terashima & Hikosaka 1995). Values for leaf area index range from less than 1 in sparsely vegetated communities like deserts or tundra to 5–7 for crops to 5–10 for forests (Schulze et al. 1994).

The **spectral composition** of shade light differs from that above a canopy, due to the selective absorption of photosynthetically active radiation by leaves. Transmittance of photosynthetically active radiation is typically less than 10%, whereas transmittance of far-red (FR, 730 nm) light is substantial (Fig. 6 in Chapter 8 on life cycles). As a result, the ratio of red (R, 660 nm) to far-red (the R/FR ratio) is lower in canopy shade. This affects the photoequilibrium of **phytochrome**, a pigment that allows a plant to perceive shading by other plants (Box 7.2), and requires adjustment of the photosynthetic apparatus.

Another characteristic of the light climate in and under a leaf canopy is that direct sunlight may arrive as "packages" of high intensity: **sunflecks**.

So there are short spells of high irradiance against a background of a low irradiance. Such sunflecks are due to the flutter of leaves, movement of branches and the changing angle of the sun. Their duration ranges from less than a second to minutes. Sunflecks typically have lower irradiance than direct sunlight due to penumbral effects, but large sunflecks (those greater than an angular size of 0.5 degrees) can approach irradiances of direct sunlight (Chazdon & Pearcy 1991).

3.2 Physiological, Biochemical, and Anatomical Differences Between Sun and Shade Leaves

Shade leaves exhibit a number of traits that make them quite distinct from leaves that developed in full daylight. We first discuss these traits and then some of the problems that may arise in leaves from exposure to high irradiance. In the last section we discuss signals and transduction pathways that allow the formation of sun vs. shade leaves.

3.2.1 The Light-Response Curve of Sun and Shade Leaves

The steady-state rate of CO_2 assimilation increases asymptotically with increasing irradiance. Below the **light-compensation point** ($A_n = 0$), there is insufficient light to compensate for respiratory carbon loss due to photorespiration and dark respiration (Fig. 8). At low light intensities, A_n increases linearly with irradiance, with the light-driven electron transport limiting photosynthesis. The initial slope of the light-response curve based on *absorbed* light (**quantum yield**) describes the efficiency with which light is converted into fixed carbon (typically about 0.06 moles CO_2 fixed per mole of quanta under favorable conditions and a normal atmospheric CO_2 concentration). When the light-response curve is based on *incident* light, the leaf's absorptance also determines the quantum yield; this initial slope is called the **apparent quantum yield**. At high irradiance, photosynthesis becomes light-saturated and is limited by carboxylation rate, which is governed by some combination of CO_2 diffusion into the leaf and carboxylation capacity. The shape of the light-response curve can be satisfactorily described by a nonrectangular hyperbola (Fig. 9):

$$A_n = \frac{\phi I + A_{max} - \sqrt{\{(\phi I + A_{max})^2 - 4\,\Theta\,\phi_{max}\}}}{2\Theta} - R_d \quad (7)$$

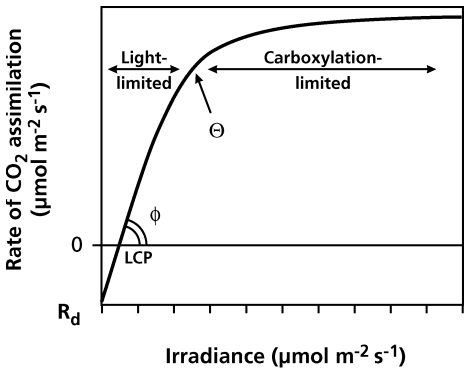

FIGURE 8. Typical response of net photosynthesis to irradiance, drawn according to Equation (7) in the text. The intercept with the *x*-axis is the light-compensation point (LCP), the initial slope of the line gives the quantum yield (ϕ) and the intercept with the *y*-axis is the rate of dark respiration (R_d). The curvature of the line is described by θ. At low irradiance, the rate of CO_2 assimilation is light-limited; at higher irradiance A_n is carboxylation limited. A_{max} is the light-saturated rate of CO_2 assimilation at ambient C_a.

where A_{max} is the light-saturated rate of gross CO_2 assimilation (net rate of CO_2 assimilation + dark respiration) at infinitely high irradiance, ϕ is the (apparent) quantum yield (on the basis of either incident or absorbed photons), Θ is the curvature factor, which can vary between 0 and 1, and R_d is the dark respiration during photosynthesis. The Equation can also be used to describe the light dependence of electron transport, when A is then replaced by J and A_{max} by J_{max} (Box 2A.1). This mathematical description is useful because it contains variables with a clear physiological meaning that can be derived from light-response curves and used to model photosynthesis.

Sun leaves differ from shade leaves primarily in their higher light-saturated rates of photosynthesis (A_{max}) (Fig. 9). The rate of dark respiration typically covaries with A_{max}. The initial slope of the light-response curves of light-acclimated and shade-acclimated plants (the **quantum yield**) is the same, except when shade-adapted plants become inhibited or damaged at high irradiance (photoinhibition or photodestruction) which reduces the quantum yield. The apparent quantum yield (i.e., based on incident photon irradiance) may also vary with variation in absorptance due to differences in chlorophyll concentration per unit leaf area. This is typically not important in the case of acclimation to light (Sect. 3.2.3), but cannot be ignored when factors such as nutrient availability and senescence

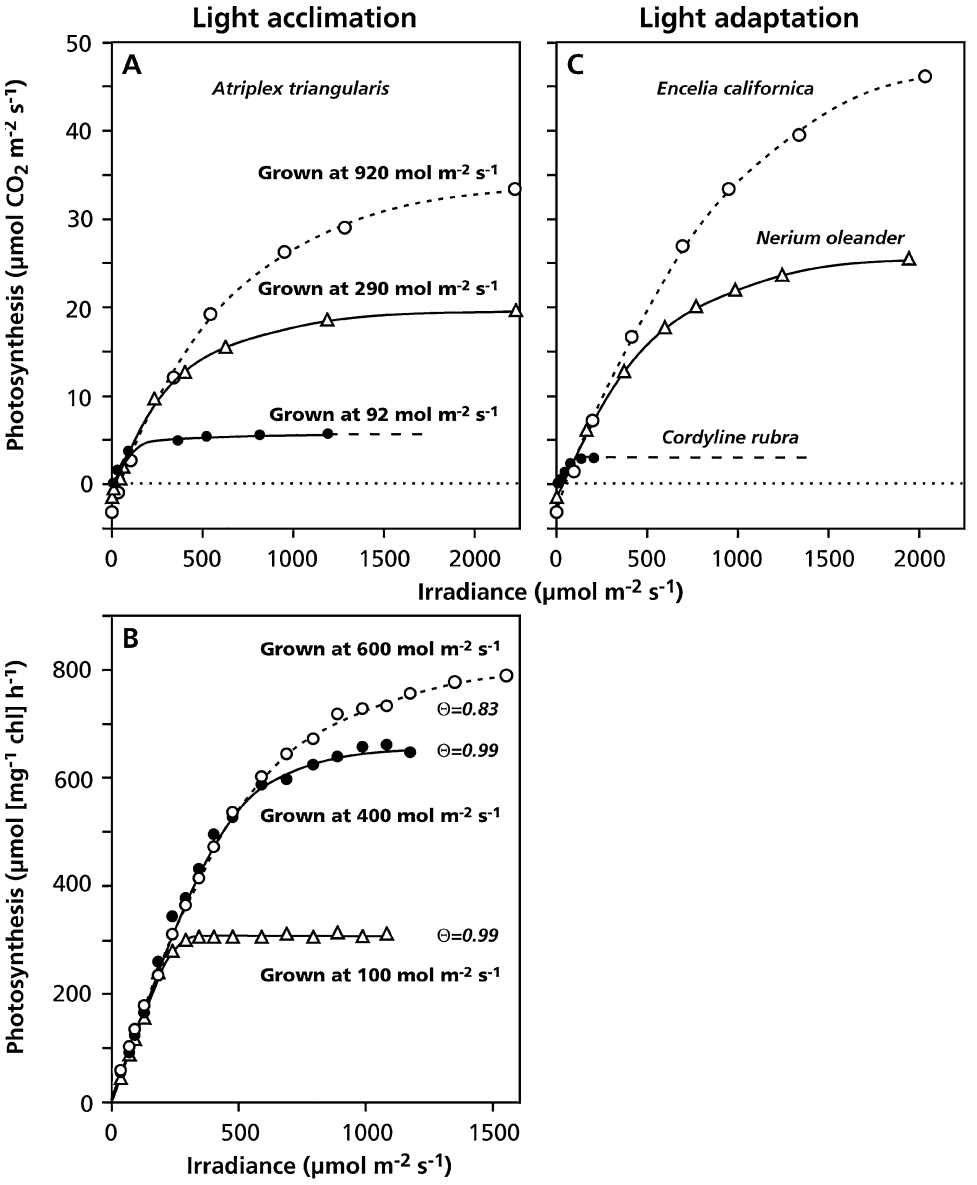

FIGURE 9. Photosynthesis as a function of irradiance for different species and growing conditions. Light acclimation: (A) for *Atriplex triangularis* (Björkman 1981) and (B) for a thin algal culture (*Coccomyxa* sp.) grown at different levels of irradiance 100, 400, or 600 µmol m^{-2} s^{-1} (B) note the difference in "curvature", for which the Θ values (Equation 6) are given in B, between the three curves (after Ögren 1993). Copyright American Society of Plant Biologists. Light adaptation: (C) for species which naturally occur at a high, intermediate, or low irradiance (after Björkman 1981).

play a role. The transition from the light-limited part to the light-saturated plateau is generally abrupt in shade leaves, but more gradual in sun leaves (higher A_{max} and lower Θ in sun leaves). Although shade leaves typically have a low A_{max}, they have lower light-compensation points and higher rates of photosynthesis at low light because of their lower respiration rates per unit leaf area (Fig. 9).

Just as in acclimation, most plants that have evolved under conditions of high light have higher light-saturated rates of photosynthesis (A_{max}), higher light-compensation points, and lower rates

of photosynthesis at low light than do shade-adapted plants when grown under the same conditions.

3.2.2 Anatomy and Ultrastructure of Sun and Shade Leaves

One mechanism by which sun-grown plants, or sun leaves on a plant, achieve a high A_{max} (Fig. 9) is by producing **thicker** leaves (Fig. 10) which provides space for more chloroplasts per unit leaf area. The increased thickness is largely due to the formation of longer palisade cells in the mesophyll and, in species that have this capacity, the development of multiple palisade layers in sun leaves (Hanson 1917). Plants that naturally occur in high-light environments (e.g., grasses, *Eucalyptus* and *Hakea* species) may have palisade parenchyma on both sides of the leaf (Fig. 10). Such leaves are naturally positioned (almost) vertically, so that both sides of the leaf receive a high irradiance. Anatomy constrains the potential of leaves to acclimate, e.g., the acclimation potential of shade leaves to a high-light environment is limited by the space in mesophyll cells bordering intercellular spaces (Oguchi et al. 2005). Full acclimation to a new light environment, therefore, typically requires the production of new leaves.

The spongy mesophyll in dorsiventral leaves of dicotyledons increases the **path length** of light in leaves by reflection at the gas-liquid interfaces of these irregularly oriented cells. The relatively large proportion of spongy mesophyll in shade leaves therefore enhances leaf absorptance, due to the greater internal light scattering (Vogelmann et al. 1996). When air spaces of shade leaves of *Hydrophyllum canadense* (broad-leaved waterleaf) or *Asarum canadense* (Canadian wild-ginger) are infiltrated with mineral oil to eliminate this phenomenon, light absorptance at 550 and 750 nm is reduced by 25 and 30%, respectively (Fig. 11). In sun leaves, which have relatively less spongy mesophyll, the effect of infiltration with oil is much smaller. The optical path length in leaves ranges from 0.9 to 2.7 times that of an equivalent amount of pigment in water, greatly increasing the effectiveness of light absorption in thin leaves of shade plants (Rühle & Wild 1979).

Leaves of obligate shade plants, as can for instance be found in the understory of a tropical rainforest, may have specialized anatomical structures that enhance light absorption even further. Epidermal and sub-epidermal cells may act as lenses that concentrate light on chloroplasts in a thin layer of mesophyll.

There are fewer chloroplasts per unit area in shade leaves as compared with sun leaves due to the reduced thickness of mesophyll. The **ultrastructure** of the chloroplasts of sun and shade leaves shows distinct differences (Fig. 12). Shade

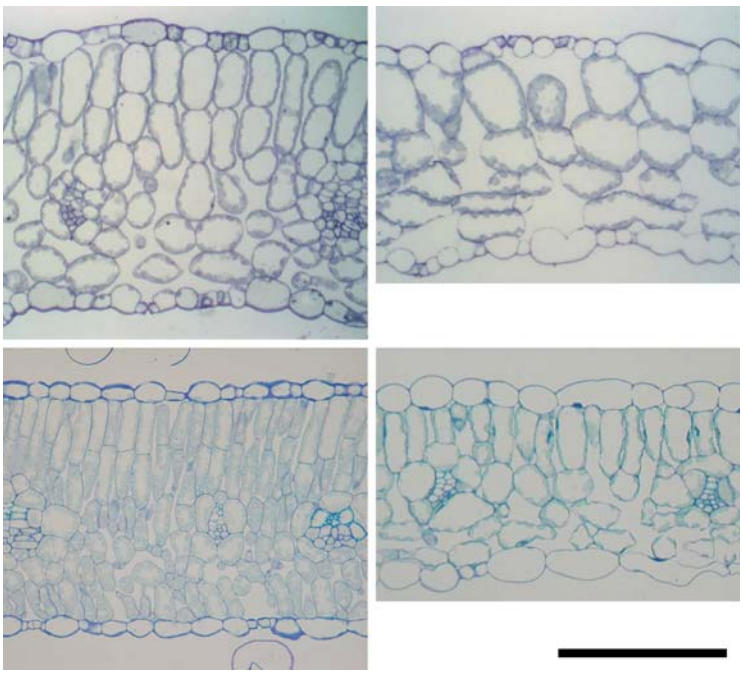

Figure 10. Light-microscopic transverse sections of sun and shade leaves of two species: (*Top*) *Arabidopsis thaliana* (thale cress) and (*Bottom*) *Chenopodium album* (pigweed). Note that the sun leaves of *Arabidopsis thaliana* have two cell layers for the palisade tissue while those of *Chenopodium album* have only one layer. Shade leaves of both species have only one cell layer. Scale bar = 100 μm (courtesy S. Yano, National Institute for Basic Biology, Okazaki, Japan).

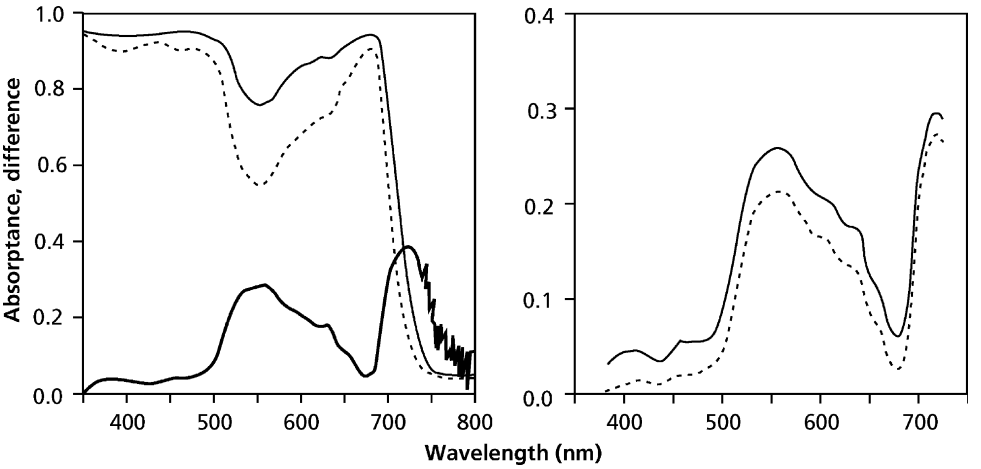

FIGURE 11. (A) Light absorptance in a shade leaf of *Hydrophyllum canadense* (broad-leaved waterleaf). The *solid line* gives the absorptance of a control leaf. The broken line shows a leaf infiltrated with mineral oil, which reduces light scattering. The difference between the two lines is given as the thick solid line. (B) The difference in absorptance between an oil-infiltrated leaf and a control leaf of *Acer saccharum* (sugar maple). The solid line gives the difference for a shade leaf, the broken line for a sun leaf (after DeLucia et al. 1996).

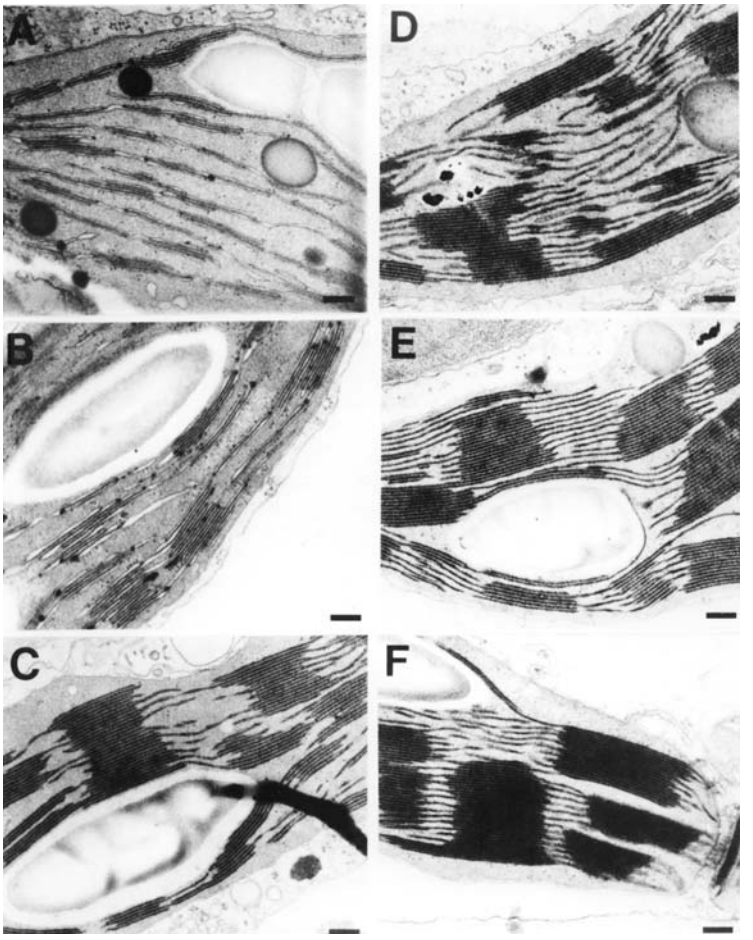

FIGURE 12. Electron micrographs of chloroplasts in sun (A–C) and shade (D–F) leaves of *Schefflera arboricola* (dwarf umbrella plant). Chloroplasts found in upper palisade parenchyma tissue (A, D), lower palisade parenchyma tissue (B, E) and spongy mesophyll tissue (C, F). Note the difference in grana between sun and shade leaves and between the upper and lower layer inside the leaf. Scale bar = 0.2 μm (courtesy A.M. Syme and C. Critchley, Department of Botany, The University of Queensland, Australia).

Box 2A.3
Carbon–Fixation and Light–Absorption Profiles Inside Leaves

We are already familiar with differences in biochemistry and physiology *between* sun and shade leaves (Sect. 3.2). If we consider the gradient in the level of irradiance inside a leaf, however, then should we not expect similar differences *within* leaves? Indeed, palisade mesophyll cells at the adaxial (upper) side of the leaf tend to have characteristics associated with acclimation to high irradiance: a high Rubisco/chlorophyll and chl *a*/chl *b* ratio, high levels of xanthophyll-cycle carotenoids, and less stacking of the thylakoids (Fig. 13; Terashima & Hikosaka 1995). On the other hand, the spongy mesophyll cells at the abaxial (lower) side of the leaf have chloroplasts with a lower Rubisco/chlorophyll and chl *a*/chl *b* ratio, characteristic for acclimation to low irradiance. What are the consequences of such profiles within the leaf for the exact location of carbon fixation in the leaf?

To address this question we first need to know the light profile within a leaf which can be measured with a fiberoptic microprobe that is moved through the leaf, taking light readings at different wavelengths (Vogelmann 1993). Chlorophyll is not homogeneously distributed in a cell; rather, it is concentrated in the chloroplasts that may have an heterogeneous distribution within and between cells. In addition, inside the leaf, absorption varies because of scattering at the air-liquid interfaces that modify pathlength (e.g., between palisade and spongy mesophyll) (Sect. 3.2.4). How can we obtain information on light absorption?

After a period of incubation in the dark, chlorophyll fluorescence of a healthy leaf is proportional to the light absorbed by that leaf (Box 2A.4). Vogelmann & Evans (2002) illuminated leaves at the adaxial side and at the side of a transversal cut, and measured the distribution of fluorescence over the cut surface using imaging techniques. Fluorescence obtained with adaxial light represents light absorption, whereas lighting the cut surface represents chlorophyll concentration. In leaves of *Spinacia oleracea* (spinach), going from the upper leaf surface deeper into the leaf, the chlorophyll concentration increases to 50 μmol m^{-2}over the first 250 μm in the palisade layer, remains similar deeper down in the palisade and spongy mesophyll, but then declines steeply toward the lower surface over the last 100 μm of the spongy mesophyll layer (Fig. 1A). As expected from the absorption characteristics of chlorophyll (Fig. 2), green light is less strongly absorbed than blue and red, penetrates deeper into the leaf, and, consequently, shows there a higher absorption (Fig. 1A). The data on light absorption and chlorophyll concentration allow the calculation of an extinction coefficient, which varies surprisingly little across a leaf. Differences in scattering between the two mesophyll layers are apparently not very important as is also evident from measurements of infiltrated leaves (Fig. 11; Vogelmann & Evans 2002).

What are the consequences of the profiles of absorption and chlorophyll concentration for the distribution of photosynthetic activity across a section of a leaf? The profile of photosynthetic capacity (A_{max}) can be measured following fixation of $^{14}CO_2$ ensuring light saturation for all chloroplasts (Evans & Vogelmann 2003); alternatively, the profile of Rubisco concentration can be used (Nishio et al. 1993). Both techniques require making thin sections parallel to the leaf surface. A_{max}peaks where chlorophyll reaches its maximum in the palisade mesophyll, and declines to a lower value in the spongy mesophyll (Fig. 1A). A_{max} per chlorophyll decreases similarly from the palisade to the spongy mesophyll. We can use the profiles of A_{max} and absorbed irradiance to calculate photosynthetic activity (A) in each layer from the light-response curve, using virtually the same equation as introduced in Sect. 3.2.1 (the only difference being that R_{day} is left out):

$$A = \frac{\phi I + A_{max} - \{(\phi I + A_{max})^2 - 4\theta\phi I A_{max}\Big)^{0.5}\}}{2\theta} \quad (1)$$

where ϕ is the maximum quantum yield, I is the absorbed irradiance and θ describes the curvature. The calculated light-response curves of the adaxial layers are like those of sun leaves, whereas those of the abaxial layers are like the ones of shade leaves. Photosynthetic activity peaks close to the adaxial surface in low light, but the maximum shifts to deeper layers at higher irradiances (Fig. 1B). Since green light

continued

Box 2A.3 *Continued*

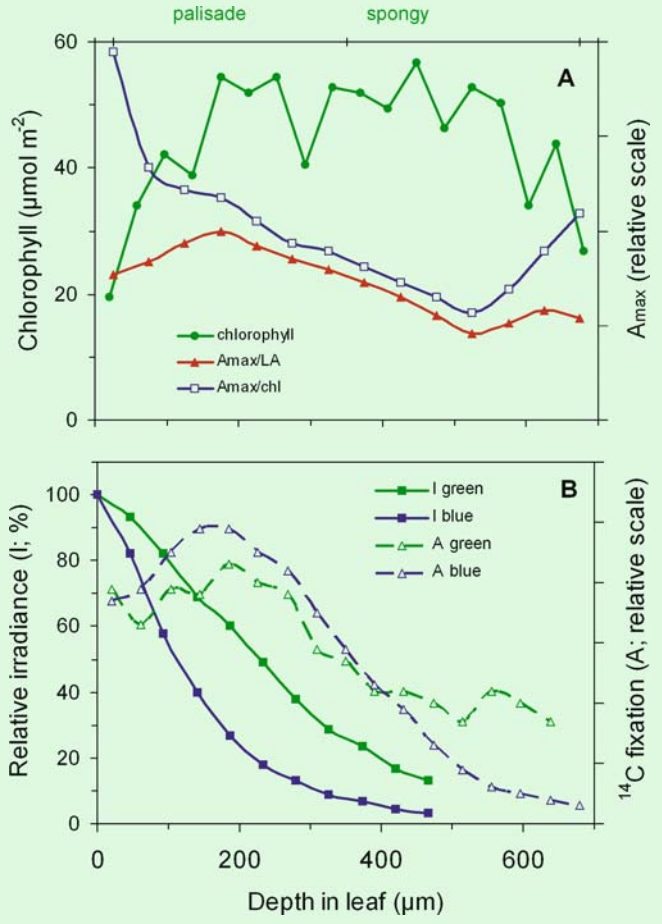

FIGURE 1. Profiles of chlorophyll and light absorption (A), and photosynthesis (B) in a leaf of *Spinacia oleracea* (spinach). The distribution of chlorophyll was derived from measurements of chlorophyll fluorescence, using a light source to illuminate the cut surface of a transversal section of the leaf. The absorption of green and blue light was also measured with chlorophyll fluorescence, but with light striking the upper leaf surface. The light-saturated photosynthetic electron transport rate (A_{max}) was derived from ^{14}C-fixation profiles and photosynthetic activity at and irradiance of 500 and 50 µmol m^{-2} s^{-1} in green and blue light were calculated using Equation (1) (Vogelmann & Evans 2002; Evans & Vogelmann 2003).

has a lower absorptance, *A* in that spectral region is more homogeneously distributed across the leaf profile, whereas blue light causes a sharp peak closer to the upper surface. Calculated profiles of *A* show a close match with the experimental data of the ^{14}C-fixation profile.

chloroplasts have a smaller volume of stroma, where the Calvin-cycle enzymes are located, but larger grana, which contain the major part of the chlorophyll. Such differences are found both between plants grown under different light conditions and between sun and shade leaves on a single plant, as well as when comparing chloroplasts from the upper and lower side of one, relatively thick, leaf of *Schefflera arboricola* (dwarf umbrella plant) (Fig. 12). The adaxial (upper) regions have a chloroplast ultrastructure like sun leaves, whereas shade acclimation is found in the abaxial (lower) regions of the leaf (Box 2A.3).

3.2.3 Biochemical Differences Between Shade and Sun Leaves

Shade leaves **minimize light limitation** through increases in capacity for light capture and decreased carboxylation capacity and mesophyll conductance, but this does not invariably lead to higher chlorophyll concentrations per unit leaf area which

determines their absorptance (Terashima et al. 2001, Warren et al. 2007). Some highly shade-adapted species [e.g., *Hedera helix* (ivy) in the juvenile stage], however, may have substantially higher chlorophyll levels per unit leaf area in shade. This might be due to the fact that their leaves do not get much thinner in the shade; however, there may also be some photodestruction of chlorophyll in high light in such species. In most species, however, higher levels of chlorophyll per unit fresh mass and per chloroplast in shade leaves are compensated for by the smaller number of chloroplasts and a lower fresh mass per area. This results in a rather constant chlorophyll level per unit area in sun- and shade leaves.

The **ratio** between **chlorophyll *a*** and **chlorophyll *b*** (chl *a*/chl *b*) is lower in shade-acclimated leaves. These leaves have relatively more chlorophyll in the **light-harvesting complexes**, which contain large amounts of chl *b* (Lichtenthaler & Babani 2004). The decreased chl *a*/chl *b* ratio is therefore a reflection of the greater investment in LHCs (Evans 1988). The larger proportion of LHC is located in the **larger grana** of the shade-acclimated chloroplast (Fig. 12). Sun leaves also contain more xanthophyll carotenoids, relative to chlorophyll (Box 2A.3; Lichtenthaler 2007).

Sun leaves have larger amounts of Calvin-cycle enzymes per unit leaf area as compared with shade leaves, due to more cell layers, a larger number of chloroplasts per cell, and a larger volume of stroma, where these enzymes are located, per chloroplast, compared with shade leaves. Sun leaves also have more stroma-exposed thylakoid membranes, which contain the b_6f cytochromes and ATPase (Fig. 13). All these components enhance the **photosynthetic capacity** of sun leaves. Since the amount of chlorophyll per unit area is more or less equal among leaf types, sun leaves also have a higher photosynthetic capacity per unit chlorophyll. The biochemical gradients for Rubisco/chlorophyll across a leaf are similar to those observed within a canopy, with adaxial (upper) cells having more Rubisco, but less chlorophyll than abaxial (lower) cells (Terashima & Hikosaka 1995).

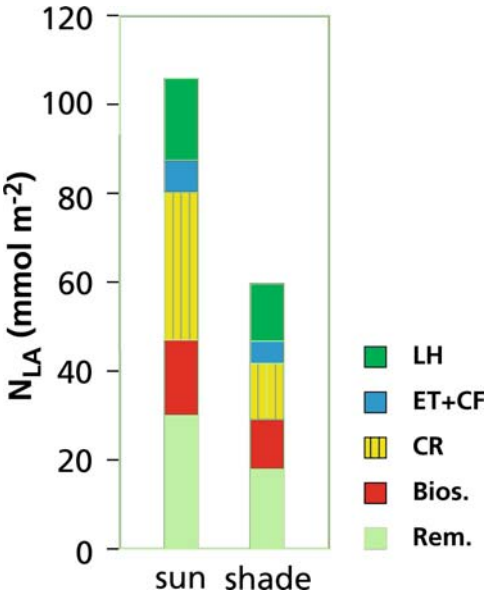

FIGURE 13. Nitrogen partitioning among various components in shade- and sun-acclimated leaves. Most of the leaf's N in herbaceous plants is associated with photosynthesis. Some of the fractions labeled Bios. (Biosynthesis) and Rem. (Remainder) are indirectly involved in synthesis and maintenance processes associated with the photosynthetic apparatus. LH = light harvesting (LHC, PS I, PS II), ET+CF = electron transport components and coupling factor (ATPase), CR = enzymes associated with carbon reduction (Calvin cycle, mainly Rubisco), Bios = biosynthesis (nucleic acids and ribosomes), Rem = remainder, other proteins and N-containing compounds (e.g., mitochondrial enzymes, amino acids, cell wall proteins, alkaloids) (after Evans & Seemann 1989).

3.2.4 The Light-Response Curve of Sun and Shade Leaves Revisited

Table 2 summarizes the differences in characteristics between shade-acclimated and sun-acclimated leaves (Walters 2005). The higher A_{max} of sun leaves as compared with shade leaves is associated with a greater amount of compounds that determine photosynthetic capacity which are located in the greater number of chloroplasts per area and in the larger stroma volume and the stroma-exposed thylakoids in chloroplasts. The increase of A_{max} with increasing amount of these compounds is almost linear (Evans & Seemann 1989). Hence, investment in compounds determining photosynthetic capacity is proportionally translated into photosynthetic rate at high irradiance levels.

The higher rate of dark respiration in sun leaves is not only due to a greater demand for respiratory energy for the maintenance of the larger number of leaf cells and chloroplasts, because respiration rates drop rapidly upon shading, whereas A_{max} is still high (Pons & Pearcy 1994). Much of the demand for ATP is probably associated with the export of the products of photosynthesis from the leaf and other processes

Table 2. Overview of generalized differences in characteristics between shade- and sun-acclimated leaves.

	Sun	Shade
Structural		
Leaf dry mass per area	High	Low
Leaf thickness	Thick	Thin
Palisade parenchyma thickness	Thick	Thin
Spongy parenchyma thickness	Similar	Similar
Stomatal density	High	Low
Chloroplast per area	Many	Few
Thylakoids per stroma volume	Low	High
Thylakoids per granum	Few	Many
Biochemical		
Chlorophyll per chloroplast	low	high
Chlorophyll per area	similar	similar
Chlorophyll per dry mass	low	high
Chlorophyll *a*/*b* ratio	high	low
Light-harvesting complex per area	low	high
Electron transport components per area	high	low
Coupling factor (ATPase) per area	high	low
Rubisco per area	high	low
Nitrogen per area	high	low
Xanthophylls per area	high	low
Gas exchange		
Photosynthetic capacity per area	high	low
Dark respiration per area	high	low
Photosynthetic capacity per dry mass	similar	similar
Dark respiration per dry mass	similar	similar
Carboxylation capacity per area	high	low
Electron transport capacity per area	high	low
Quantum yield	similar	similar
Curvature of light-response curve	gradual	acute

associated with a high photosynthetic activity (Sect. 4.4 in Chapter 2B on plant respiration).

The preferential absorption of photons in the red and blue regions of the spectrum by a leaf is not a simple function of its irradiance and chlorophyll concentration. A relationship with a negative exponent would be expected, as described for monochromatic light and pigments in solution (Lambert-Beer's law). The situation in a leaf is more complicated, however, because preferential absorption of red light by chlorophyll causes changes in the spectral distribution of light through the leaf. Moreover, the path length of light is complicated, due to reflection inside the leaf and to changes in the proportions of direct and diffuse light. Empirical equations, such as a hyperbole, can be used to describe light absorption by chlorophyll. For a healthy leaf, the quantum yield based on incident light is directly proportional to the amount of photons absorbed.

The cause of the decrease in convexity (Equation 7) of the light-response curve with increasing growth irradiance (Fig. 9) is probably partly associated with the level of light-acclimation of the chloroplast in the cross-section of a leaf in relation to the distribution of light within the leaf (Leverenz 1987).

A high A_{max} per unit area and per unit chlorophyll (but not per unit biomass) of sun leaves is beneficial in high-light conditions, because the prevailing high irradiance can be efficiently exploited, and photon absorption per unit photosynthetic capacity is not limiting photosynthetic rates. Such a high A_{max}, however, would not be of much use in the shade, because the high irradiance required to utilize the capacity occurs only infrequently, and a high A_{max} is associated with high rates of respiration and a large investment of resources. On the other hand, a high chlorophyll concentration per unit photosynthetic capacity and per unit biomass in thin shade leaves maximizes the capture of limiting photons in

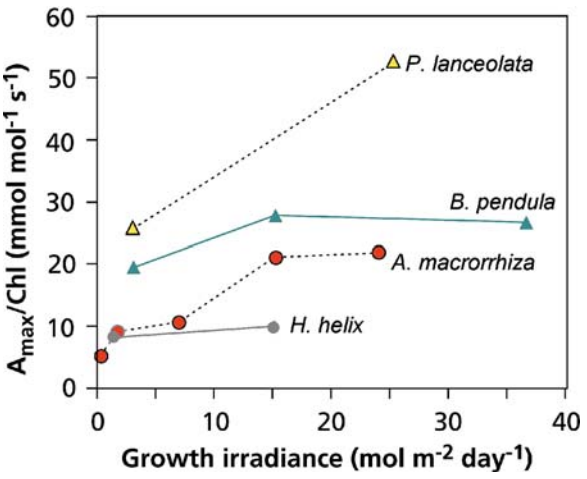

FIGURE 14. Light-saturated rate of CO_2 assimilation (A_{max}) per unit chlorophyll in relation to growth irradiance for four different species. *Plantago lanceolata* (snake plantain) (Poot et al. 1996), *Betula pendula* (European white birch, Bp) (Öquist et al. 1982), *Alocasia macrorrhiza* (giant taro, Am) (Sims & Pearcy 1989), *Hedera helix* (ivy, Hh) (T.L. Pons, unpublished data).

low-light conditions which is advantageous at low irradiance. Apparently, there is a "trade-off" between investment of resources in carbon-assimilating capacity and in light harvesting as reflected in the ratio of photosynthetic capacity to chlorophyll concentration. This ratio represents light acclimation at the chloroplast level.

Although A_{max}per unit chlorophyll responds qualitatively similar to growth irradiance in all plants, there are differences among species (Fig. 14; Murchie & Horton 1997). Four functional groups can be discerned:

1. Shade-avoiding species, such as the pioneer tree *Betula pendula* (European white birch) have a high A_{max}/chlorophyll ratio. This ratio, however, does not change much with growth irradiance.
2. Fast-growing herbaceous species from habitats with a dense canopy and/or a variable light availability have high A_{max}/chlorophyll ratios, which decrease strongly with decreasing irradiance. *Plantago lanceolata* (snake plantain) and *Arabidopsis thaliana* (thale cress) (Bailey et al. 2001) are examples.
3. A plastic response is also found in shade-adapted plants such as herbaceous understory species [*Alocasia macrorrhiza* (giant taro)] that depend on gaps for reproduction, and forest trees that tolerate shade as seedlings. The A_{max}/chlorophyll ratio, however, is much lower over the entire range of irradiance levels.
4. A low A_{max}/chlorophyll ratio that changes little with growth irradiance is found in woody shade-adapted species, such as juvenile *Hedera helix* (ivy).

3.2.5 The Regulation of Acclimation

As mentioned in previous sections, light acclimation consists of changes in leaf structure and chloroplast number at the leaf level, and changes in the photosynthetic apparatus at the chloroplast level. Some aspects of leaf anatomy, including morphology of epidermal cells and the number of stomata, are controlled by **systemic signals** originating in mature leaves (Lake et al. 2001, Coupe et al. 2006). Chloroplast properties are mostly determined by the **local light environment** of the developing leaves (Yano & Terashima 2001).

Studies of regulation at the chloroplast level have yielded significant insights. Each of the major components of the photosynthetic apparatus has part of their subunits encoded in the chloroplast and others in the nucleus. Acclimation of chloroplast composition thus likely entails coordinated changes in transcription of both genomes. The abundance of mRNAs coding for photosynthetic proteins, however, does not respond clearly during acclimation which suggests that post-transcriptional modifications play an important role (Walters 2005). Several perception mechanisms of the spectral and irradiance component of the light climate have been proposed.

Mutants lacking cryptochrome and phytochrome photoreceptors (CRY1, CRY2, PHYA), or having defects in their signaling pathway, show changes in chloroplast composition and disturbance of normal acclimation (Smith et al. 1993, Walters et al. 1999). Hence, these photoreceptors are either actually involved in perception of the light environment with respect to photosynthetic acclimation, or their action is a prerequisite for normal development of the photosynthetic apparatus. There is also evidence for a role of signals from photosynthesis itself in the regulation of acclimation, either directly or indirectly. Several of these have been identified, such as the redox state of components of the photosynthetic membrane or in the stroma, the ATP/ADP ratio, reactive oxygen species,

and the concentration of carbohydrates, including glucose and trehalose-6-phosphate (Walters 2005), but a definitive answer about their precise role is still lacking. **Systemic signals** play a role in the effect of the light environment of mature leaves on the acclimation of young, growing leaves, irrespective of their own light environment (Yano & Terashima 2001).

3.3 Effects of Excess Irradiance

All photons absorbed by the photosynthetic pigments result in excited chlorophyll, but at irradiance levels beyond the linear, light-limited region of the light-response curve of photosynthesis, not all excited chlorophyll can be used in photochemistry (Figs. 8, 15). The fraction of excitation energy that cannot be used increases with irradiance and under conditions that restrict the rate of electron transport and Calvin-cycle activity such as low temperature and desiccation. This is potentially harmful for plants, because the excess excitation may result in serious damage, if it is not dissipated. To avoid damage, plants have mechanisms to safely dispose of this excess excitation energy. When these mechanisms are at work, the quantum yield of photosynthesis is **temporarily** reduced (minutes), a normal phenomenon at high irradiance. The excess excitation energy, however, may also cause damage to the photosynthetic membranes if the dissipation mechanisms are inadequate. This is called **photoinhibition**, which is due to an imbalance between the rate of photodamage to PS II and the rate of repair of damaged PS II. Photodamage is initiated by the direct effects of light on the O_2-evolving complex and, thus, photodamage to PS II is unavoidable (Nishiyama et al. 2006). A reduction in quantum yield that is re-established within minutes to normal healthy values is referred to as **dynamic photoinhibition** (Osmond 1994); it is predominantly associated with changes in the xanthophyll cycle (Sect. 3.3.1). More serious damage that takes hours to revert to control conditions leads to **chronic photoinhibition**; it is mostly related to temporarily impaired D1 (Sect. 2.1.1; Long et al. 1994). Even **longer-lasting** photoinhibition (days) can be referred to as **sustained photoinhibition** (Sect. 7.2). A technique used for the quantification of photoinhibition is the measurement of quantum yield by means of chlorophyll fluorescence (Box 2A.4).

3.3.1 Photoinhibition—Protection by Carotenoids of the Xanthophyll Cycle

Plants that are acclimated to high light dissipate excess energy through reactions mediated by a particular group of **carotenoids** (Fig. 16). This dissipation process is induced by accumulation of protons in the thylakoid lumen which is triggered by excess light. Acidification of the lumen induces an enzymatic conversion of the carotenoid violaxanthin into antheraxanthin and zeaxanthin (Gilmore 1997). The

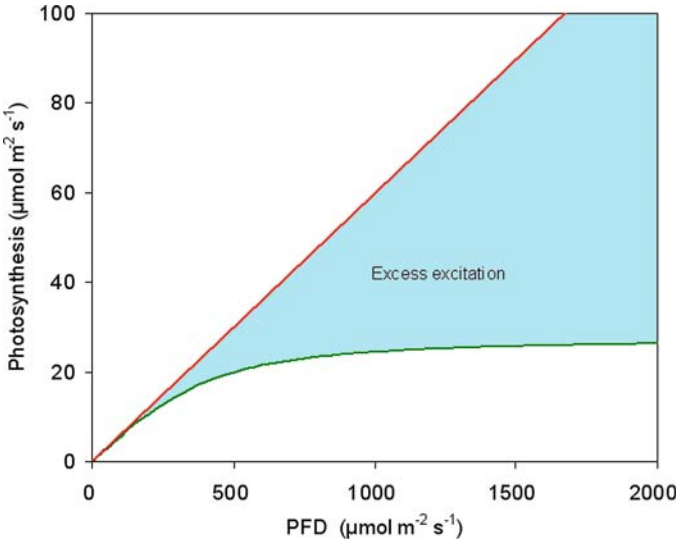

FIGURE 15. Response of photosynthesis to light intensity. Photosynthesis increases hyperbolically with irradiance, but photon absorption, and thus the generation of excited chlorophylls, increases linearly. The difference (blue area) between the two processes increases with increasing irradiance and represents the excess excitation energy.

Box 2A.4
Chlorophyll Fluorescence

When chlorophyllous tissue is irradiated with photosynthetically active radiation (400–700 nm) or wavelengths shorter than 400 nm, it emits radiation of longer wavelengths (approx. 680–760 nm). This fluorescence originates mainly from chlorophyll *a* associated with photosystem II (PS II). The measurement of the kinetics of chlorophyll fluorescence has been developed into a sensitive tool for probing state variables of the photosynthetic apparatus in vivo. In an ecophysiological context, this is a useful technique to quantify effects of stress on photosynthetic performance that is also applicable under field conditions.

Photons absorbed by chlorophyll give rise to (1) an excited state of the pigment which is channelled to the reaction center and may give rise to photochemical charge separation. The quantum yield of this process is given by ϕ_P. Alternative routes for the excitation energy are (2) dissipation as heat (ϕ_D) and (3) fluorescent emission (ϕ_F). These three processes are competitive. This leads to the assumption that the sum of the quantum yields of the three processes is unity:

$$\phi_P + \phi_D + \phi_F = I \qquad (1)$$

Since only the first two processes are subject to regulation, the magnitude of fluorescence depends on the added rates of photochemistry and heat dissipation. Measurement of fluorescence, therefore, provides a tool for quantification of these processes.

Basic Fluorescence Kinetics

When a leaf is subjected to strong white light after incubation in darkness, a characteristic pattern of fluorescence follows, known as the Kautsky curve (Bolhàr-Nordenkampf & Ögren 1993, Schreiber et al. 1995). It rises immediately to a low value (F_0), which is maintained only briefly in strong light, but can be monitored for a longer period in weak intermittent light (Fig. 1, left). This level of fluorescence (F_0) is indicative of open reaction centers due to a fully oxidized state of the primary electron acceptor Q_A. In strong saturating irradiance, fluorescence

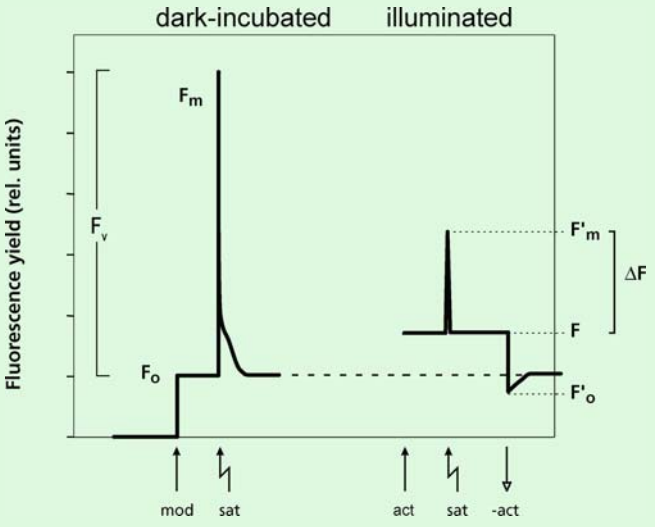

FIGURE 1. Fluorescence kinetics in dark-incubated and illuminated leaves in response to a saturating pulse of white light. mod = modulated measuring light on; sat = saturating pulse on; act=actinic light on for a prolonged period together with modulated measuring light; -act = actinic light off. For explanation of fluorescence symbols see text (after Schreiber et al. 1995).

continued

Box 2A.4 *Continued*

rises quickly to a maximum value (F_m) (Fig. 1, left) which indicates closure of all reaction centers as a result of fully reduced Q_A. When light is maintained, fluorescence decreases gradually (quenching) to a stable value as a result of induction of photosynthetic electron transport and dissipation processes.

After a period of illumination at a subsaturating irradiance, fluorescence stabilizes at a value F, somewhat above F_0 (Fig. 1, right). When a saturating pulse is given under these conditions, fluorescence does not rise to F_m, but to a lower value called F_m'. Although reaction centers are closed at saturating light, dissipation processes compete now with fluorescence which causes the quenching of F_m to F_m'.

Since all reaction centers are closed during the saturating pulse, the photochemical quantum yield (ϕ_P) is practically zero and, therefore, the quantum yields of dissipation at saturating light (ϕ_{Dm}) and fluorescence at saturating light (ϕ_{Fm}) are unity:

$$\phi_{Dm} + \phi_{Fm} = 1 \tag{2}$$

It is further assumed that there is no change in the relative quantum yields of dissipation and fluorescence during the saturating pulse:

$$\frac{\phi_{Dm}}{\phi_{Fm}} = \frac{\phi_D}{\phi_F} \tag{3}$$

Photochemical quantum yield (ϕ_P) is also referred to as ϕ_{II} because it originates mainly from PSII. It can now be expressed in fluorescence parameters only, on the basis of Equations (1), (2), and (3).

$$\phi_{II} = \frac{\phi_{Fm} - \phi_F}{\phi_{Fm}} \tag{4}$$

The fluorescence parameters F_0 and F_m can be measured with time-resolving equipment, where the sample is irradiated in darkness with $\lambda < 680\,\text{nm}$ and fluorescence is detected as emitted radiation at $\lambda > 680\,\text{nm}$. White light sources, however, typically also have radiation in the wavelength region of chlorophyll fluorescence. For measurements in any light condition, systems have been developed that use a weak modulated light source in conjunction with a detector that monitors only the fluorescence emitted at the frequency and phase of the source. A strong white light source for generating saturating pulses ($>5,000\ \mu\text{mol}\ m^{-2}s^{-1}$) and an actinic light source typically complete such systems. The modulated measuring light is sufficiently weak for measurement of F_0. This is the method used in the example given in Fig. 1. The constancy of the measuring light means that any change in fluorescence signal is proportional to ϕ_F. This means that the maximum quantum yield (ϕ_{IIm}) as measured in dark-incubated leaves is

$$\phi_m = (F_m - F_0)/F_m = F_v/F_m \tag{5}$$

where F_v is the variable fluorescence, the difference between maximal and minimal fluorescence. In illuminated samples the expression becomes

$$\phi_{II} = (F_m' - F)/F_m' = \Delta F/F_m' \tag{6}$$

where ΔF is the increase in fluorescence due to a saturating pulse superimposed on the actinic irradiance. $\Delta F/F_m'$ has values equal to or lower than F_v/F_m; the difference increases with increasing irradiance.

The partitioning of fluorescence quenching due to photochemical (qP) and nonphotochemical (qN) processes can be determined. These are defined as

$$qP = (F_m' - F)/(F_m' - F_0') = \Delta F/F_v' \tag{7}$$

$$qN = 1 - (F_m' - F_0')/(F_m - F_0) = 1 - F_v'/F_v \tag{8}$$

F_0 may be quenched in light, and is then called F_0' (Fig. 1 right). The measurement of this parameter may be complicated, particularly under field conditions. We can also use another term for nonphotochemical quenching (NPQ) which does not require the determination of F_0':

$$\text{NPQ} = (F_m - F_m')/F_m' \tag{9}$$

The theoretical derivation of the fluorescence parameters as based on the assumptions described above is supported by substantial empirical evidence. The biophysical background of the processes, however, is not always fully understood.

continued

Box 2A.4 *Continued*

Relationships with Photosynthetic Performance

Maximum quantum yield after dark incubation (F_v/F_m) is typically very stable at values around 0.8 in healthy leaves. F_v/F_m correlates well with the quantum yield of photosynthesis measured as O_2 production or CO_2 uptake at low irradiance (Fig. 2). In particular, the reduction of the quantum yield by photoinhibition can be evaluated with this fluorescence parameter. A decrease in F_v/F_m can be due to a decrease in F_m and/or an increase in F_0. A fast- and a slow-relaxing component can be distinguished. The fast component is alleviated within a few hours of low light or darkness and is therefore only evident during daytime; it is supposed to be involved in protection of PS II against over-excitation. The slow-relaxing component remains several days and is considered as an indication of (longer-lasting) damage to PS II. Such damage can be the result of sudden exposure of shade leaves to full sun light, or a combination of high irradiance and extreme (high or low) temperature. The way plants cope with this combination of stress factors determines their performance in particular habitats where such conditions occur.

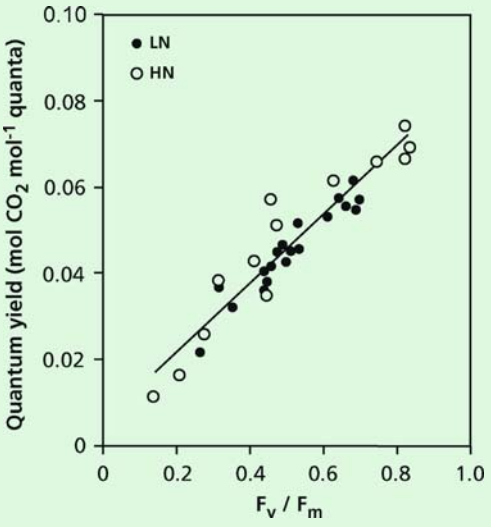

FIGURE 2. The relationship between quantum yield, as determined from the rate of O_2 evolution at different levels of low irradiance, and the maximum quantum yield of PS II determined with chlorophyll fluorescence (F_v/F_m, ϕ_{IIm}). Measurements were made on *Glycine max* (soybean) grown at high (*open symbols*) and low (*filled symbols*) N supply and exposed to high light for different periods prior to measurement (after Kao & Forseth 1992).

Quantum yield in light ($\Delta F/F_m'$) can be used to derive the rate of electron transport (J_F).

$$J_F = I\,\Delta F/F_m'\,\text{abs}\,0.5 \qquad (10)$$

where I is the irradiance and abs is the photon absorption by the leaf and 0.5 refers to the equal partitioning of photons between the two photosystems (Genty et al. 1989). For comparison of J_F with photosynthetic gas-exchange rates, the rate of the carboxylation (V_c) and oxygenation (V_o) reaction of Rubisco must be known. In C_4 plants and in C_3 plants at low O_2 and/or high CO_2, V_o is low and can be ignored. Hence, the rate of electron transport can also be derived from the rate of O_2 production or CO_2 uptake (J_c). For a comparison of J_F with J_c in normal air in C_3 plants, V_o must be estimated from the intercellular partial pressure of CO_2 (Box 2A.1). Photosynthetic ratesgenerally show good correlations with J_F (Fig. 3). J_F may be somewhat higher than J_c (Fig. 3). This can be ascribed to electron flow associated with nonassimilatory processes, or with assimilatory processes that do not result in CO_2 absorption, such as nitrate reduction. Alternatively, the chloroplast population monitored by fluorescence is not representative for the functioning of all chloroplasts across the whole leaf depth. The good correlation of gas exchange and fluorescence data in many cases indicates that J_F is representative for the whole-leaf photosynthetic rate, at least in a relative sense. Hence, J_F is also referred to as the relative rate of electron transport.

continued

Box 2A.4 *Continued*

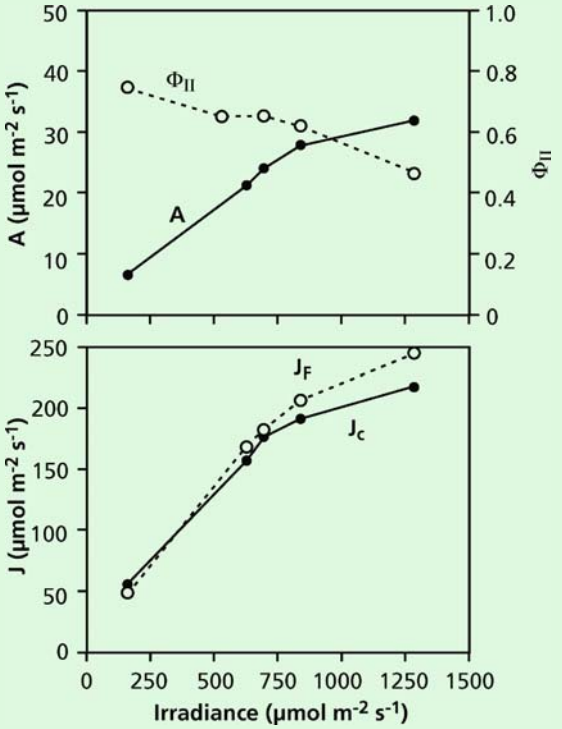

FIGURE 3. Relationship of chlorophyll fluorescence parameters and rates of CO_2 assimilation in the C_3 plant *Flaveria pringlei*. A = rate of CO_2 assimilation; ϕ_{II} = quantum yield of PS II in light ($F/F_{m'}$); J_F = electron-transport rate calculated from ϕ_{II} and irradiance; J_c = electron-transport rate calculated from gas-exchange parameters (after Krall & Edwards 1992). Copyright Physiologia Plantarum.

dissipation process also requires a special **photosystem II subunit S** (**PsbS**) (Li et al. 2002). Mutants of *Arabidopsis thaliana* (thale cress) that are unable to convert violaxanthin to zeaxanthin in excessive light exhibit greatly reduced nonphotochemical quenching, and are more sensitive to photoinhibition than wild-type plants (Niyogi et al. 1998). Similarly, PsbS-deficient mutants have a reduced fitness at intermittent, moderate levels of excess light (Külheim et al. 2002).

Zeaxanthin triggers a kind of "lightning rod" mechanism. It is involved in the induction of conformational changes in the light-harvesting antennae of PS II which facilitates the dissipation of excess excitations (Fig. 17; Pascal et al. 2005). This energy dissipation can be measured by chlorophyll fluorescence (Box 2A.4) and is termed high-energy-dependent or pH-dependent fluorescence quenching. In the absence of a properly functioning **xanthophyll cycle**, excess energy could, among others, be passed on to O_2. This leads to photooxidative damage when scavenging mechanisms cannot deal with the resulting **reactive oxygen species** (ROS). For example, **herbicides** that inhibit the synthesis of carotenoids cause the production of vast amounts of ROS that cause chlorophyll to bleach and thus kill the plant (Wakabayashi & Böger 2002). In the absence of any inhibitors, ROS inhibit the repair of PS II, in particular the synthesis of the **D1 protein** of PS II, by their effect on mRNA translation. It is a normal phenomenon when plants are exposed to full sunlight even in the absence of other stress factors (Nishiyama et al. 2006).

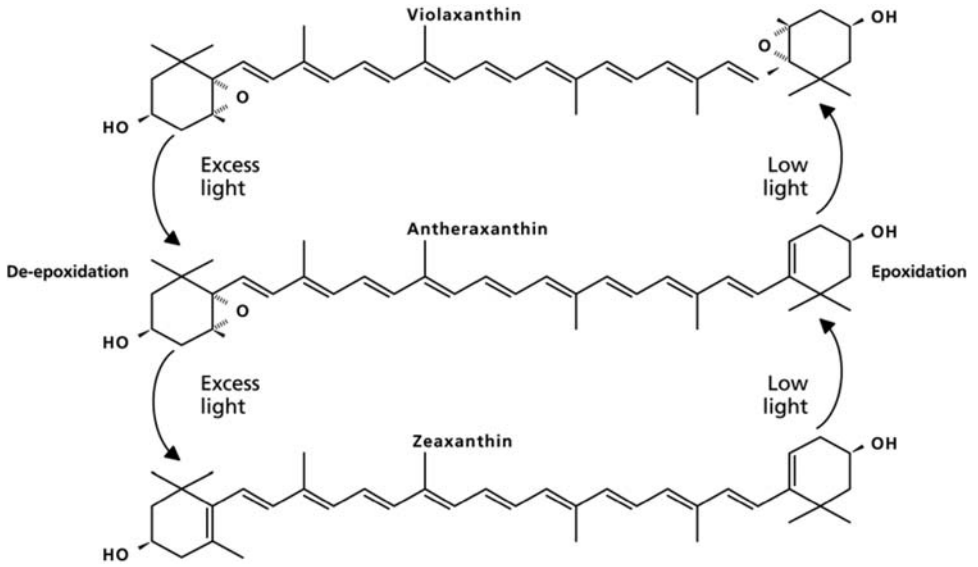

FIGURE 16. Scheme of the xanthophyll cycle and its regulation by excess or limiting light. Upon exposure to excess light, a rapid stepwise removal (de-epoxidation) of two oxygen functions (the epoxy groups) in violaxanthin takes place; the pH optimum of this reaction, which is catalyzed a de-epoxidase, is acidic. This de-epoxidation results in a lengthening of the conjugated system of double bonds from 9 in violaxanthin 10 and 11 in antheraxanthin and zeaxanthin, respectively. The de-epoxidation step occurs in minutes. Under low-light conditions, the opposite process, epoxidation, takes place. It may take minutes, hours, or days, depending on environmental conditions (Demmig-Adams & Adams 1996, 2006).

However, when shade plants are exposed to full sunlight, or when other stresses combine with high irradiance (e.g., desiccation, high or low temperature) then more excessive damage can occur, involving destruction of membranes and oxidation of chlorophyll (bleaching), causing a longer-lasting reduction in photosynthesis.

In sun-exposed sites, diurnal changes in irradiance are closely tracked by the level of **antheraxanthin** and **zeaxanthin**. In shade conditions, sunflecks lead to the rapid appearance of antheraxanthin and zeaxanthin and reappearance of **violaxanthin** between subsequent sunflecks. This regulation mechanism ensures that no competing dissipation of energy occurs when light is limiting for photosynthesis, whereas damage is prevented when light is absorbed in excess. Typically, sun-grown plants not only contain a larger fraction of the carotenoids as zeaxanthin in high light, but their total pool of **carotenoids** is larger also (Fig. 18; Adams et al. 1999). The pool of reduced **ascorbate**, which plays a role in the xanthophyll cycle (Fig. 17), is also several-fold greater in plants acclimated to high light (Logan et al. 1996).

3.3.2 Chloroplast Movement in Response to Changes in Irradiance

The leaf's absorptance is affected by the concentration of chlorophyll in the leaf and the path length of light in the leaf, as well as by the location of the chloroplasts. **Light-induced movements** of chloroplasts are affected only by wavelengths below 500 nm. High intensities in this wavelength region cause the chloroplasts to line up along the vertical walls, parallel to the light direction, rather than along the lower cell walls, perpendicular to the direction of the radiation, as in control leaves. Chloroplasts are anchored with **actin networks** and their final positioning relies on connections to actin (Staiger et al. 1997). Chloroplast movements are pronounced in aquatic plants, such as *Vallisneria gigantea* (giant vallis) and shade-tolerant understory species, such as *Oxalis oregana* (redwood sorrel) where they may decrease the leaf's absorptance by as much as 20%, thereby increasing both transmittance and reflectance. Other species [e.g., the shade-avoiding *Helianthus annuus* (sunflower)] show no blue light-induced chloroplast movement or change

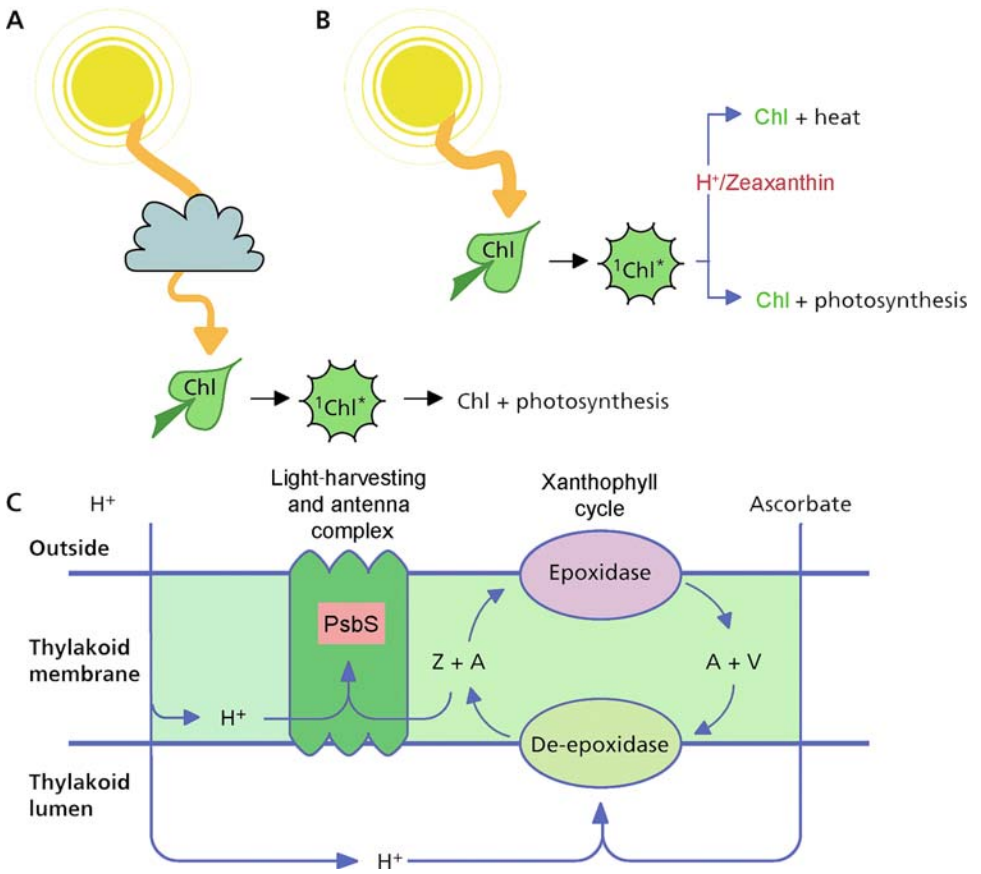

FIGURE 17. *Top*: Depiction of the conditions where (A) all or (B) only part of the sunlight absorbed by chlorophyll within a leaf is used for photosynthesis. Safe dissipation of excess energy requires the presence of zeaxanthin as well as a low pH in the photosynthetic membranes. The same energized form of chlorophyll is used either for photosynthesis or loses its energy as heat. *Bottom*: Depiction of the regulation of the biochemistry of the xanthophyll cycle as well as the induction of xanthophyll-cycle-dependent energy dissipation by pH. De-epoxidation to antheraxanthin (A) and zeaxanthin (Z) from violaxanthin (V), catalyzed by a de-epoxidase with an acidic pH optimum, takes place at a low pH in the lumen of the thylakoid as well in the presence of reduced ascorbate. Protonation of a residue of a photosystem II subunit S (PsbS) is essential for the functioning of the cycle. In addition, a low pH of certain domains within the membrane, together with the presence of zeaxanthin or antheraxanthin, is required to induce the actual energy dissipation. This dissipation takes place within the light-collecting antenna complex of PS II (modified after Demmig-Adams & Adams 1996).

in absorptance. Chloroplast movements in shade plants exposed to high light avoid photoinhibition (Brugnoli & Björkman 1992).

3.4 Responses to Variable Irradiance

So far we have discussed mostly steady-state responses to light, meaning that a particular environmental condition is maintained until a constant response is achieved. Conditions in the real world, however, are typically not constant, irradiance being the most rapidly varying environmental factor. Since photosynthesis primarily depends on irradiance, the dynamic response to variation in irradiance deserves particular attention.

The irradiance level above a leaf canopy changes with time of day and with cloud cover, often by more than an order of magnitude within seconds. In a leaf canopy, irradiance, particularly direct radiation, changes even more. In a forest, direct sunlight may penetrate through holes in

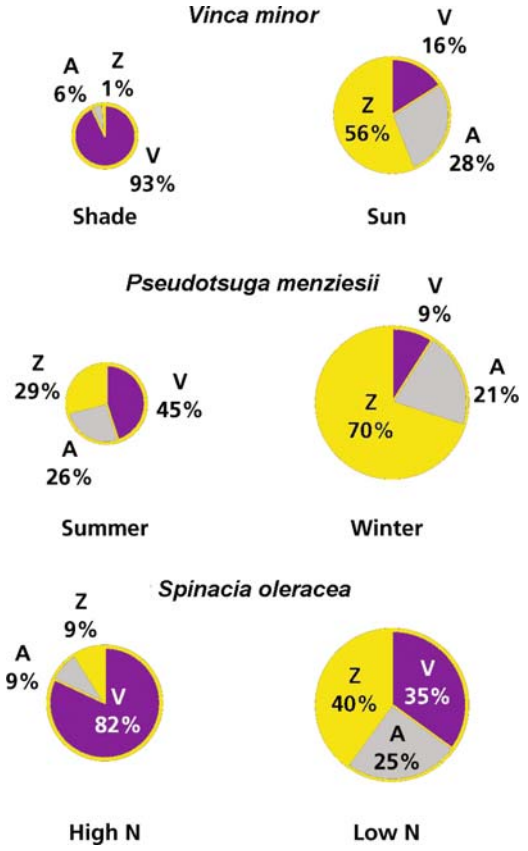

FIGURE 18. Differences in zeaxanthin (Z), violaxanthin (V) and antheraxanthin (A) contents of leaves upon acclimation to the light level [*Vinca minor* (periwinkle)], season [*Pseudotsuga menziesii* (Douglas fir)] and N supply [*Spinacia oleracea* (spinach)]. The total areas reflect the concentration of the three carotenoids relative to that of chlorophyll (after Demmig-Adams & Adams 1996).

the overlying leaf canopy, casting **sunflecks** on the forest floor. These move with wind action and position of the sun, thus exposing both leaves in the canopy and shade plants in the understory to short periods of bright light. Sunflecks typically account for 40–60% of total irradiance in understory canopies of dense tropical and temperate forests and are quite variable in duration and intensity (Chazdon & Pearcy 1991).

3.4.1 Photosynthetic Induction

When a leaf that has been in darkness or low light for hours is transferred to a saturating level of irradiance, the photosynthetic rate increases only gradually over a period of up to one hour to a new steady-state rate (Fig. 19), with stomatal conductance increasing more or less in parallel. We cannot conclude, however, that limitation of photosynthesis during induction is invariably due to stomatal opening (Allen & Pearcy 2000). If stomatal conductance limited photosynthesis, the intercellular CO_2 concentration (C_i) should drop immediately upon transfer to high irradiance, but, in fact, there is a more gradual decline over the first minutes, and then a slow increase until full induction (Fig. 19). Stomatal patchiness might play a role (Sect. 5.1), but there are also additional limitations at the chloroplast level. The demand for CO_2 increases faster than the supply in the first minutes as evident from the initial decline in C_i. Its subsequent rise indicates that the supply increases faster than the demand, as shown in Fig. 20, where $A_n$is plotted as a function of C_i during photosynthetic induction. During the first one or two minutes there is a fast increase in demand for CO_2 (fast induction component) which is due to fast light induction of some Calvin-cycle enzymes and build-up of metabolite pools (Sassenrath-Cole et al. 1994). The slower phase of increase in demand until approximately 10 minutes is dominated by the light-activation of Rubisco. After that, C_i increases and A_n increases along the A_n–C_i curve, indicating that a decrease in stomatal limitation dominates further rise in photosynthetic rate (Fig. 20).

Loss of photosynthetic induction occurs in low light, but at a lower rate than induction in high light, particularly in forest understory species. Hence, in a sequence of sunflecks, photosynthetic induction increases from one sunfleck to the next, until a high induction state is reached, when sunflecks can be used efficiently (Fig. 19).

3.4.2 Light Activation of Rubisco

Rubisco, as well as other enzymes of the Calvin cycle, are **activated by light,** before they have a high catalytic activity (Fig. 21; Portis 2003). The increase in Rubisco activity, due to its activation by light, closely matches the increased photosynthetic rate at a high irradiance apart from possible stomatal limitations. Two mechanisms are involved in the activation of Rubisco. Firstly, CO_2 binds covalently to a lysine residue at the enzyme's active site (**carbamylation**), followed by binding of Mg^{2+} and RuBP. In this activated state, Rubisco is able to catalyze the reaction with CO_2 or O_2. Rubisco is **deactivated** when (1) RuBP binds to a decarbamylated

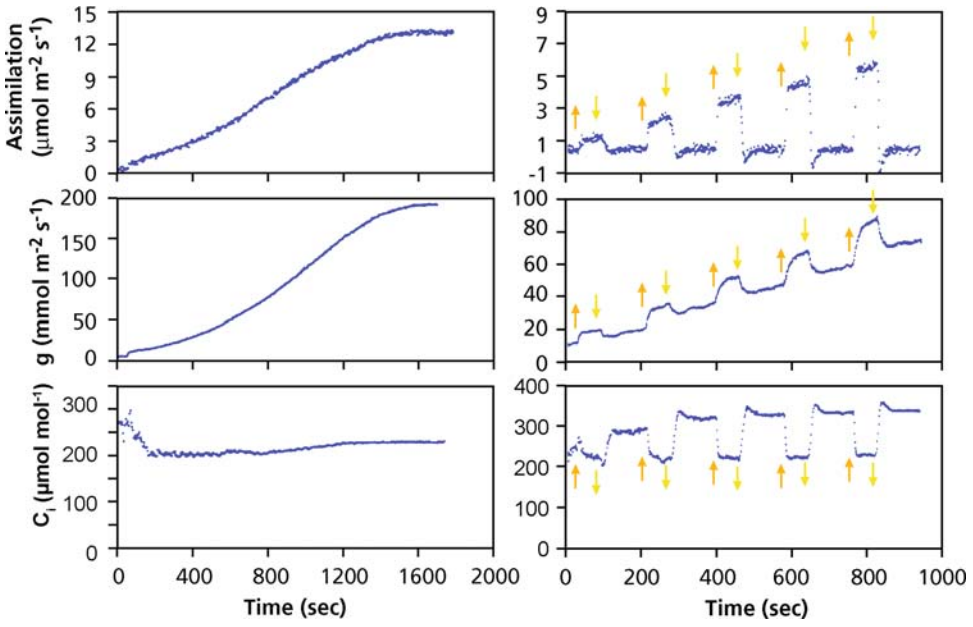

FIGURE 19. Photosynthetic induction in *Toona australis*, which is an understory species from the tropical rainforest in Australia. (*Left panels*) Time course of the rate of CO_2 assimilation (A_n) (*top*), stomatal conductance (g_s) (*middle*), and the intercellular CO_2 concentration (C_i) (*bottom*) of plants that were first exposed to a low irradiance level and then transferred to high saturating irradiance. (*Right panels*) Leaves are exposed to five "sunflecks", indicated by arrows, with a low background level of irradiance in between (Chazdon & Pearcy 1986).

Rubisco, (2) 2-**carboxy-D-arabinitol 1-phosphate** (CA1P), an analogue of the extremely short-lived intermediate of the RuBP carboxylation reaction, binds to the carbamylated Rubisco, and (3) a product produced by the catalytic "misfire" of Rubisco ("misprotonation"), xylulose-1,5-bisphosphate (Salvucci & Crafts-Brandner 2004a), binds to a carbamylated Rubisco. Secondly, **Rubisco activase** plays a role in catalyzing the dissociation of inhibitors from the active site of Rubisco; its activity increases with increasing rate of electron transport (Fig. 21). The activity of Rubisco activase is regulated by ADP/ATP and redox changes mediated by thioredoxin in some species.

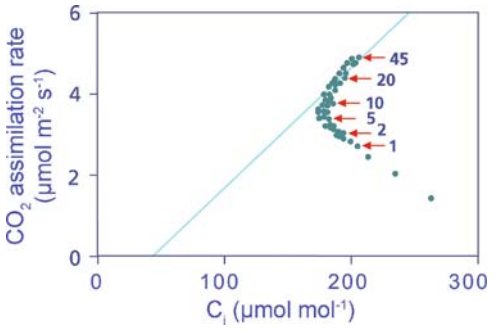

FIGURE 20. Photosynthetic response of *Alocasia macrorrhiza* (giant taro) to intercellular CO_2 concentration (C_i) during the induction phase after a transition from an irradiance level of 10 to 500 µmol m^{-2} s^{-1} (light saturation). The solid line represents the A_n–C_i relationship of a fully induced leaf calculated as Rubisco-limited rates. Numbers indicate minutes after transition (after Kirschbaum & Pearcy 1988).

Light activation of Rubisco, a natural process that occurs at the beginning of the light period in all plants, is an important aspect of the regulation (fine-tuning) of photosynthesis. In the absence of such light activation, the three phases of the Calvin cycle (carboxylation, reduction, and regeneration of RuBP) may compete for substrates, leading to oscillation of the rate of CO_2 fixation upon the beginning of the light period. It may also protect active sites of Rubisco during inactivity in darkness (Portis 2003), but the regulation mechanism occurs at the expense of low rates of CO_2 assimilation during periods of low induction.

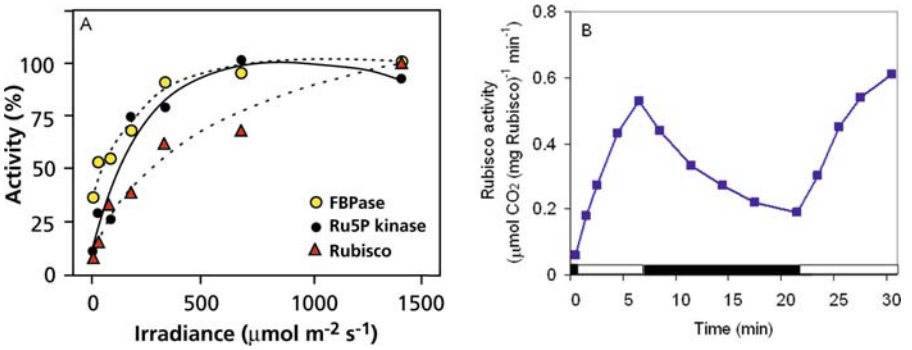

FIGURE 21. (A) Light activation of Rubisco and two other Calvin cycle enzymes, Ribulose-5-phosphate kinase and fructose-bisphosphatase (Salvucci 1989). Copyright Physiologia Plantarum. (B) Time course of Rubisco activation level during sequential light open symbols) and dark (filled symbols) periods (after Portis et al. 1986). Copyright American Society of Plant Biologists.

3.4.3 Post-illumination CO_2 Assimilation and Sunfleck-Utilization Efficiency

The rate of O_2 evolution, the product of the first step of electron transport, stops immediately after a sunfleck, whereas CO_2 assimilation continues for a brief period thereafter. This is called **post-illumination CO_2 fixation** (Fig. 22). CO_2 assimilation in the Calvin cycle requires both NADPH and ATP, which are generated during the light reactions. Particularly in short sunflecks, this post-illumination CO_2 fixation is important relative to photosynthesis during the sunfleck, thus increasing total CO_2 assimilation due to the sunfleck above what would be expected from steady-state measurements (Fig. 23).

CO_2 assimilation due to a sunfleck also depends on **induction state**. Leaves become increasingly induced with longer sunflecks of up to a few minutes (Fig. 25). At low induction states, sunfleck-utilization efficiency decreases below what would be expected from steady-state rates (Fig. 23). Forest understory plants tend to utilize sunflecks more efficiently than plants from short vegetation, particularly flecks of a few seconds to a few minutes. Accumulation of larger Calvin-cycle metabolite pools and longer maintenance of photosynthetic induction are possible reasons. Efficient utilization of sunflecks is crucial for understory plants, since most radiation comes in the form of relatively long-lasting sunflecks, and half the plant's assimilation may depend on these short periods of high irradiance.

3.4.4 Metabolite Pools in Sun and Shade Leaves

As explained in Sect. 2.1.3, the photophosphorylation of ADP depends on the proton gradient across

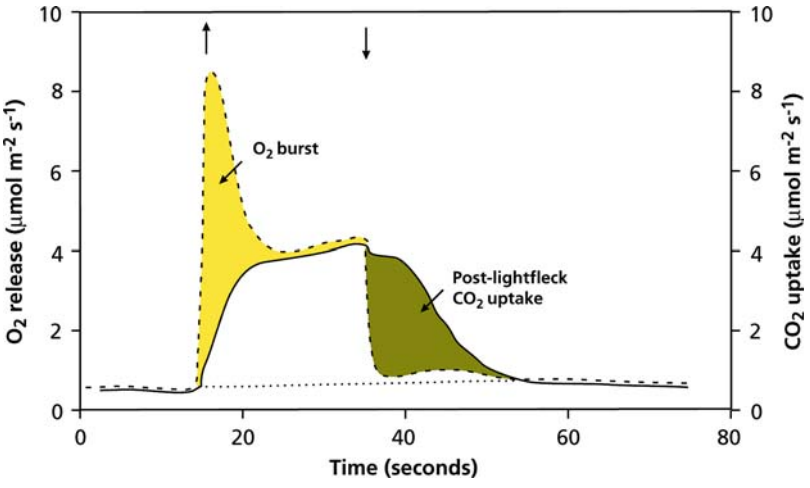

FIGURE 22. CO_2 uptake and O_2 release in response to a "sunfleck". Arrows indicate the beginning and end of the "sunfleck" (Pearcy 1990). With kind permission from the Annual Review of Plant Physiology Plant Molecular Biology, Vol. 41, copyright 1990, by Annual Reviews Inc.

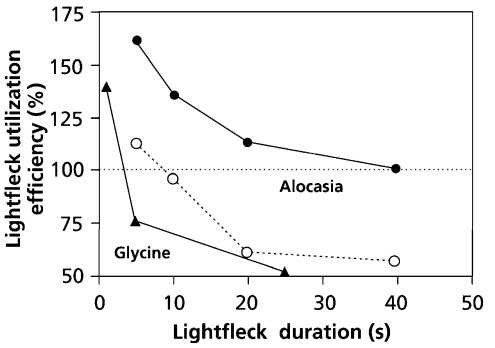

FIGURE 23. Efficiency of "sunfleck" utilization as dependent on duration of the "sunfleck" and induction state in two species. *Alocasia macrorrhiza* (giant taro, an understory species) measured at high (closed symbols) and low induction state (open symbols). Induction state of *Glycine max* (soybean, a sun species) is approximately 50% of maximum. Efficiencies are calculated as total CO_2 assimilation due to the sunfleck relative to that calculated from the steady-state rates at the high irradiance (sunfleck) and the low (background) irradiance (Pearcy 1988, Pons & Pearcy 1992).

the thylakoid membrane. This gradient is still present immediately following a sunfleck, and ATP can therefore still be generated for a brief period. The formation of NADPH, however, directly depends on the flux of electrons from water, via the photosystems and the photosynthetic electron-transport chain, and therefore comes to an immediate halt after the sunfleck. Moreover, the concentration of NADPH in the cell is too low to sustain Calvin-cycle activity. Storage of the reducing equivalents takes place in **triose-phosphates** (Table 3), which are intermediates of the Calvin cycle.

To allow the storage of reducing power in intermediates of the Calvin cycle, the phosphorylating step leading to the substrate for the reduction reaction must proceed. This can be realized by regulating the activity of two enzymes of the Calvin cycle which both utilize ATP: phosphoglycerate kinase and ribulose-phosphate kinase (Fig. 4). When competing for ATP in vitro, the second kinase tends to dominate, leaving little ATP for phosphoglycerate kinase. If this were to happen in vivo as well, no storage of reducing equivalents in triose-phosphate would be possible, and CO_2 assimilation would not continue beyond the sunfleck. The concentration of triose-phosphate at the end of a

TABLE 3. The potential contribution of triose-phosphates and ribulose-1,5-bisphosphate to the post-illumination CO_2 assimilation of *Alocasia macrorrhiza* (giant taro) and *Phaseolus vulgaris* (common bean), grown either in full sun or in the shade. *

	Alocasia macrorrhiza		*Phaseolus vulgaris*	
	Shade	Sun	Shade	Sun
RuBP (μmol m^{-2})	2.0	14.5	2.9	5.3
Triose phosphates (μmol m^{-2})	16.3	18.0	19.8	10.5
Total potential CO_2 fixation (μmol m^{-2})	12	25	15	12
Potential efficiency (%)	190	204	154	120
Triose-P/RuBP	4.9	0.7	4.1	1.2
Post-illumination ATP required (μmol g^{-1} Chl)	13	22	63	29

Source: Sharkey et al. (1986a).

*The values for the intermediates give the difference in their pool size at the end of the lightfleck and 1 min later. The total potential CO_2 assimilation is RuP_2 + 3/5 triose-P pool size. The potential efficiency was calculated on the assumption that the rate of photosynthesis during the 5 s lightfleck was equal to the steady-state value measured after 20 minute in high light.

sunfleck is relatively greater in shade leaves than in sun leaves, whereas the opposite is found for ribulose-1,5-bisphosphate (Table 3). This indicates that the activity of the steps in the Calvin cycle leading to ribulose-phosphate is suppressed. Thus competition for ATP between the kinase is prevented, and the reducing power from NADPH can be transferred to 1,3-bisphosphoglycerate, leading to the formation of triose-phosphate. Storage of reducing power occurs in species that are adapted to shade, e.g., *Alocasia macrorrhiza* (giant taro), as well as in leaves acclimated to shade, e.g., shade leaves of common bean (*Phaseolus vulgaris*).

3.4.5 Net Effect of Sunflecks on Carbon Gain and Growth

Although most understory plants can maintain a positive carbon balance with diffuse light in the absence of sunflecks, daily carbon assimilation and growth rate in moist forests correlates closely with irradiance received in sunflecks (Fig. 24). Moreover, sunflecks account for an increasing proportion of total carbon gain (9–46%) as their size and frequency increase. In dry forests, where understory plants experience both light and water limitation, sunflecks may reduce daily carbon gain on cloud-free days (Allen & Pearcy 2000). Thus, the net impact of sunflecks on carbon gain depends on both cumulative irradiance and other potentially limiting factors.

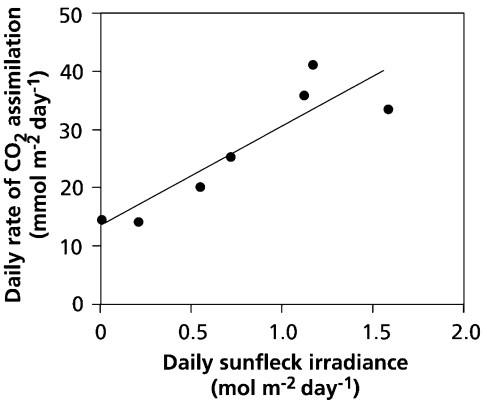

FIGURE 24. (A) Total carbon gain of *Adenocaulon bicolor* as a function of daily photon flux contributed by sunflecks in the understorey of a temperate redwood forest. (B) Relative growth rate of *Euphorbia forbesii* (*filled circles*) and *Claoxylon sandwicense* (*open circles*) as a function of average duration of potential sunflecks (estimated from hemispherical photographs) in the understorey of a tropical forest (after Chazdon & Pearcy 1991).

4. Partitioning of the Products of Photosynthesis and Regulation by "Feedback"

4.1 Partitioning Within the Cell

Most of the products of photosynthesis are exported out of the chloroplast to the cytosol as **triose-phosphate** in exchange for P_i. Triose-phosphate is the substrate for the synthesis of sucrose in the cytosol (Fig. 25) and for the formation of cellular components in the **source** leaf. Sucrose is largely exported to other parts (**sinks**) of the plant, via the phloem.

Partitioning of the products of the Calvin cycle within the cell is controlled by the concentration of P_i in the cytosol. If this concentration is high, rapid exchange for triose-phosphate allows export of most of the products of the Calvin cycle. If the concentration of P_i drops, the exchange rate will decline, and the concentration of triose-phosphate in the chloroplast increases. Inside the chloroplasts, the triose-phosphates are used for the synthesis of **starch**, releasing P_i within the chloroplast. So, the partitioning of the products of photosynthesis between export to the cytosol and storage compounds in the chloroplasts is largely determined by the availability of P_i in the cytosol. This regulation can be demonstrated by experiments using leaf discs in which the concentration of cytosolic P_i is manipulated (Table 4).

In intact plants the rate of photosynthesis may also be reduced when the plant's demand for carbohydrate (reduced sink strength) is decreased, for example by the removal of part of the fruits or "girdling" of the petiole (Table 4). [Girdling involves damaging the phloem tissue of the stem, either by a temperature treatment or mechanically, leaving the xylem intact.] Restricting the export of assimilates by reduced sink capacity or more directly by blocking the phloem sequesters the cytosolic P_i in phosphorylated sugars, leading to **feedback inhibition** of photosynthesis. When the level of P_i in the cytosol is increased, by floating the leaf discs on a phosphate buffer, the rate of photosynthesis may also drop [e.g., in *Cucumis sativus* (cucumber) Table 4], but there is no accumulation of starch. This is likely due to the very rapid export of triose-phosphate from the chloroplasts, in exchange for P_i, depleting the Calvin cycle of intermediates.

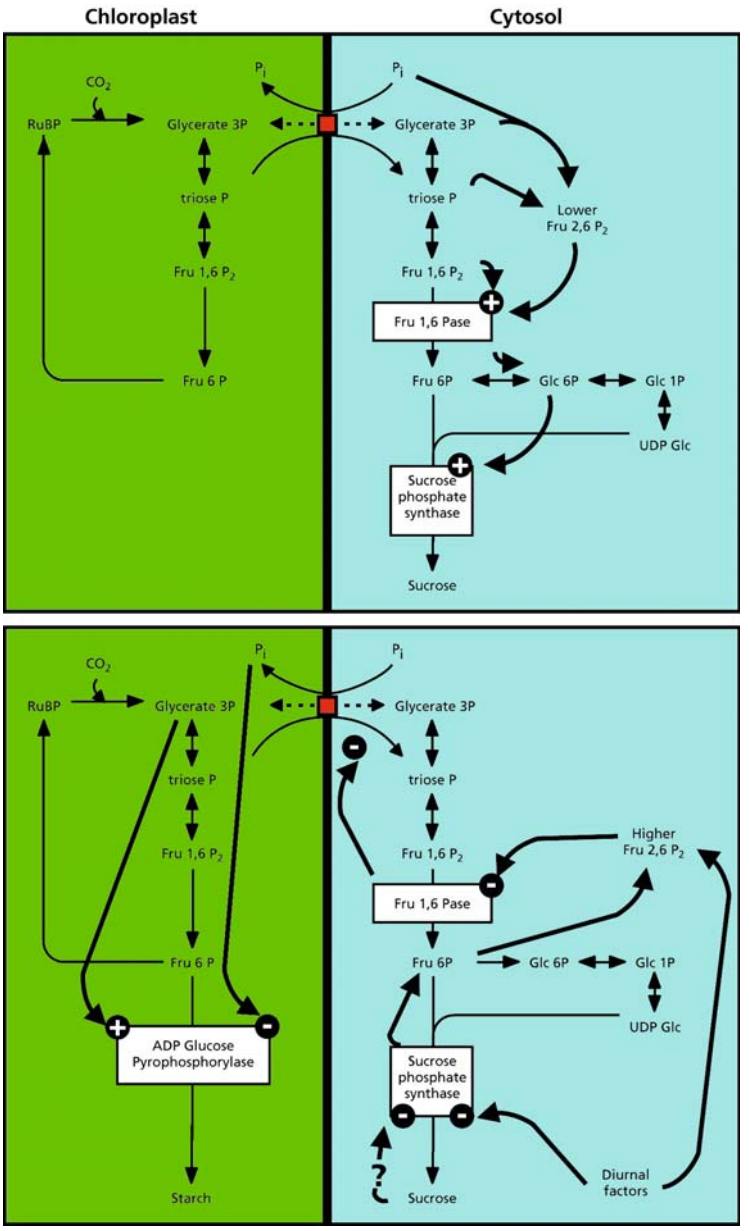

FIGURE 25. The formation of triose-phosphate in the Calvin cycle. Triose-P is exported to the cytosol, in exchange for inorganic phosphate (P_i), or used as a substrate for the synthesis of starch in the chloroplast.

4.2 Short-Term Regulation of Photosynthetic Rate by Feedback

Under conditions of "feedback inhibition" (Sect. 4.1), phosphorylated intermediates of the pathway leading to sucrose accumulate, inexorably decreasing the cytosolic P_i concentration. In the absence of sufficient P_i in the chloroplast, the formation of ATP is reduced and the activity of the Calvin cycle declines. That is, less intermediates are available and less RuBP is regenerated, so that the carboxylating activity of Rubisco and hence the rate of photosynthesis drops.

How important is feedback inhibition in plants whose sink has not been manipulated? To answer this question, we can determine the **O_2 sensitivity** of photosynthesis. Normally, the rate of net CO_2 assimilation increases when the O_2 concentration is lowered from a normal 21% to 1 or 2%, due to the suppression of the oxygenation reaction. When the

TABLE 4. Rates of CO_2 assimilation (μmol $m^{-2}s^{-1}$) and the accumulation of ^{14}C in soluble sugars ("ethanol-soluble") and starch ("$HClO_4$-soluble") (^{14}C as % of total ^{14}C recovered) in leaf discs of *Gossypium hirsutum* (cotton) and *Cucumis sativus* (cucumber) floating on a Tris-maleate buffer, a phosphate buffer, or a mannose solution.*

	Control			Girdled		
	CO_2 Fixation	Ethanol-Soluble	$HClO_4$-Soluble	CO_2 Fixation	Ethanol-Soluble	$HClO_4$ Soluble
Cotton						
Tris-maleate	18	83	17	12	76	24
Phosphate	18	87	13	10	83	17
Mannose	12	54	46	10	76	24
Cucumber						
Tris-maleate	13	76	24	6	40	60
Phosphate	9	82	18	5	76	24
Mannose	9	55	45	4	40	60

Source: Plaut et al. (1987).

* Leaves were taken from control plants ("control") or from plants whose petioles had been treated in such a way as to restrict phloem transport ("girdled"). The concentration of cytosolic P_i can be decreased by incubating leaf discs in a solution containing mannose. Mannose is readily taken up and enzymatically converted into mannose phosphate, thus sequestering some of the P_i originally present in the cytosol. Under these conditions starch accumulates in the chloroplasts. At extremely low cytosolic P_i concentrations, the rate of photosynthesis is also reduced. When leaf discs are taken from plants with reduced sink capacity, the addition of mannose has very little effect, because the cytosolic P_i concentration is already low before mannose addition.

activity of Rubisco is restricted by the regeneration of RuBP, lowering the O_2 concentration enhances the net rate of CO_2 assimilation to a lesser extent. Feedback inhibition is found at a high irradiance and also at a low temperature, which restricts phloem loading. Under these conditions the capacity to assimilate CO_2 exceeds the capacity to export and further metabolize the products of photosynthesis. Consequently, phosphorylated intermediates of the pathway from triose-phosphate to sucrose accumulate which sequesters phosphate. As a result, P_i starts to limit photosynthesis, and the rate of photosynthesis declines as soon as the capacity to channel triose-phosphate to starch is saturated. Figure 26, showing the response of the net rate of CO_2 assimilation to $N_2 + CO_2$ at four levels of irradiance and a leaf temperature of 15°C, illustrates this point.

The assessment of feedback inhibition of photosynthesis using the O_2 sensitivity of this process is complicated by the fact that the relative activities of the carboxylating and oxygenating reactions of Rubisco also depend on temperature (Sect. 7.1). To resolve this problem, a mathematical model of photosynthesis has been used (Box 2A.1). This model incorporates biochemical information on the photosynthetic reactions and simulates the effect of

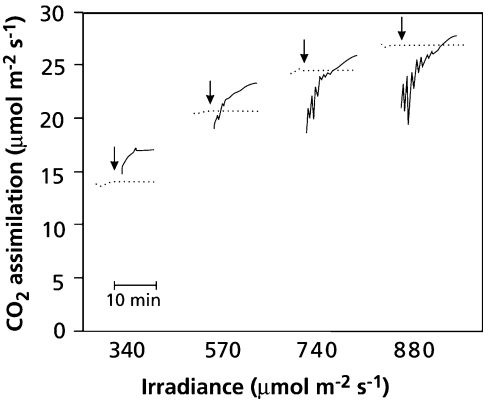

FIGURE 26. The response of the CO_2 assimilation rate to a change in O_2 concentration at four levels of irradiance. The broken lines give the steady-state rate of CO_2 assimilation. The gas phase changes from air to $N_2 + CO_2$ at the time indicated by the arrows. The CO_2 concentration in the atmosphere surrounding the leaf is maintained at 550 μmol mol^{-1} and the leaf temperature at 15°C. At a relatively low irradiance (340 μmol m^{-2} s^{-1}) the rate of CO_2 assimilation is rapidly enhanced when the O_2 concentration is decreased, whereas at high irradiance (880 μmol m^{-2} s^{-1}), CO_2 assimilation first decreases and is only marginally enhanced after several minutes, indicative of feedback inhibition (after Sharkey et al. 1986b). Copyright American Society of Plant Biologists.

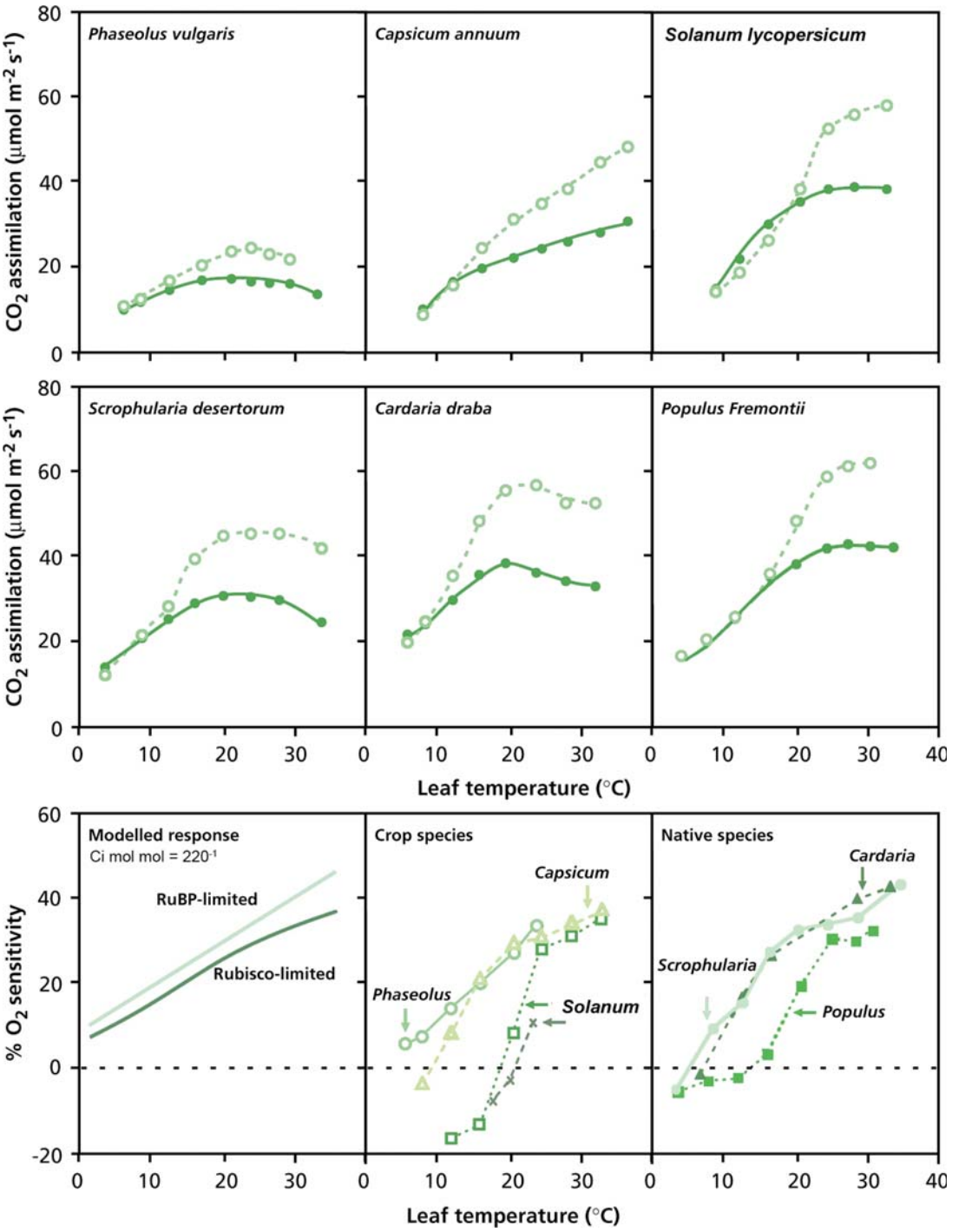

FIGURE 27. The effect of temperature on the net rate of CO_2 assimilation at 18% (v/v; filled symbols) and 3% (v/v; open symbols) O_2 (*top*), and the O_2 sensitivity of photosynthesis (*bottom*) for a number of species. All plants were grown outdoors (after Sage & Sharkey 1987). Copyright American Society of Plant Biologists.

lowering the O_2 concentration at a range of temperatures. Comparison of the observed effect of the decrease in O_2 concentration (Fig. 27, lower middle and right panels) with the experimental observations (Fig. 27, lower left panel), allows conclusions on the extent of feedback inhibition in plants under normal conditions. The lower right panels show distinct feedback inhibition for *Solanum lycopersicum* (tomato) and *Populus fremontii* (Fremont cottonwood) at low temperatures, and less feedback inhibition for *Phaseolus vulgaris* (common bean), *Capsicum annuum* (pepper), *Scrophularia desertorum* (figwort), and *Cardaria draba* (hoary cress).

Comparison of the modeled results in the lower left panel with the experimental results in the other lower panels in Fig. 27 shows that photosynthesis of plants growing under natural conditions can be restricted by feedback, especially at relatively low temperatures. Feedback inhibition is predominantly associated with species accumulating starch in their chloroplasts, rather than sucrose and hexoses in the cytosol and vacuoles. Since genetically transformed plants of the same species, lacking the ability to store starch, behave like the starch-accumulating wild type, the reason for this difference remains obscure (Goldschmidt & Huber 1992). Perhaps it reflects the mode of phloem loading (i.e., either symplastic or apoplastic; Chapter 2C on long-distance transport).

4.3 Sugar-Induced Repression of Genes Encoding Calvin-Cycle Enzymes

The feedback mechanism outlined in Sect. 4.2 operates in the short term, adjusting the activity of the existing photosynthetic apparatus to the capacity of export and sink activity, but mechanisms at the level of **gene transcription** play a more important role in the long term. They modify photosynthetic capacity and can override regulation by light, tissue type, and developmental stage (Smeekens & Rook 1998). Leaves of *Triticum aestivum* (wheat) fed with 1% glucose have a lower photosynthetic capacity as well as lower levels of mRNA coding for several Calvin-cycle enzymes, including the small subunit of Rubisco (Jones et al. 1996). Regulation of photosynthetic gene expression by **carbohydrates** plays an important role in the control of the activity of the "source" (leaves) by the demand in the "sink" (e.g., fruits) (Paul & Foyer 2001). Sensing of carbohydrate levels is mediated by a specific **hexokinase**, which is an enzyme that phosphorylates hexose while hydrolyzing ATP (Smeekens 2000). This regulation at the level of gene transcription plays a role in the acclimation of the photosynthetic apparatus to elevated concentrations of atmospheric CO_2 (Sect. 12), and, more generally in adjusting photosynthetic capacity to environmental and developmental needs.

4.4 Ecological Impacts Mediated by Source-Sink Interactions

Many ecological processes affect photosynthesis through their impact on plant demand for carbohydrate (Sect. 4.2). In general, processes that increase carbohydrate demand increase the rate of photosynthesis, whereas factors that reduce demand reduce photosynthesis.

Although defoliation generally reduces carbon assimilation by the defoliated plant by reducing the biomass of photosynthetic tissue, it may cause a compensatory increase in photosynthetic rate of remaining leaves through several mechanisms. The increased sink demand for carbohydrate generally leads to an increase in A_{max} in the remaining leaves. Defoliation also reduces environmental constraints on photosynthesis by increasing light penetration through the canopy, and by increasing the biomass of roots available to support each remaining leaf. The resulting increases in light and water availability may enhance photosynthesis under shaded and dry conditions, respectively.

Growth at elevated atmospheric [CO_2] may lead to a down-regulation of photosynthesis, involving sensing of the leaves' carbohydrate status (Sect. 12.1), and other ecological factors discussed here probably act on photosynthesis in a similar manner. Box 2A.5 provides a brief overview of gas-exchange equipment, especially portable equipment that can be used in the field for ecological surveys.

5. Responses to Availability of Water

The inevitable loss of water, when the stomata are open to allow photosynthesis, may lead to a decrease in leaf relative water content (RWC), if the water supply from roots does not match the loss from leaves. The decline in RWC may directly or indirectly affect photosynthesis. In this section we describe effects of the water supply on photosynthesis, and discuss genetic adaptation and phenotypic acclimation to water shortage.

Box 2A.5
The Measurement of Gas Exchange

The uptake and release of CO_2 in photosynthesis and respiration and the release of H_2O during transpiration of plants or leaves is measured using gas-exchange systems. Several types exist (e.g., Field et al. 1989, Long & Hällgren 1993). Here we briefly address the operation of so-called open systems and potential complications with their use, with particular attention to the now commonly used portable systems that are commercially available.

The essence of a gas-exchange system is a transparent chamber that encloses the photosynthetically active tissue. Air enters the chamber at a specified flow rate (f_m) measured and controlled by a flow-controller. The leaf changes the concentrations of CO_2 and H_2O inside the chamber. The magnitude of the difference in CO_2 and H_2O concentration between the air entering the chamber (C_e and W_e) and at the outlet (C_o and W_o) depends on its gas-exchange activity. The net photosynthetic rate (A_n) is then calculated following Von Caemmerer & Farquhar (1981).

$$A_n = f_m/L_a \{C_e - C_o(1 - W_e)/(1 - W_o)\} \quad (1)$$

A_n is expressed per unit leaf area (L_a), but another basis, e.g., dry mass can also be used. The last part of the equation refers to the correction for the volume increase and, consequently, concentration decrease caused by the simultaneously occurring transpiration (E). E can be calculated similarly by substituting W_e and W_o for C_e and C_o. When leaf temperature is also measured, stomatal conductance (g_s) can be calculated using E and assuming a saturated vapor pressure in the intercellular spaces of the leaf. From g_s and A_n, intercellular CO_2 concentration (C_i) can be calculated. The principle is explained in Sect. 2.2.2, but corrections are necessary (Von Caemmerer & Farquhar 1981). The calculations assume homogeneity of parameter values across the measured area. A powerful analysis of photosynthetic performance can be made when these four gas-exchange parameters are available, as explained in the text. A further development is the combination of gas-exchange with the measurement of chlorophyll fluorescence (Box 2A.4) that gives a measure of electron-transport rate allowing estimates of the CO_2 concentration in the chloroplast (C_c), conductance for CO_2 transport in the mesophyll (g_m), photorespiration, and engagement of alternative electron sinks (Long & Bernacchi 2003).

A typical leaf chamber contains a fan that homogenizes the air which makes C_o and W_o representative of the air around the leaf (C_a and W_a, respectively). The fan further increases the boundary layer conductance (Chapter 4A), which allows a better control of leaf temperature and reduces possible errors associated with the estimation of g_s. It further contains a sensor for leaf and/or air temperature and a light sensor is attached. Most of the recent models of portable systems are also equipped with temperature control. Concentrations of CO_2 and H_2O at the inlet and outlet of the leaf chamber are measured with an infra-red gas analyzer (IRGA). The concentration of CO_2 and H_2O can be manipulated in the more advanced models that are also equipped with a light source. The systems are completed with computerized control, data-acquisition and data-processing. This versatile equipment can be used to measure photosynthetic performance in ambient conditions and for measuring the response of gas-exchange activity to environmental factors such as humidity, CO_2, temperature and light.

The ease of gas-exchange measurement brings the danger of less critical use. Some sources of error and guidelines for their avoidance are given by Long & Bernacchi (2003); here, the most important problems are addressed. Modern systems have small chambers that clamp with gaskets on a leaf, thus limiting the measurement to a part of the leaf. This has the advantage that also small leaves can easily be measured and that the condition of homogeneity mentioned above is more easily met. However, the use of a small area has its draw-backs. In these chambers, a significant part of the leaf is covered by the gasket. The leaf area under the gasket continues to respire, and part of the CO_2 produced diffuses to the leaf chamber where it

continued

Box 2A.5 *Continued*

results in overestimation of respiration rates (Pons & Welschen 2002). In homobaric leaves, air can escape through the intercellular spaces depending on the overpressure in the chamber which complicates matters further (Jahnke & Pieruschka 2006). CO_2 and H_2O can also diffuse through the gasket, and more likely along the interface between gasket and leaf. This is particularly important when concentrations inside and outside the chamber are different, such as when measuring a CO_2 response and at high humidity in a dry environment (Flexas et al. 2007b, Rodeghiero et al. 2007). Large errors can be caused by these imperfections, particularly when using small chambers at low gas-exchange rates. Suggestions are given in the above-mentioned publications for minimizing and correcting these errors, but that is not always straightforward and sometimes not possible.

When measuring gas-exchange rates under ambient conditions in the field, glasshouse, or growth chamber, ambient light is attenuated, particularly around the edges. Ambient air is often used for such measurements. The uptake of CO_2 results in a decreased CO_2 concentration in the chamber, causing a further underestimation of A_n compared with in situ rates. The reading for E deviates also from in situ rates due to a chamber climate in terms of humidity, temperature, and turbulence that differs from outside. When using short periods of enclosure, g_s is probably not affected by the chamber climate. Corrections of A_n and E can be made from assumed or separately measured short-term humidity, temperature, light, and CO_2 effects, using measurements of environmental parameters in undisturbed conditions.

5.1 Regulation of Stomatal Opening

Stomatal opening tends to be regulated such that photosynthesis is approximately **co-limited** by CO_2 diffusion through stomata and light-driven electron transport. This is seen in Fig. 6 as the intersection between the line describing the leaf's conductance for CO_2 transport (**supply function**) and the A-C_c curve (**demand function**). A higher conductance and higher C_c would only marginally increase CO_2 assimilation, but would significantly increase transpiration, since transpiration increases linearly with g_s, as a result of the constant difference in water vapor concentration between the leaf and the air (w_i-w_a) (Sect. 2.2.2, Fig. 28; Sect. 5.4.3 of Chapter 3 on plant water relations). At lower conductance, water loss declines again linearly with g_s; however, C_c also declines, because the demand for CO_2 remains the same, and the difference with C_a increases. This increased CO_2 concentration gradient across the stomata counteracts the decrease in g_s. Hence, photosynthesis declines less than does transpiration with decreasing $C_c$and C_i. The result is an increasing **water-use efficiency** (WUE) (carbon gain per water lost) with decreasing g_s. Less of the total photosynthetic capacity is used at a low $C_c$and C_i, however, leading to a reduced **photosynthetic N-use efficiency** (PNUE) (carbon gain per unit leaf N; Sect. 6.1).

Plants tend to reduce stomatal opening under water stress so that WUE is maximized at the expense of PNUE. Under limited availability of N, stomata may open further, increasing PNUE at the

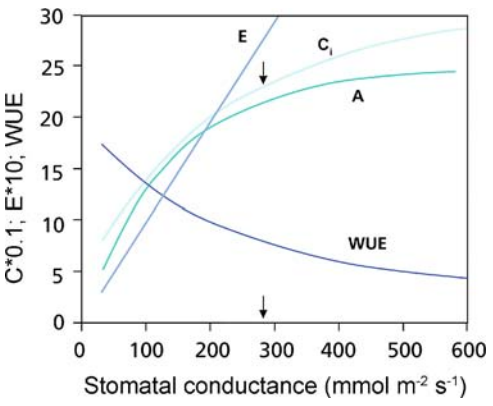

FIGURE 28. The effect of stomatal conductance (g_s) on the transpiration rate (E, mmol m^{-2} s^{-1}), rate of CO_2 assimilation (A, μmol m^{-2} s^{-1}), intercellular CO_2 concentration (C_i, μmol mol^{-1}) and photosynthetic water-use efficiency (WUE, mmol CO_2 (mol H_2O) $^{-1}$ s^{-1}) as a function of stomatal conductance. Calculations were made assuming a constant leaf temperature of 25°C and a negligible boundary layer resistance. The arrow indicates g_s at the co-limitation point of carboxylation and electron transport. For the calculations, Equations as described in Box 2A.1 and Sect. 2.2.2 have been used.

TABLE 5. Intrinsic water-use efficiency (WUE, A/g_s) and nitrogen-use efficiency of photosynthesis (PNUE, A/N_{LA}) of leaves of *Helianthus annuus* (sunflower), growing in a field in the middle of a hot, dry summer day in California.*

	N_{LA} Mmol m^{-2}	A μmol m^{-2} s^{-1}	g_s mol m^{-2} s^{-1}	C_i μmol mol^{-1}	WUE μmol mol^{-1}	PNUE μmol mol^{-1} s^{-1}
High N + W	190	37	1.2	240	31	195
Low W	180	25	0.4	200	63	139
Low N	130	27	1.0	260	27	208

Source: Fredeen et al. (1991).

* Plants were irrigated and fertilized (high N + W), only irrigated but not fertilized (low N), or only fertilized but not irrigated (low W). Since transpiration is approximately linearly related to g_s, A/g_s is used as an approximation of WUE.

expense of WUE (Table 5). This trade-off between efficient use of water or N explains why perennial species from lower-rainfall sites in eastern Australia have higher leaf N concentration, lower light-saturated photosynthetic rates at a given leaf N concentration, and lower stomatal conductance at a given rate of photosynthesis (implying lower C_i) when compared with similar species from higher-rainfall sites. By investing heavily in photosynthetic enzymes, a larger draw-down of C_i is achieved, and a given photosynthetic rate is possible at a lower stomatal conductance. The benefit of the strategy is that dry-site species reduce water loss at a given rate of photosynthesis, down to levels similar to wet-site species, despite occurring in lower-humidity environments. The cost of high leaf N is higher costs incurred by N acquisition and possibly increased herbivory risk (Wright et al. 2001).

When a plant is subjected to water stress, stomata tend to close. This response is regulated initially by **abscisic acid** (ABA), a phytohormone that is produced by roots in contact with dry soil and is transported to the leaves (Sect. 5.4.1 of Chapter 3 on plant water relations; Box 7.2). There are also effects that are not triggered by ABA arriving from the roots, mediated via ABA produced in the leaf (Holbrook et al. 2002, Christmann et al. 2005). In addition, both electrical and hydraulic signals control stomatal conductance in response to soil moisture availability (Grams et al. 2007). Stomatal conductance may also decline in response to increasing vapor pressure deficit (VPD) of the air (Sect. 5.4.3 of Chapter 3 on plant water relations). The result of these regulatory mechanisms is that, in many cases, transpiration is fairly constant over a range of VPDs, and leaf water potential is constant over a range of soil water potentials. Water loss is therefore restricted when dry air likely imposes water stress (a **feedforward response**) or when the plant experiences incipient water stress (a **feedback response**). In dry environments these two regulatory mechanisms often cause midday stomatal closure and therefore a decline in photosynthesis (Fig. 34 in Chapter 3 on plant water relations).

It was long assumed that stomata respond homogeneously over the entire leaf; however, leaves of water-stressed plants exposed to $^{14}CO_2$ show often a heterogeneous distribution of fixed ^{14}C. This shows that some stomata close completely (there is no radioactivity close to these stomata), whereas others hardly change their aperture (label is located near these stomata) (Downton et al. 1988, Terashima et al. 1988). This patchy stomatal closure can also be visualized dynamically and nondestructively with thermal and chlorophyll fluorescence imaging techniques (Mott & Buckley 2000); patches with closed stomata are identified by their high temperature and low quantum yield. **Patchiness** of stomatal opening complicates the calculation of C_i (Sect. 2.2.2), because the calculation assumes a homogeneous distribution of gas exchange parameters across the leaf lamina.

Leaves of plants that reduce stomatal conductance during the middle of the day may only close some of their stomata, while others remain open. This nonuniform reaction of stomata may occur only when plants are rapidly exposed to water stress, whereas stomata may respond in a more uniform manner when the stress is imposed more slowly (Gunasekera & Berkowitz 1992). Stomatal patchiness can also occur in dark-adjusted leaves upon exposure to bright light (Eckstein et al. 1996, Mott & Buckley 2000).

5.2 The A–C_c Curve as Affected by Water Stress

Water stress alters both the **supply** and the **demand** functions of photosynthesis (Flexas & Medrano

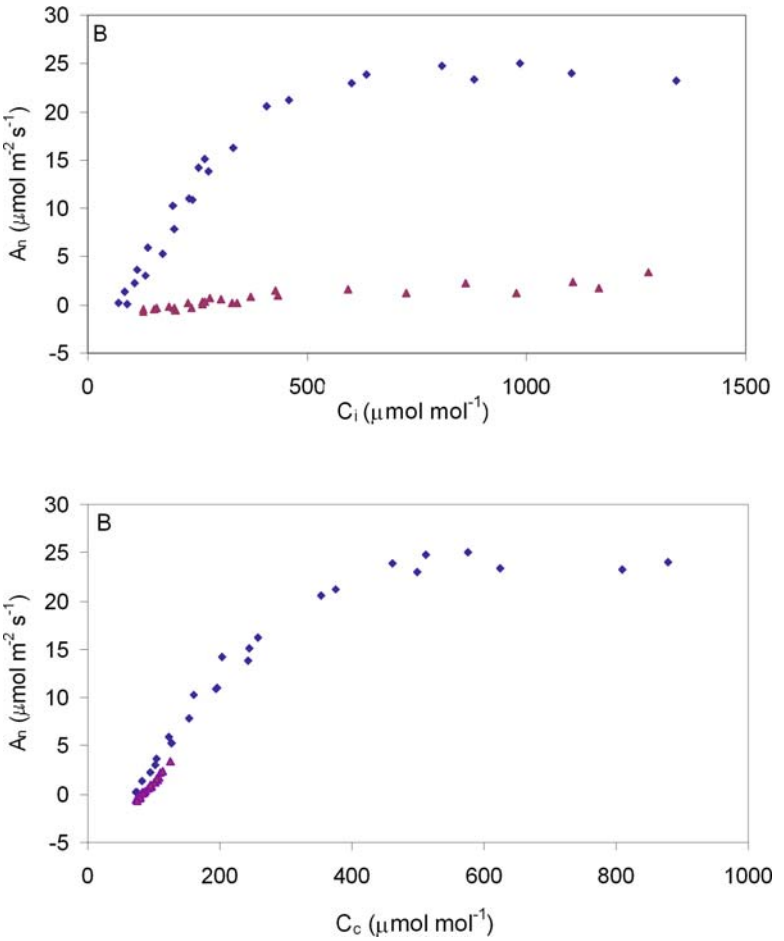

FIGURE 29. The response of net photosynthesis to (A) intercellular CO_2 concentration (C_i), and (B) CO_2 concentration in the chloroplasts (C_c), for well watered (blue symbols) and severely water-stressed plants (purple symbols) (after Flexas et al. 2006b).

2002, Grassi & Magnani 2005), but the main effect is on stomatal and mesophyll conductance, unless the stress is very severe (Fig. 29; Flexas et al. 2004). When only the conductance declines with plant desiccation, the slope of the A_n–C_c curve is unaffected (Fig. 29B). Because high irradiance and high temperature often coincide with drought, however, photoinhibition may be involved which reduces the demand function. Similarly, if growth is inhibited more strongly than photosynthesis by water stress, feedback inhibition may play an additional role. The net effect of the down-regulation of photosynthetic capacity under severe water stress is that C_c is higher than would be expected if a decrease in conductance were the only factor causing a reduction in assimilation in water-stressed plants. The reduction in photosynthetic capacity allows photosynthesis to continue operating near the break-point between the RuBP-limited and the CO_2-limited regions of the A–C_c curve. Thus drought-acclimated plants maximize the effectiveness of both light and dark reactions of photosynthesis under dry conditions at the cost of reduced photosynthetic capacity under favorable conditions. The decline in photosynthetic capacity in water-stressed plants is associated with declines in all biochemical components of the photosynthetic process.

The changes in stomatal regulation of gas exchange in species and cultivars that are genetically adapted to drought are similar to those described above for drought acclimation. Drought-adapted wheat (*Triticum aestivum*) cultivars have a lower stomatal conductance and operate at a lower C_i than do less adapted cultivars. In addition, stomatal conductance and photosynthesis in desert shrubs are lower than in less drought-adapted plants and they decline less in response to water stress, largely due to osmotic adjustment (Sect. 4.1 of Chapter 3 on plant water relations).

5.3 Carbon-Isotope Fractionation in Relation to Water-Use Efficiency

Carbon-isotope composition of plant tissues provides an integrated measure of the photosynthetic water-use efficiency (WUE = A/E) or, more precisely, the intrinsic WUE (A/g_s) during the time when the carbon in these tissues was assimilated (Fig. 30). As explained in Box 2A.2, air has a $\delta^{13}C$ of approximately –8‰, and the major steps in C_3 photosynthesis that fractionate are diffusion (4.4‰) and carboxylation (30‰, including dissolution of CO_2). The isotopic composition of a leaf will approach that of the process that most strongly limits photosynthesis. If stomata were almost closed and diffusion were the rate-limiting step, $\delta^{13}C$ of leaves would be about –12.4‰ (i.e., –8 + –4.4); if carboxylation were the only limiting factor, we would expect a $\delta^{13}C$ of –38‰ (i.e., –8 + –30). A typical range of $\delta^{13}C$ in C_3 plants is –25 to –29‰, indicating co-limitation by diffusion and carboxylation (O'Leary 1993); however, $\delta^{13}C$ values vary among plant species and environment depending on the rate of CO_2 assimilation and stomatal and mesophyll conductance. The fractionation, $\Delta^{13}C$, is defined as (Box 2A.2):

$$\begin{aligned}\Delta^{13}C &= [4.4 + 22.6(C_i/C_a)] \times 10^{-3}, \text{or :}\\ \delta^{13}C_{air} - \delta^{13}C_{leaf} &= 4.4 + 22.6(C_i/C_a),\end{aligned} \quad (8)$$

which indicates that a high C_i/C_a (due to high stomatal conductance or low rate of CO_2 assimilation) results in a large fractionation (strongly negative $\delta^{13}C$). We can now use this information to estimate an integrated WUE for the plant, but we must be aware of one significant problem: Equation (8) uses C_i, and does not take **mesophyll conductance** into account; it uses C_i, and assumes that the mesophyll conductance scales with stomatal conductance. Therefore, some of the fractionation data have to be interpreted with great care, because they may reflect differences in mesophyll conductance, rather than (only) stomatal conductance (Grassi & Magnani 2005, Warren & Adams 2006).

The water-use efficiency (WUE = A_n/E) is given by

$$\begin{aligned}\text{WUE} = A_n/E &= g_c(C_a - C_i)/g_w(w_i - w_a)\\ &= C_a(1 - C_i/C_a)/1.6(w_i - w_a)\end{aligned} \quad (9)$$

given that $g_w/g_c = 1.6$ (the molar ratio of diffusion of water vapor and CO_2 in air). Equation (9) tells us that the WUE is high, if the conductance is low in comparison with the capacity to assimilate CO_2 in the mesophyll. Under these circumstances C_i (and C_i/C_a) will be small. The right-hand part of Equation (9) then approximates [$C_a/(1.6(w_i–w_a)$] and diffusion is the predominant component determining fractionation of carbon isotopes and approaches a value of 4.4‰. On the other hand, if the stomatal conductance is large, WUE is small, C_i approximates C_a and the right-hand part of Equation (8) approaches 27‰. Fractionation of the carbon isotopes is now largely due to the biochemical fractionation by Rubisco. Values for WUE thus obtained can only be compared at the same vapor pressure difference (w_i–w_a), e.g., within one experiment or a site at the same atmospheric conditions. Therefore, the WUE derived from $\delta^{13}C$ of plant carbon is mostly referred to as **intrinsic WUE** (A_n/g_s), which is equivalent to a value normalized at a constant VPD of 1 mol mol^{-1}.

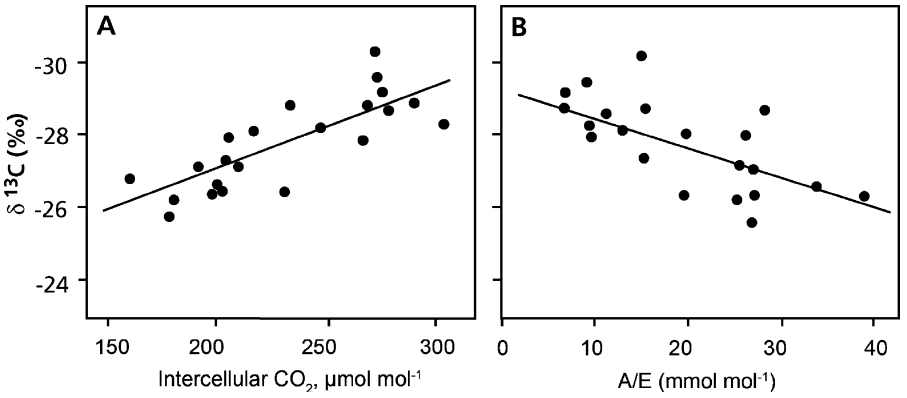

FIGURE 30. The relationship between carbon-isotope composition ($\delta^{13}C$) and (A) average intercellular CO_2 concentration, and (B) daily photosynthetic water-use efficiency, assimilation/transpiration (A/E). The data points refer to mistletoes and host plants in central Australia (Ehleringer et al. 1985). Copyright by the American Association for the Advancement of Science.

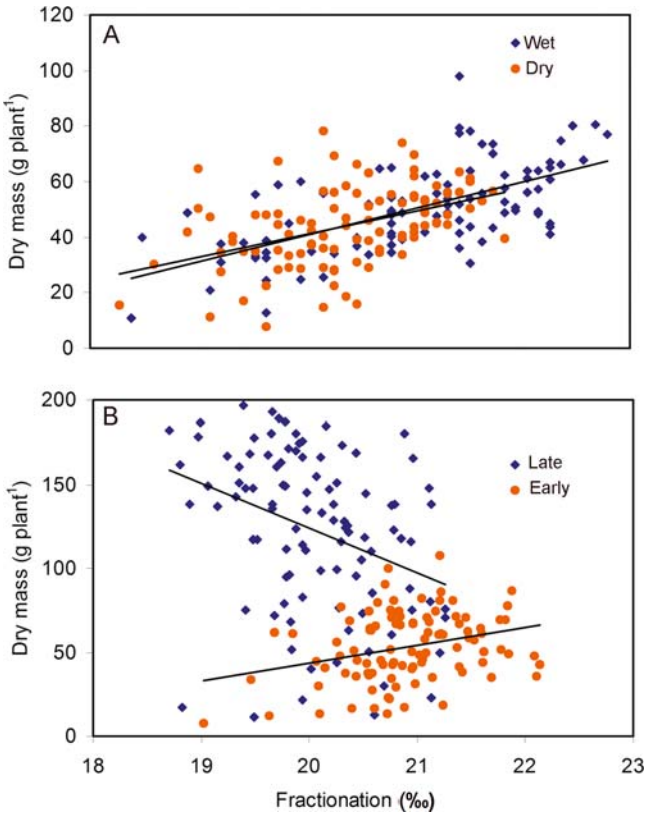

FIGURE 31. Association between dry mass and carbon-isotope fractionation in the F_2 generation of *Solanum lycopersicum* x *Solanum pennellii* (tomato) grown in a wet and a dry environment in 1995 (A) and terminated early and late in 1996 (B). The regression is across the two environments in 1995, whereas in 1996 the regressions are for the early and the late environments separately (Martin et al. 1999). Copyright Crop Science Society of America.

As expected from the theoretical analysis above, there is a good correlation between WUE and the carbon-isotope fractionation (Fig. 30). *Triticum aestivum* (wheat) grown under dry conditions has a higher WUE and a lower carbon-isotope fractionation than plants well supplied with water (Farquhar & Richards 1984). Moreover, those genotypes that perform best under drought (greatest WUE) have the lowest carbon-isotope fractionation, so that isotopic composition can be used to select for genotypes with improved performance under conditions where water is limiting (Fig. 31). A similar correlation between WUE and $\delta^{13}C$ has been found for cultivars of other species [e.g., *Hordeum vulgare* (barley) (Hubick & Farquhar 1989) and *Arachis hypogaea* (peanut) (Wright et al. 1988, Hubick 1990)].

5.4 Other Sources of Variation in Carbon-Isotope Ratios in C_3 Plants

Given the close relationship between WUE and $\delta^{13}C$, carbon-isotopic composition can be used to infer average WUE during growth (Fig. 30; Sect. 6 of Chapter 3 on plant water relations). For example, $\delta^{13}C$ is higher (less negative) in **desert plants** than in **mesic plants**, and it is higher in tissue produced during dry seasons (Smedley et al. 1991) or in dry years. This indicates that plants growing in dry conditions have a lower C_i than those in moist conditions. Other factors can alter isotopic composition without altering WUE. For example, $\delta^{13}C$ of plant tissue is higher at the bottom than at the top of the canopy. This is to a limited extent due to the contribution of ^{13}C-depleted CO_2 from soil respiration, but mostly to the lower C_i of sunlit top leaves compared with the shaded understory leaves (Buchmann et al. 1997). A complicating factor with the derivation of WUE from $\delta^{13}C$ is that isotope fractionation is operating at the level of Rubisco in the chloroplast, whereas the theoretical model is based on C_i. Possible variation in the draw-down of CO_2 from the intercellular spaces to the chloroplast (Sect. 2.2.3), due to the mesophyll resistance, is not taken into account, and may cause variation in $\delta^{13}C$ that is not associated with WUE.

Annuals fractionate more strongly against ^{13}C than **perennials**; additionally, herbs fractionate more than grasses, and **root parasites** [e.g.,

Comandra umbellata (pale bastard toadflax)] more than any of the surrounding species (Smedley et al. 1991). These patterns suggest a high stomatal conductance and low WUE in annuals, herbs, and hemiparasites. The low WUE of hemiparasitic plants is important in nutrient acquisition (Sect. 3 in Chapter 9D on parasitic associations).

6. Effects of Soil Nutrient Supply on Photosynthesis

6.1 The Photosynthesis–Nitrogen Relationship

Since the photosynthetic machinery accounts for more than half of the N in a leaf (Fig. 13) and much of the remainder is indirectly associated with its photosynthetic function, photosynthesis is strongly affected by N availability. A_{max} increases linearly with leaf N per unit area (Fig. 32), regardless of whether the variation in leaf N is caused by differences in soil N availability, growth irradiance, or leaf age, and holds also when similar species are compared (Fig. 32). The slope of this relationship is much steeper for C_4 plants than for C_3 plants (Sect. 9.5), and differs also among C_3 plants (Sect. 4.2.1 of Chapter 6 on mineral nutrition; Evans 1989). When leaves with different N concentration are compared of plants grown at different N availability, the photosynthetic rate per unit N (**photosynthetic N-use efficiency**; PNUE) at the growth irradiance is highest in leaves with low N concentrations. This is due to the higher degree of utilization of the photosynthetic apparatus (Fig. 33); hence, a higher efficiency at the expense of photosynthetic rate.

The strong A_{max} vs. N relationship cannot be due to any simple direct N limitation of photosynthesis, because both carbon-isotope studies and A–C_c curves generally show that photosynthesis is co-limited by CO_2 diffusion and photosynthetic capacity. Rather, the entire photosynthetic process is down-regulated under conditions of N limitation, with declines in Rubisco, chlorophyll, and stomatal conductance (Sect. 5.1, Table 5). The net effect of this coordinated response of all photosynthetic components is that C_i/C_a and $\delta^{13}C$ show no consistent relationship with leaf N (Rundel & Sharifi 1993).

In some field studies, especially in conifers, which often grow on low-P soils, photosynthesis may show little correlation with tissue N, but a strong correlation with tissue [P] (Reich & Schoettle 1988). The low photosynthetic rate of plants grown at low P supply may reflect feedback inhibition due to slow growth and low concentrations of P_i in the cytosol (Sect. 4.1) or low concentrations of Rubisco and other photosynthetic enzymes.

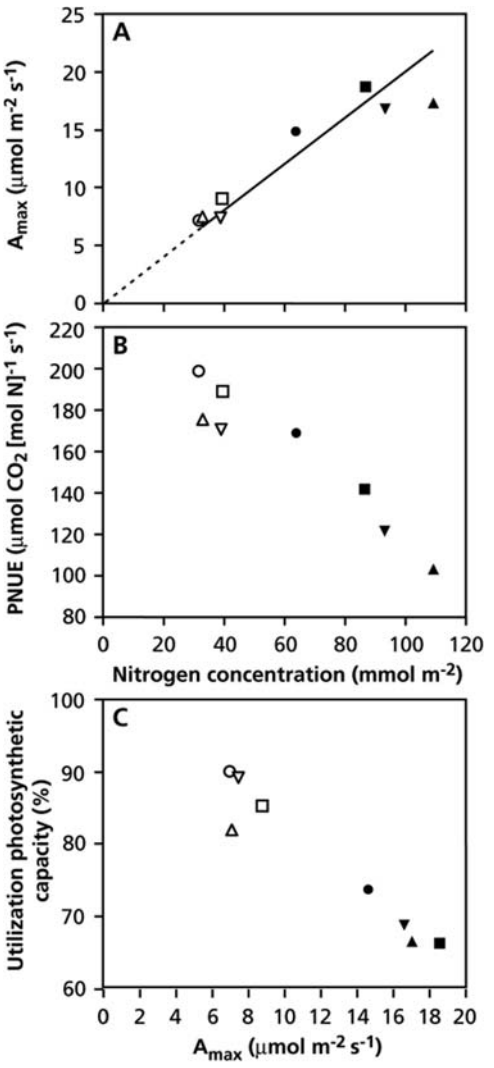

FIGURE 32. The light-saturated rate of photosynthesis (A_{max}) of four grasses grown at high (filled symbols) and low (open symbols) N supply (A) and their photosynthetic N-use efficiency (PNUE) determined at growth irradiance (B) plotted against leaf N per unit area. Note the higher PNUE for plants grown at a low N supply. (C) The proportional utilization of the total photosynthetic capacity at growth irradiance, calculated as the ratio of the rate at growth irradiance and A_{max} in relation to A_{max} (Pons et al. 1994). Copyright SPB Academic Publishing.

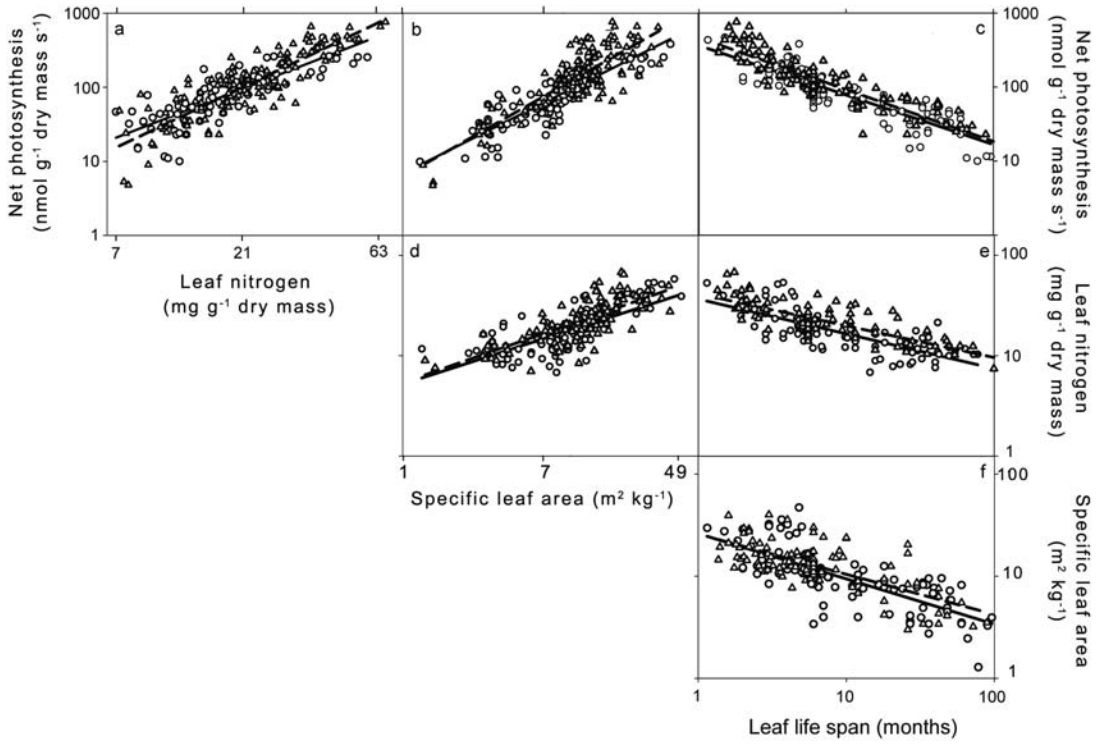

FIGURE 33. Relations of (A) mass-based maximum rate of CO_2 assimilation, (B) leaf N concentration, and (C) specific leaf area of young mature leaves as a function of their expected leaf life-span. The symbols refer to a data set for 111 species from six biomes (after Reich et al. 1997).

6.2 Interactions of Nitrogen, Light, and Water

Because of the coordinated responses of all photosynthetic processes, any environmental stress that reduces photosynthesis will reduce both the diffusional and the biochemical components (Table 5). Therefore, N concentration per unit leaf area is typically highest in sun leaves, and declines toward the bottom of a canopy. In canopies of *Nicotiana tabacum* (tobacco), this partially reflects higher rates of CO_2 assimilation of young, high-N leaves in high-light environments (Boonman et al. 2007). In multi-species canopies, however, the low leaf [N] per area in understory species clearly reflects the adjustment of photosynthetic capacity to the reduced light availability (Table 5; Niinemets 2007).

6.3 Photosynthesis, Nitrogen, and Leaf Life Span

As discussed in Chapter 6 on mineral nutrition and Chapter 7 on growth and allocation, plants acclimate and adapt to low soil N and low soil moisture by producing long-lived leaves that are thicker and have a high leaf mass density, a low specific leaf area (SLA; i.e., leaf area per unit leaf mass) and a low leaf N concentration. Both broad-leaved and conifer species show a single strong negative correlation between leaf life-span and either leaf N concentration or mass-based photosynthetic rate (Fig. 33; Reich et al. 1997). The low SLA in long-lived leaves relates to structural properties required to withstand unfavorable environmental conditions (Chapter 7 on growth and allocation). There is a strong positive correlation between SLA and leaf N concentration for different data sets (Fig. 33). Together, the greater leaf thickness and low N concentrations per unit leaf mass result in low rates of photosynthesis on a leaf-mass basis in long-lived leaves (Fig. 33). Maximum stomatal conductance correlates strongly with leaf N, because g_s scales with A_{max} (Wright et al. 2004).

7. Photosynthesis and Leaf Temperature: Effects and Adaptations

Temperature has a major effect on enzymatically catalyzed reactions and membrane processes, and therefore affects photosynthesis. Because the **activation energy** of different reactions often differs among plants acclimated or adapted to different temperature regimes, photosynthesis may be affected accordingly (for a discussion of the concepts of **acclimation** and **adaptation**, see Fig. 3 and Sect. 4 of Chapter 1 on assumptions and approaches). In this section temperature effects on photosynthesis will be explained in terms of underlying biochemical, biophysical, and molecular processes.

Differences among plants in their capacity to perform at extreme temperatures often correlate with the plant's capacity to photosynthesize at these temperatures. This may reflect both the adjustment of photosynthesis to the demand of the sinks (Sect. 4) and changes in the photosynthetic machinery during acclimation and adaptation.

7.1 Effects of High Temperatures on Photosynthesis

Many plants exhibit an optimum temperature for photosynthesis close to their normal growth temperature, showing **acclimation** (Fig. 34; Berry & Björkman 1980, Yamori et al. 2005). Below this optimum, enzymatic reaction rates, primarily associated with the "**dark reactions**", are temperature limited. At high temperatures the **oxygenating** reaction of Rubisco increases more than the **carboxylating** one so that photorespiration becomes proportionally more important. This is partly because the **solubility** of CO_2 declines with increasing temperature more strongly than does that of O_2. Part of the effect of temperature on photosynthesis of C_3 plants is due to the effects of temperature on **kinetic properties** of Rubisco. V_{max} increases with increasing temperature, but the K_m-values increase also, and more steeply for CO_2 than for O_2 (Fig. 35). This means that the affinity for CO_2 decreases more strongly than that for O_2. Additionally, electron transport (Cen & Sage 2005) and g_m (Yamori et al. 2006a, Warren 2007) may decline at elevated temperatures. The combined temperature effects on solubility, affinity, and mesophyll conductance cause a proportional increase in **photorespiration**, resulting in a decline in net photosynthesis at high temperature when electron-transport rates cannot keep up with the increased inefficiency.

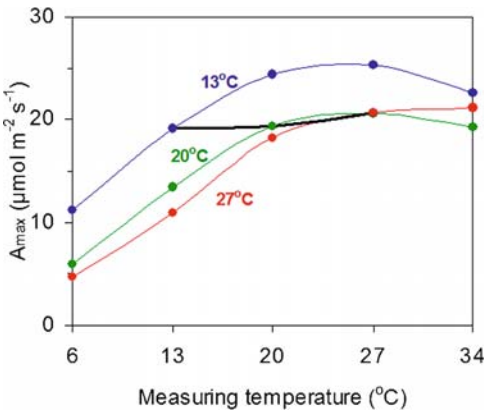

FIGURE 34. Temperature dependence of light-saturated rates of photosynthesis of *Plantago major* (common plantain) grown at three temperatures. The black line connects measurements at the growth temperatures (after Atkin et al. 2006). Copyright Blackwell Science Ltd.

Adaptation to high temperature typically causes a shift of the temperature optimum for net photosynthesis to higher temperatures (Fig. 36; Berry & Björkman 1980). Similarly, the temperature optimum for photosynthesis shifts to higher temperatures when coastal and desert populations of *Atriplex lentiformis* **acclimate** to high temperatures (Pearcy 1977).

Apart from the increase in photorespiration discussed above, there are several other factors important for determining **acclimation** and **adaptation** of photosynthesis to temperature. In leaves of *Spinacia oleracea* (spinach) the **Rubisco activation state** decreases with increasing temperatures above the optimum temperatures for photosynthesis, irrespective of growth temperature, while the activation state remains high at lower temperatures. Rubisco thermal stabilities of spinach leaves grown at low temperature are lower than those of leaves grown at high temperature. Photosynthetic performance in spinach is largely determined by the Rubisco kinetics at low temperature and by Rubisco kinetics and Rubisco activation state at high temperature (Yamori et al. 2006b). Furthermore, Rubisco can become inactivated at moderately high temperatures. Species adapted to hot environments often show temperature optima for photosynthesis that are quite close to the temperature at which enzymes are inactivated. The lability of **Rubisco activase** plays a major role in the decline of photosynthesis at high temperatures (Salvucci & Crafts-Brandner 2004b, Hikosaka et al. 2006). Thermal acclimation of *Acer rubrum* (red

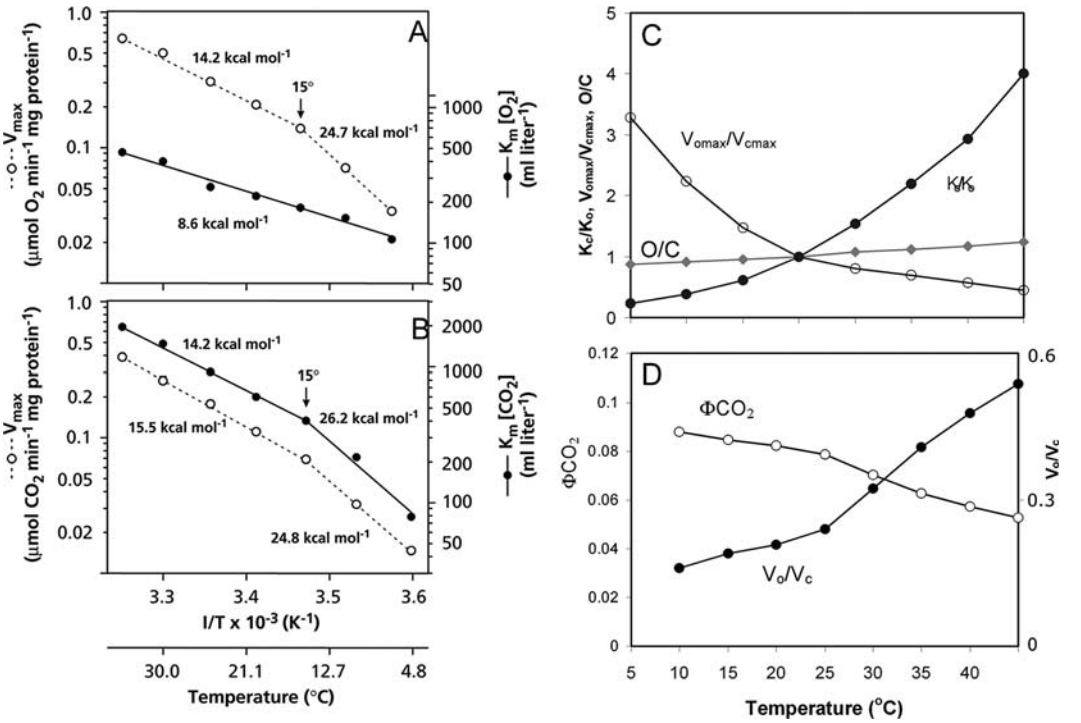

FIGURE 35. Temperature dependence of V_{max} and the K_m of (A) the oxygenating and (B) the carboxylating reaction of Rubisco. V_{max} is the rate of the carboxylating or oxygenating reaction at a saturating concentration of CO_2 and O_2, respectively. The K_m is the concentration of CO_2 and O_2 at which the carboxylating and oxygenating reaction, respectively, proceed at the rate which equals $1/2\,V_{max}$. Note that a logarithmic scale is used for the *y*-axis and that the inverse of the absolute temperature is plotted on the *x*-axis ("Arrhenius-plot"). In such a graph, the slope gives the activation energy, a measure for the temperature dependence of the reaction (Berry & Raison 1981). (C) The combined effects of temperature on kinetic properties as shown in (A) and (B) and relative solubility of O_2 and CO_2 (O/C) have been modeled, normalized to values at 20°C. (D) Relative rates of the oxygenation and carboxylation reactions of Rubisco (V_o/V_c) and quantum yield (ϕ CO_2) modeled using the same parameter values as in (C). For calculation of V_o/V_c and ϕ CO_2, it was assumed that partial pressures of CO_2 and O_2 in the chloroplast were 27 Pa and 21 kPa, respectively. Kinetic parameters used were calculated from Jordan and Ogren (1981) (courtesy I. Terashima, The University of Tokyo, Japan).

maple) from Florida in comparison with genotypes from Minnesota, US, is associated with maintenance of a high ratio of Rubisco activase to Rubisco (Weston et al. 2007). In *Gossypium hirsutum* (cotton) expression of the gene encoding Rubisco activase is influenced by post-transcriptional mechanisms that probably contribute to acclimation of photosynthesis during extended periods of heat stress (DeRidder & Salvucci 2007).

High temperatures also require a high degree of saturation of the membrane lipids of the thylakoid for integrated functioning of its components and prevention of leakiness (Sharkey 2005). Therefore, not only Rubisco activity, but also membrane-bound processes of electron transport may be limiting photosynthesis at high temperatures.

7.2 Effects of Low Temperatures on Photosynthesis

When plants grown at a moderate temperature are transferred to a lower temperature, but within the range normal for the growing season, photosynthesis is initially reduced (Fig. 34). Photon absorption is not affected by temperature, but the rate of electron transport and biochemical processes are reduced as a direct consequence of the lower temperature. Particularly, sucrose metabolism and/or phloem loading can become limiting for photosynthesis, causing feedback inhibition (Fig. 27). Acclimation to the lower growth temperature involves up-regulation of the limiting components of the photosynthetic apparatus. Hence, the capacity

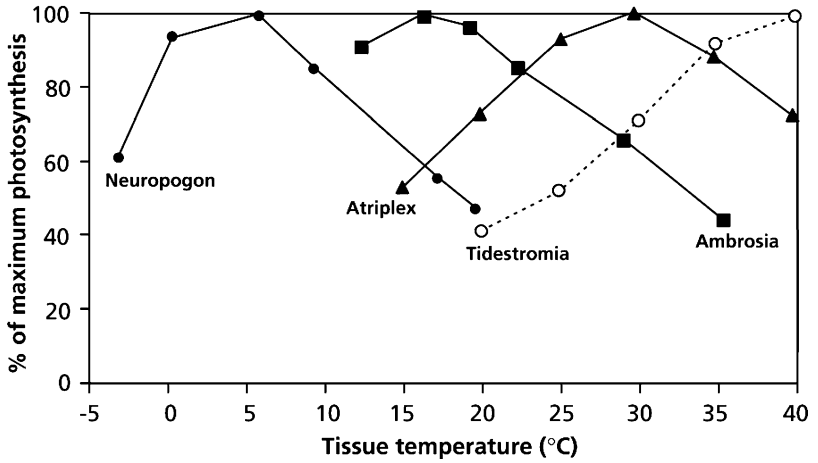

FIGURE 36. Photosynthetic response to temperature in plants from contrasting temperature regimes. Curves from left to right are for *Neuropogon acromelanus*, an Antarctic lichen, *Ambrosia chamissonis*, a cool coastal dune plant, *Atriplex hymenelytra*, an evergreen desert shrub, and *Tidestromia obliongifolia*, a summer-active desert perennial (after Mooney 1986).

for electron transport (J_{max}) is increased, and Rubisco levels increase as well with the proportional increase in carboxylation capacity (V_{cmax}) (Atkin et al. 2006). Feedback inhibition is alleviated by increased expression of enzymes of the sucrose synthesis pathway (Stitt & Hurry 2002). Acclimation comprises therefore an increase in photosynthetic capacity which is associated with an increase in leaf thickness, whereas chlorophyll concentrations remains more or less similar, thus causing an increase in A_{max} per unit chlorophyll. The change is accompanied by a decrease in antenna size of PS II. Hence, acclimation to low temperature resembles to a considerable extent acclimation to high irradiance (Huner et al. 1998). In *Plantago major* (common plantain) species, the result of acclimation is that, just as with respiration (Fig. 17 in Chapter 2B on respiration), photosynthetic rates are virtually independent of growth temperature (Fig. 35).

When cold is more extreme, damage is likely to occur. Many (sub)tropical plants grow poorly or become damaged at temperatures between 10 and 20°C. Such damage is called "**chilling injury**" and differs from frost damage, which only occurs below 0°C. Part of the chilling injury is associated with the photosynthetic apparatus. The following aspects play a role:

1. Decrease in membrane fluidity
2. Changes in the activity of membrane-associated enzymes and processes, such as the photosynthetic electron transport
3. Loss of activity of cold-sensitive enzymes.

Chilling resistance probably involves **reduced saturation** of membrane fatty acids which increases membrane fluidity and so compensates for the effect of low temperature on membrane fluidity (Chapter 4B on effects of radiation and temperature).

Chilling often leads to **photoinhibition** and **photooxidation**, because the biophysical reactions of photosynthesis (photon capture and transfer of excitation energy) are far less affected by temperature than the biochemical steps, including electron transport and activity of the Calvin cycle (Sect. 3.3). The leaves of evergreen plants in cold climates typically develop and expand during the warm spring and summer months, and are retained during the winter months when all growth ceases. Upon exposure to low temperature and high irradiance, the conversion of the light-harvesting **violaxanthin** to the energy-quenching **zeaxanthin** (Sect. 3.3.1) occurs within minutes. In addition to this ubiquitous process of "flexible dissipation", several forms of "**sustained dissipation**" exist. The sustained dissipation does not relax upon darkening of the leaves, but it is still ΔpH-dependent; it is flexible in the sense that, e.g., warming of leaves allows this state to be quickly reversed. The difference in the underlying mechanism between flexible and sustained ΔpH-independent dissipation is not related to zeaxanthin, because this xanthophyll is involved in both types of thermal dissipation (Demmig-Adams & Adams 2006). Therefore, under lasting stress conditions and in some plant species, the flexible, ΔpH-independent engagement and disengagement of zeaxanthin in dissipation is replaced by a

Table 6. Differences in the response of photosynthesis and photoprotection between crops/weeds and evergreens. Typical changes in intrinsic photosynthetic capacity, ΔpH-independent dissipation, zeaxanthin and antheraxanthin (Z + A) retention, in annual crops/biennial weeds *vs.* evergreen species in response to transfer of shade-acclimated plants to high light or in response to the transition from summer to winter conditions.

	Shade to sun transfer		Summer to winter transition	
	Annual crop	Evergreen	Tropical annual/biennial Crop/weed	Temperate evergreen
Photosynthetic capacity	↑	↓	↑	↓↓
ΔpH-independent dissipation	*	↑↑	*	↑↑
Z+A retention	*	↑↑	*	↑↑

***Source*: Demmig-Adams & Adams (2006).**
***Seen only transiently and at moderate levels upon transition.**

highly effective, but less flexible continuous engagement of zeaxanthin in dissipation that does not require a ΔpH. It is not yet known which factors other than zeaxanthin are involved in the ΔpH-dependent, less flexible, but potent form of dissipation that is particularly pronounced in long-lived, slow-growing evergreen species (Table 6).

Hardening of *Thuja plicata* (western red cedar) seedlings (i.e., acclimation to low temperatures) is associated with some loss of chlorophyll and with increased levels of carotenoids, giving the leaves a red-brown color. Exposure to low temperatures causes a decline in photosynthetic capacity and the quantum yield of photosynthesis, as evidenced by the decline in chlorophyll fluorescence (i.e., in the ratio F_v/F_m; Box 2A.4). The carotenoids prevent damage that might otherwise occur as a result of photooxidation (Sect. 3.3.1). Upon transfer of the seedlings to a normal temperature (dehardening) the carotenoids disappear within a few days (Weger et al. 1993). Other temperate conifers such as *Pinus banksiana* (jack pine) exhibit "purpling", which is caused by the accumulation of anthocyanin in epidermal cells. This appears to protect the needles against photoinhibition of PS II through a simple screening of irradiance (Huner et al. 1998). Accumulation of photoprotective anthocyanins gives rise to typical autumn colors, e.g., in *Cornus stolonifera* (red-osier dogwood) (Feild et al. 2001).

In the alpine and arctic species *Oxyria digyna* (alpine mountainsorrel), an increased resistance to photoinhibition is caused by an increased capacity to repair damaged PS II reaction centers and increased nonphotochemical quenching. Maximum rates of photosynthesis by arctic and alpine plants measured in the field are similar to those of temperate-zone species, but are reached at lower temperatures–often 10–15°C (Fig. 36). These substantial photosynthetic rates at low temperatures are achieved in part by high concentrations of Rubisco, as found in acclimation of lowland plants. This may account for the high tissue N concentration of arctic and alpine plants despite low N availability in soils (Körner & Larcher 1988). Although temperature optima of arctic and alpine plants are 10–30°C lower than those of temperate plants, they are still 5–10°C higher than average summer leaf temperatures in the field.

8. Effects of Air Pollutants on Photosynthesis

Many air pollutants reduce plant growth, partly through their negative effects on photosynthesis. Pollutants like SO_2 and ozone (O_3) that enter the leaf through stomata, directly damage the photosynthetic cells of the leaf. In general, any factor that increases stomatal conductance (e.g., high supply of water, high light intensity, high N supply) increases the movement of pollutants into the plant, and therefore their impact on photosynthesis. At low [O_3], decreased production *Glycine max* (soybean) corresponds to a decrease in leaf photosynthesis, but at higher [O_3] the larger loss in production is associated with decreases in both leaf photosynthesis and leaf area (Morgan et al. 2003). Rates of net photosynthesis and stomatal conductance in *Fagus sylvatica* (beech) are about 25% lower when the O_3 concentration is double that of the background concentration in Kranzberg Forest (Germany), while V_{cmax} is and g_m are not affected (Warren et al. 2007). The major effect of SO_2 on growth and yield of *Vicia faba* (faba bean) is due to leaf injury (necrosis

and abscission of leaves), rather than direct effects on gas exchange characteristics (photosynthesis and respiration) (Kropf 1989).

9. C_4 Plants

9.1 Introduction

The first sections of this chapter dealt primarily with the characteristics of photosynthesis of C_3 species. There are also species with photosynthetic characteristics quite different from these C_3 plants. These so-called **C_4 species** belong to widely different taxonomic groups (Table 7); the C_4 syndrome is very rare among tree species; *Chamaesyce olowaluana* (Euphorbiaceae) is a canopy-forming C_4 tree from Hawaii (Sage 2004). Although their different anatomy has been well documented for over a century, the biochemistry and physiology of C_4 species has been elucidated more recently. It is hard to say who first "discovered" the C_4 pathway of photosynthesis (Hatch & Slack 1998); however, Hatch & Slack (1966) certainly deserve credit for combining earlier pieces of information with their own findings and proposing the basic pathway as outlined in this section.

None of the metabolic reactions or anatomical features of C_4 plants are really unique to these species; however, they are all linked in a manner quite different from that in C_3 species. Based on differences in biochemistry, physiology, and anatomy, three subtypes of C_4 species are discerned (Table 8). In addition, there are intermediate forms between C_3 and C_4 metabolism (Sect. 9.6).

9.2 Biochemical and Anatomical Aspects

The anatomy of C_4 plants differs strikingly from that of C_3 plants (Fig. 37). C_4 plants are characterized by their **Kranz anatomy**, a sheath of thick-walled cells surrounding the vascular bundle ("Kranz" is the German word for "wreath"). These thick walls of the bundle sheath cells may be impregnated with suberin, but this does not appear to be essential to reduce

Table 7. The 19 families containing members with the C_4 photosynthetic pathway.*

Family	Number of lineages	Subtypes
Monocots		
Poaceae	11	NADP-ME, NAD-ME, PCK
Cyperaceae	4	NADP-ME, NAD-ME
Hydrocharitaceae	1	Single-cell NADP-ME
Dicots		
Acanthaceae	1	–
Aizoaceae	2	NADP-ME
Amaranthaceae	3	NADP-ME, NAD-ME
Asteraceae	3	NADP-ME
Boraginaceae	1	NAD-ME
Brassicaceae	1	–
Caryophyllaceae	1	NAD-ME
Chenopodiaceae	10	NADP-ME, NAD-ME & single-cell NAD-ME
Euphorbiaceae	1	NADP-ME
Gisekiaceae	1	NAD-ME
Molluginaceae	1	NAD-ME
Nyctaginaceae	1	NAD-ME
Polygonaceae	1	–
Portulacaceae	2	NADP-ME, NAD-ME
Scrophulariaceae	1	–
Zygophyllaceae	2	NADP-ME

Source: Sage (2004).

*The number of lineages represents the putative times of independent evolution of C_4 in the family. The biochemical subtypes (not known for all species) are as defined in Table 8 and Fig. 37. Single-cell C_4 is explained in the text.

Table 8. Main differences between the three subtypes of C_4 species.*

Subtype	Major decarboxylase in BSC	Decarboxylation occurs in	Major substrate moving from		Photosystems in BSC
			MC to BSC	BSC to MC	
NADP-ME	NADP-malic enzyme	Chloroplast	Malate	Pyruvate	I and II[a]
NAD-ME	NAD-malic enzyme	Mitochondria	Aspartate	Alanine	I and II
PCK	PEP carboxykinase	Cytosol	Aspartate + malate	Alanine + PEP	I and II

*MC is mesophyll cells; BSC is vascular bundle sheath cells.
[a]Some NADP-ME monocots, including *Zea mays* (corn) have only PS I in BSC chloroplasts.

the gas diffusion between the bundle sheath and the mesophyll. In some C_4 species (NADP-ME types), the cells of the bundle sheath contain large chloroplasts with mainly stroma thylakoids and very little grana. The bundle sheath cells are connected via **plasmodesmata** with the adjacent thin-walled mesophyll cells, with large intercellular spaces.

CO_2 is first assimilated in the mesophyll cells, catalyzed by **PEP carboxylase**, a light-activated enzyme, located in the cytosol. PEP carboxylase uses phospho*enol*pyruvate (PEP) and HCO_3^- as substrates. HCO_3^- is formed by hydratation of CO_2, catalyzed by **carbonic anhydrase**. The high affinity of PEP carboxylase for HCO_3^- reduces C_i to about 100 µmol mol^{-1}, less than half the C_i of C_3 plants (Sect. 2.2.2). PEP is produced in the light from pyruvate and ATP, catalyzed by pyruvate P_i-dikinase, a light-activated enzyme located in the chloroplast. The product of the reaction catalyzed by PEP carboxylase is oxaloacetate, which is reduced to malate. Alternatively, oxaloacetate may be transaminated in a reaction with alanine, forming aspartate. Whether malate or aspartate, or a mixture of the two, are formed, depends on the subtype of the C_4 species (Table 8). Malate (or aspartate) diffuses via plasmodesmata to the vascular bundle sheath cells, where it is decarboxylated, producing CO_2 and pyruvate (or alanine). CO_2 is then fixed by Rubisco in the chloroplasts of the **bundle sheath cells**, which have a normal Calvin cycle, as in C_3 plants. Rubisco is not present in the mesophyll cells, which do not have a complete Calvin cycle and only store starch when the bundle sheath chloroplasts reach their maximum starch concentrations.

Fixation of CO_2 by PEP carboxylase and the subsequent decarboxylation occur relatively fast,

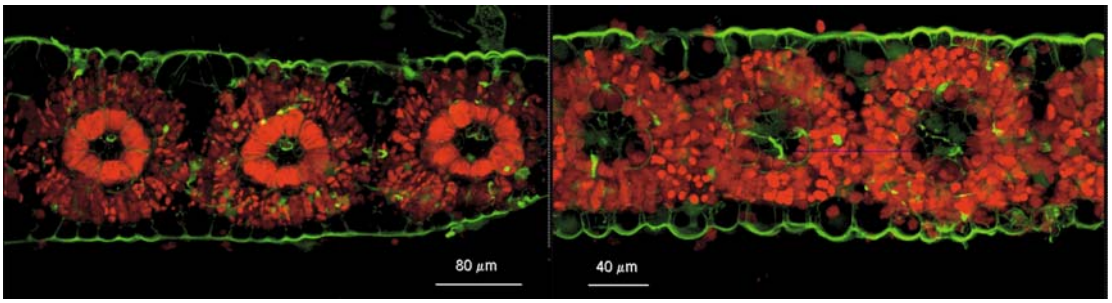

Figure 37. (Facing page) Schematic representation photosynthetic metabolism in the three C_4 types distinguished according to the decarboxylating enzyme. NADP-ME, NADP-requiring malic enzyme; PCK, PEP carboxykinase; NAD-ME, NAD-requiring malic enzyme. Numbers refer to enzymes. (1) PEP carboxylase, (2) NADP-malate dehydrogenase, (3) NADP-malic enzyme, (4) pyruvate P_i-dikinase, (5) Rubisco, (6) PEP carboxykinase, (7) alanine aminotransferase, (8) aspartate amino transferase, (9) NAD-malate dehydrogenase, (10) NAD-malic enzyme (after Lawlor 1993). (Above) Cross-sections of leaves of monocotyledonous C_4 grasses (Ghannoum et al. 2005). Chlorophyll *a* autofluorescence of a leaf cross-section of (*Left*) *Panicum miliaceum* (French millet, NAD-ME), and (*Right*) *Sorgum bicolor* (millet, NAD-ME). The images were obtained using confocal microscopy. Cell walls are shown in green and chlorophyll *a* autofluorescence in red. Most of the autofluorescence emanates from bundle sheath cells in the NAD-ME species (*Left*) and from the mesophyll cells in the NADP-ME species (*Right*), showing the difference in chlorophyll distribution between the two subtypes (courtesy O. Ghannoum, Centre for Horticulture and Plant Sciences, University of Western Sydney, Australia). Copyright American Society of Plant Biologists.

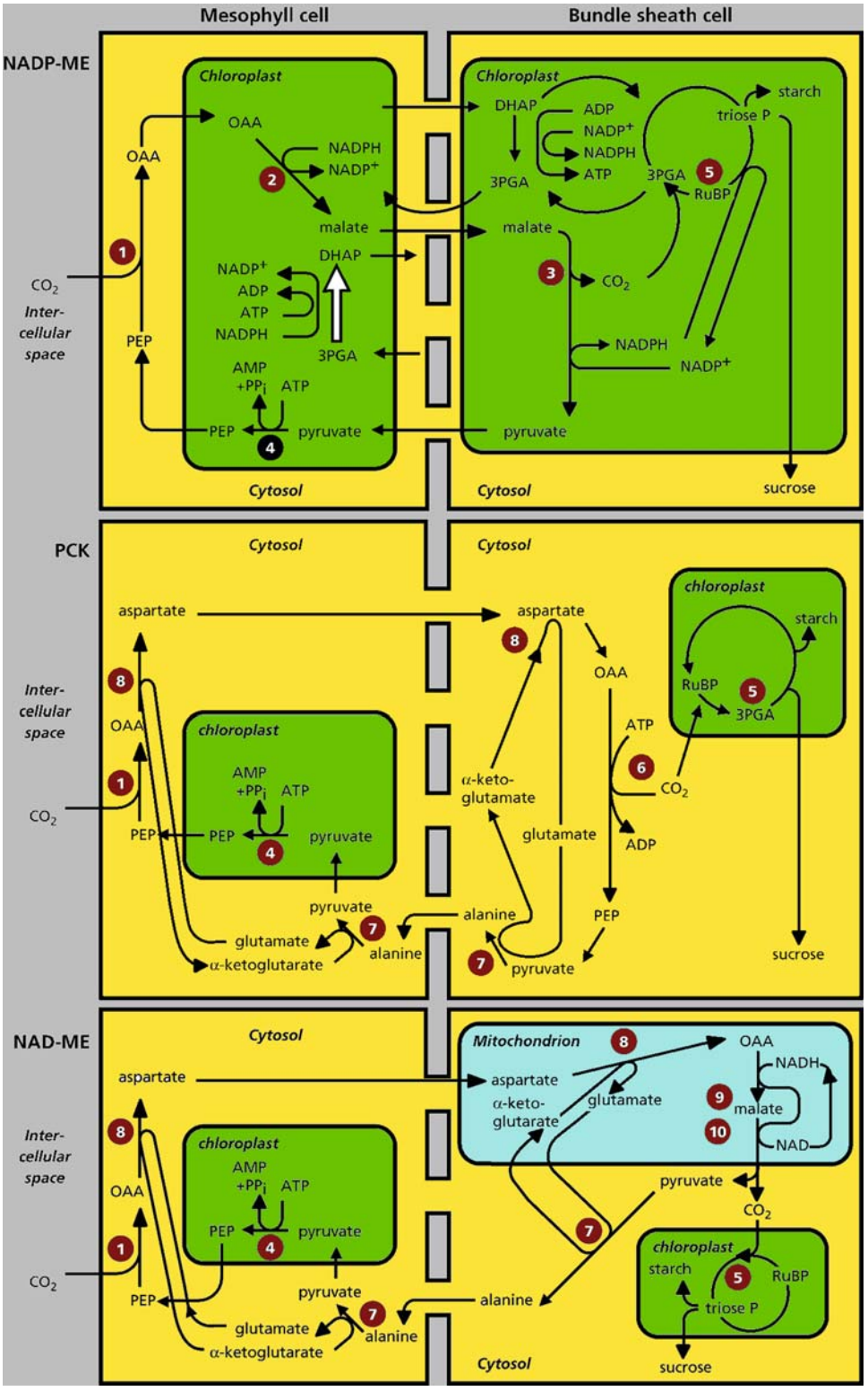

FIGURE 37. (continued)

allowing the build-up of a high concentration of CO_2 in the vascular bundle sheath. When the outside CO_2 concentration is 380 μmol mol^{-1}, that at the site of Rubisco in the chloroplasts of the vascular bundle is 1000–2000 μmol mol^{-1}. The C_i, that is the CO_2 concentration in the intercellular spaces in the mesophyll, is only about 100 μmol mol^{-1}. With such a steep gradient in the CO_2 concentration it is inevitable that some CO_2 diffuses back from the bundle sheath to the mesophyll, but this is only about 20%. In other words, C_4 plants have a mechanism to enhance the CO_2 concentration at the site of Rubisco to an extent that its **oxygenation** reaction is virtually fully inhibited. Consequently, C_4 plants have negligible rates of **photorespiration**.

Based on the enzyme involved in the decarboxylation of the C_4 compounds transported to the vascular bundle sheath, three groups of C_4 species are discerned: NADP-malic enzyme-, NAD-malic enzyme- and PEP carboxykinase-types (Table 8, Fig. 37). The difference in biochemistry is closely correlated with anatomical features of the bundle sheath and mesophyll of the leaf blade as viewed in transverse sections with the light microscope (Ellis 1977). In NAD-ME-subtypes, which decarboxylate malate (produced from imported aspartate) in the bundle sheath mitochondria, the mitochondrial frequency is several-fold higher than that in NADP-ME-subtypes. The specific activity of the mitochondrial enzymes involved in C_4 photosynthesis is also greatly enhanced (Hatch & Carnal 1992). The NAD-ME group of C_4 species tends to occupy the driest habitats, although the reason for this is unclear (Ellis et al. 1980, Ehleringer & Monson 1993).

Decarboxylation of malate occurs only during assimilation of CO_2, and vice versa. The explanation for this is that the NADP needed to decarboxylate malate is produced in the Calvin cycle, during the assimilation of CO_2. At least in the more "sophisticated" NADP-ME C_4 plants such as *Zea mays* (corn) and *Saccharum officinale* (sugar cane), the NADPH required for the photosynthetic reduction of CO_2 originates from the activity of NADP malic enzyme. Since two molecules of NADPH are required per molecule of CO_2 fixed by Rubisco, this amount of NADPH is not sufficient for the assimilation of all CO_2. Additional NADPH is required to an even larger extent if aspartate, or a combination of malate and aspartate, diffuses to the bundle sheath. It is assumed that this additional NADPH can be imported via a "shuttle", involving PGA and dihydroxyacetone phosphate (DHAP). Part of the PGA that originates in the bundle-sheath chloroplasts returns to the mesophyll. Here it is reduced, producing DHAP, which diffuses to the bundle sheath. Alternatively, NADPH required in the bundle sheath cells might originate from the removal of electrons from water. This reaction requires the activity of PS II, next to PS I. PS II is only poorly developed in the bundle sheath cells, at least in the "more sophisticated" C_4 species. The poor development of PS II activity in the bundle sheath indicates that very little O_2 is evolved in these cells that contain Rubisco, which greatly favors the carboxylation reaction over the oxygenation.

The formation of PEP from pyruvate in the mesophyll cells catalyzed by pyruvate P_i-dikinase, requires one molecule of ATP and produces AMP, instead of ADP; this corresponds to the equivalent of two molecules of ATP per molecule of PEP. This represents the metabolic costs of the **CO_2 pump** of the C_4 pathway. It reduces photosynthetic efficiency of C_4 plants, when compared with that of C_3 plants under nonphotorespiratory conditions. In summary, C_4 photosynthesis concentrates CO_2 at the site of carboxylation by Rubisco in the bundle sheath, but this is accomplished at a metabolic cost.

9.3 Intercellular and Intracellular Transport of Metabolites of the C_4 Pathway

Transport of the metabolites that move between the two cell types occurs by **diffusion** through **plasmodesmata**. The concentration gradient between the mesophyll and bundle sheath cells is sufficiently high to allow diffusion at a rate that readily sustains photosynthesis, with the exception of that of pyruvate. How can we account for rapid transport of pyruvate from the bundle sheath to the mesophyll if there is no concentration gradient?

Uptake of pyruvate in the chloroplasts of the mesophyll cells is a light-dependent process, requiring a specific energy-dependent carrier. Active uptake of pyruvate into the chloroplast reduces the pyruvate concentration in the cytosol of these mesophyll cells to a low level, creating a concentration gradient that drives diffusion from the bundle sheath cells (Flügge et al. 1985).

In the chloroplasts of the mesophyll cells, pyruvate is converted into PEP, which is exported to the cytosol in exchange for P_i. The same translocator that facilitates this transport is probably also used to export triose-phosphate in exchange for PGA. This translocator operates in the reverse direction in mesophyll and bundle sheath chloroplasts, in that PGA is imported and triose-phosphate is exported in the mesophyll chloroplasts, while the chloroplasts in the bundle sheath export PGA and import triose phosphate.

The chloroplast envelope of the mesophyll cells also contains a translocator for the transport of dicarboxylates (malate, oxaloacetate, aspartate, and glutamate). Transport of these carboxylates occurs by exchange. The uptake of oxaloacetate, in exchange for other dicarboxylates, is competitively inhibited by these other dicarboxylates, with the values for K_i being in the same range as those for K_m. [K_i is the inhibitor (i.e., dicarboxylate) concentration at which the inhibition of the transport process is half that of the maximum inhibition by that inhibitor; K_m is the substrate (oxaloacetate) concentration at which the transport process occurs at half the maximum rate.] Such a system does not allow rapid import of oxaloacetate. A special transport system, transporting oxaloacetate without exchange against other dicarboxylates, takes care of rapid import of oxaloacetate into the mesophyll chloroplasts.

9.4 Photosynthetic Efficiency and Performance at High and Low Temperatures

The differences in anatomy and biochemistry result in strikingly different A_n-C_i curves between C_3 and C_4. First, the **CO_2-compensation point** of C_4 plants is only 0–5 μmol mol^{-1} CO_2, as compared with 40–50 μmol mol^{-1} in C_3 plants (Fig. 38). Second, this compensation point is not affected by O_2 concentration, as opposed to that of C_3 plants which is considerably less at a low O_2 concentration (i.e., when photorespiration is suppressed). Thirdly, the C_i (the internal concentration of CO_2 in the mesophyll) at a C_a of 380 μmol mol^{-1} is only about 100 μmol mol^{-1}, compared with approximately 250 μmol mol^{-1} in C_3 plants (Fig. 38).

There are also major differences in the characteristics of the light-response curves of CO_2 assimilation of C_3 and C_4 species. The initial slope of the light-response represents the light-limited part and is referred to as the **quantum yield**. Photochemical activity is limited by the rate of electron transport under these conditions. Changes in quantum yield are thus caused by changes in the partitioning between carboxylation and oxygenation reactions of Rubisco. When measured at 30°C or higher, the quantum yield is considerably higher for C_4 plants and independent of the O_2 concentration, in contrast to that of C_3 plants. Therefore, at relatively high temperatures, the quantum yield of photosynthesis

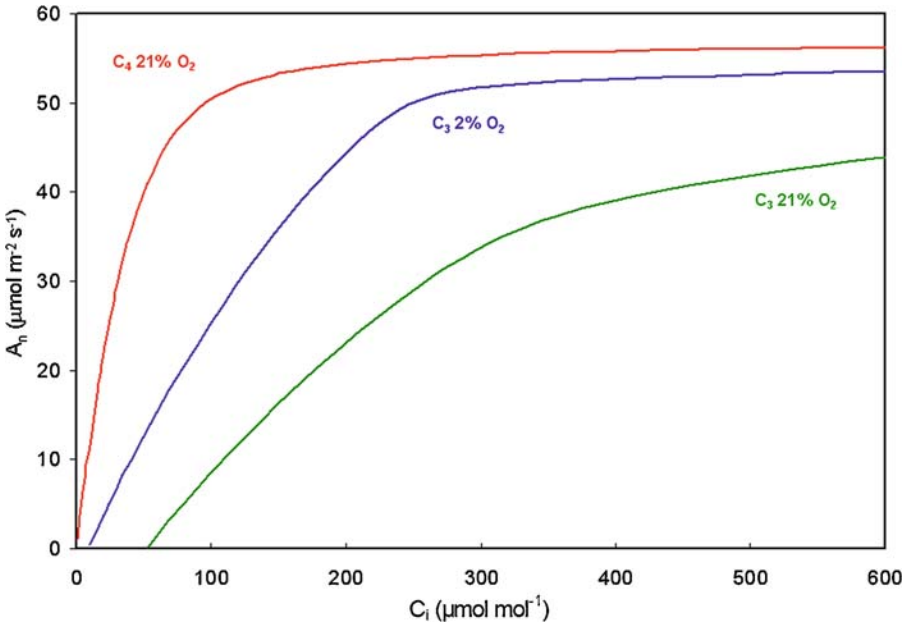

FIGURE 38. Response of net photosynthesis (A_n) to intercellular CO_2 concentration in the mesophyll (C_i) of C_3 and C_4 plants. C_3 plants respond strongly to O_2 as shown by the lines for normal atmospheric (21%) and low (2%) O_2 concentrations, whereas C_4 plants do not. The CO_2-response curves were calculated based on models described by Von Caemmerer (2000). Parameter values for the C_3 model were $V_{cmax} = 150$ and $J_{max} = 225$ μmol m^{-2} s^{-1} (see Box 2A.1), and in the C_4 model $V_{cmax} = 60$ and $V_{pmax} = 120$ μmol m^{-2} s^{-1}, where V_{pmax} is the maximum PEP carboxylase activity. Arrows indicate typical C_i values at 380 μmol CO_2 mol^{-1}air.

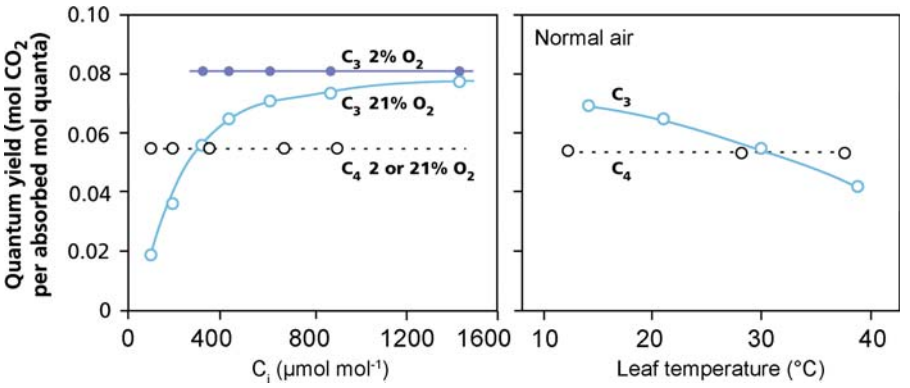

FIGURE 39. The effect of temperature and the intercellular CO_2 concentration (C_i) on the quantum yield of the photosynthetic CO_2 assimilation in a C_3 and a C_4 plant (after Ehleringer & Björkman 1977).

is higher for C_4 plants, and is not affected by **temperature**. By contrast, the quantum yield of C_3 plants declines with increasing temperature, due to the proportionally increasing oxygenating activity of Rubisco (Fig. 39). At an atmospheric O_2 and CO_2 concentration of 21% and 350 µmol mol^{-1}, respectively, the quantum yield is higher for C_4 plants at high temperatures due to photorespiration in C_3 species, but lower at low temperatures due to the additional ATP required to regenerate PEP in C_4 species. When measured at a low O_2 concentration (to suppress photorespiration) and a C_a of 350 µmol mol^{-1}, the quantum yield is invariably higher for C_3 plants.

The rate of CO_2 assimilation of C_4 plants typically saturates at higher irradiance than that of C_3 plants, because A_{max} of C_4 plants is generally higher. This is facilitated by a high C_c, the CO_2 concentration at the site of Rubisco. In C_3 plants with their generally lower A_{max}, the light-response curve levels off at lower irradiances, because CO_2 becomes the limiting factor for the net CO_2 assimilation. At

TABLE 9. Variation in kinetic parameters of the ubiquitous carboxylating enzyme Rubisco at 25°C for eight species in four groups.*

		K_m (CO_2)		
	Presence of CCM	In water µM	In air µmol mol^{-1}	k_{cat} S^{-1}
Cyanobacteria				
Synechococcus	+	293	–	12.5
Green algae				
Chlamydomonas reinhardtii	+	29	–	5.8
C_4 terrestrial plants				
Amaranthus hybridus	+	16	480	3.8
Sorghum bicolor	+	30	900	5.4
Zea mays	+	34	1020	4.4
C_3 terrestrial plants				
Triticum aestivum	–	14	420	2.5
Spinacia oleracea	–	14	420	3.7
Nicotiana tabacum	–	11	330	3.4

Source: Tcherkez et al (2006).

* Shown are the Michaelis–Menten constant $K_m(CO_2)$, inversely related to substrate (CO_2) affinity, and the catalytic turnover rate at saturating CO_2 (k_{cat}, mol CO_2 (mol catalytic sites)$^{-1}$. $K_m(CO_2)$ in air is calculated from the value provided for water using the solubility of CO_2 at 25°C (33.5 mmol L^{-1} at standard atmospheric pressure). CCM = carbon-concentrating mechanism.

Table 10. The number of chloroplasts and of mitochondria plus peroxisomes in bundle sheath cells compared with those in mesophyll cells (BSC/MC) and the CO_2-compensation point (Γ, μmol mol^{-1}, of C_3, C_4, and C_3–C_4 intermediates belonging to the genera *Panicum, Neurachne, Flaveria,* and *Moricandia.*

Species	Photosynthetic pathway	BSC/MC		Γ
		Chloroplasts	Mitochondria + peroxisomes	
P. milioides	C_3–C_4	0.9	2.4	19
P. miliaceum	C_4	1.1	8.4	1
N. minor	C_3–C_4	3.1	20.0	4
N. munroi	C_4	0.8	4.9	1
N. tenuifolia	C_3	0.6	1.2	43
F. anomala	C_3–C_4	0.9	2.3	9
F. floridana	C_3–C_4	1.4	5.0	3
F. linearis	C_3–C_4	2.0	3.6	12
F. oppositifolia	C_3–C_4	1.4	3.6	14
F. brownii	C_4-like	4.2	7.9	2
F. trinerva	C_4	2.2	2.4	0
F. pringlei	C_3	0.5	1.0	43
M. arvensis	C_3–C_4	1.4	5.2	32
M. spinosa	C_3–C_4	1.6	6.0	25
M. foleyi	C_3	1.5	3.3	51
M. moricandioides	C_3	2.0	2.8	52

***Source*: Brown & Hattersley (1989).**

increasing atmospheric CO_2 concentrations the irradiance at which light saturation is reached shifts to higher levels also in C_3 plants.

The high concentration of CO_2 in the vascular bundle sheath of C_4-plants, the site of Rubisco, allows different kinetic properties of Rubisco. Table 9 shows that indeed the $K_m(CO_2)$ of Rubisco from terrestrial C_3 plants is lower than that from C_4 plants. A high K_m, that is a low affinity, for CO_2 of Rubisco is not a disadvantage for the photosynthesis of C_4 plants, considering the high C_c in de the bundle sheath. For C_3 plants a low K_m for CO_2 is vital, since the C_i is far from saturating for Rubisco in their mesophyll cells. The advantage of the high K_m of the C_4 Rubisco is thought to be indirect in that it allows a high **maximum rate** per unit protein of the enzyme (V_{max} or k_{cat}). That is, the tighter CO_2 is bound to Rubisco, the longer it takes for the carboxylation to be completed. In C_3 plants, a high affinity is essential, so that k_{cat} cannot be high. C_4 plants, which do not require a high affinity, do indeed have an enzyme with a high k_{cat}, allowing more moles of CO_2 to be fixed per unit Rubisco and time at the high C_c (Table 10). Interestingly, the alga *Chlamydomonas reinhardtii*, which has a CO_2-concentrating mechanism (Sect. 11.3), also has a Rubisco enzyme with a high K_m (low affinity) for CO_2 and a high V_{max} and k_{cat} (Table 10). Apparently, there is a trade-off in Rubisco between CO_2 specificity [a low $K_m(CO_2)$] and catalytic capacity (a high k_{cat}).

The biochemical and physiological differences between C_4 and C_3 plants have important ecological implications. The abundance of C_4 monocots in regional floras correlates most strongly with growing season temperature, whereas C_4 dicot abundance correlates more strongly with aridity and salinity (Ehleringer & Monson 1993). At regional and local scales, areas with **warm-season rainfall** have greater C_4 abundance than regions with cool-season precipitation. Along local gradients, C_4 species occupy microsites that are warmest or have driest soils. In communities with both C_3 and C_4 species, C_3 species are most active early in the growing season when conditions are cool and moist, whereas C_4 activity increases as conditions become warmer and drier. Together these patterns suggest that high photosynthetic rates at high temperature (due to **lack of photorespiration**) and high water-use efficiency (WUE) (due to the **low C_i**, which enables C_4 plants to have a **lower stomatal conductance** for the same CO_2 assimilation rate) are the major factors governing the ecological distribution of the C_4 photosynthetic pathway. Any competitive advantage of the high WUE of C_4 plants, however, has been difficult to document experimentally (Ehleringer & Monson 1993). This

may well be due to the fact that, in a competitive situation, any water that is left in the soil by a plant with a high WUE is available for a competitor with lower WUE. Although WUE of C_4 plants is higher, the C_4 pathway does not give them a higher drought tolerance.

C_4 plants generally have lower tissue N concentrations, because they have 3–6 times less Rubisco than C_4 plants and very low levels of the photorespiratory enzymes, though some of the advantage is lost by the investment of N in the enzymes of the C_4 pathway. C_4 plants also have equivalent or higher photosynthetic rates than C_3 plants, resulting in a higher rate of photosynthesis per unit of leaf N (**Photosynthetic N-Use Efficiency**, PNUE), especially at high temperatures (Fig. 40). The higher PNUE of C_4 plants is accounted for by: (1) suppression of the oxygenase activity of Rubisco, so that the enzyme is only used for the carboxylation reaction; (2) the lack of photorespiratory enzymes; (3) the higher catalytic activity of Rubisco due to its high k_{cat} and the high C_c (Table 10). Just as in a comparison of C_3 species that differ in PNUE (Sect. 4.2.1 of Chapter 6 on mineral nutrition), there is no consistent tendency of C_4 species to have increased abundance or a competitive advantage in low-N soils (Christie & Detling 1982, Sage & Pearcy 1987a). This suggests that the high PNUE of C_4 species is less important than their high WUE and high optimum temperature of photosynthesis in explaining patterns of distribution.

One of the key enzymes of the C_4 pathway in *Zea mays* (corn), pyruvate P_i-dikinase, readily loses its activity at low temperature and hence the leaves' photosynthetic capacity declines. This accounts for part of the chilling sensitivity of most C_4 plants. Loss of activity of pyruvate P_i-dikinase at low temperatures can be prevented by protective ("compatible") compounds (Sect. 3.4.5 of Chapter 3 on plant water relations), but it remains to be investigated if this plays a major role in intact C_4 plants (Krall et al. 1989).

9.5 C_3–C_4 Intermediates

In the beginning of the 1970s, when the C_4 pathway was unraveled, there were attempts to cross C_3 and C_4 species of *Atriplex* (saltbush). This was considered a useful approach to enhance the rate or efficiency of photosynthesis and yield of C_3 parents. The complexity of anatomy and biochemistry of the C_4 plants, however, is such, that these crosses have not produced any useful progeny (Brown & Bouton 1993). Since molecular techniques have become available which allow silencing and over-expression of specific genes in specific cells, attempts have been made to reduce the activity of glycine decarboxylase, the key enzyme in photorespiration, in mesophyll cells of C_3 plants and over-express the gene in the bundle sheath. Although these attempts have been successful from a molecular point of view in that the aim of selectively modifying the enzyme activity was achieved, no results have yet been obtained to show enhanced rates of photosynthesis. This is perhaps not unexpected, in view of the rather small advantage true C_3–C_4 intermediates are likely to have in comparison with C_3 relatives.

Further attempts to transform C_3 crops into C_4 were inspired by the discovery of plants that perform a C_4 pathway without intercellular compartmentation between mesophyll and bundlesheath. *Suaeda aralocaspica* (formerly known as *Borszczowia aralocas-*

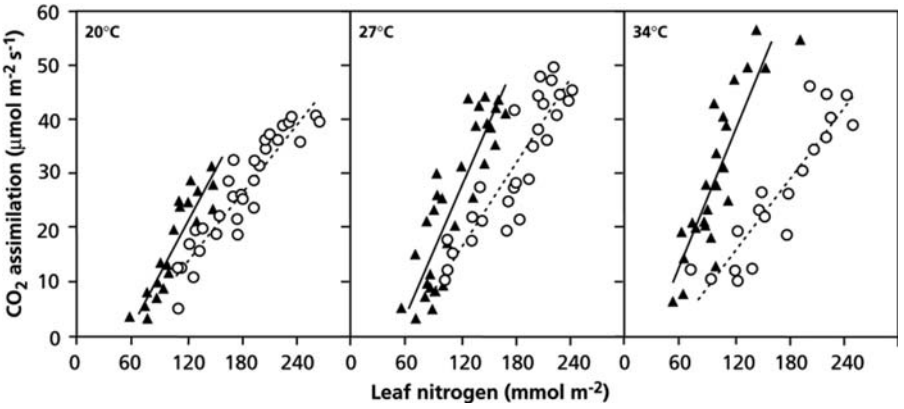

FIGURE 40. The rate of CO_2 assimilation as a function of the organic N concentration in the leaf and the temperature, as measured for the C_3 plant *Chenopodium album* (pigweed, *circles*) and the C_4 plant *Amaranthus retroflexus* (*triangles*) (after Sage & Pearcy 1987b). Copyright American Society of Plant Biologists.

pica, seepweed) and *Bienertia cycloptera* have the complete C_4 cycle operating in mesophyll cells. PEP carboxylation and regeneration occur at the distal ends of the cell exposed to the intercellular air spaces. The C_4 acids produced must therefore diffuse from here to the opposite, proximal end of the cell where they are decarboxylated. An elongated vacuole provides high resistance to CO_2 efflux and thus CO_2 accumulates where Rubisco is located. In this regard, the general layout of these C_3–C_4 intermediates is similar to that of Kranz-type C_4 plants, the major difference being the lack of a cell wall segregating the PCA and PCR compartments (Sage 2002, 2004). The existence of single-cell C_4 in terrestrial plants opens new possibilities for introducing the C_4 pathway in C_3 crops, because it does not require complicated anatomical changes (Surridge 2002).

Over 20 plant species exhibit photosynthetic traits that are intermediate between C_3 and C_4 plants (e.g., species in the genera *Alternanthera*, *Flaveria*, *Neurachne*, *Moricandia*, *Panicum*, and *Parthenium*). These show **reduced** rates of**photorespiration** and **CO_2-compensation points** in the range of 8 to 35 μmol mol^{-1}, compared with 40–50 μmol mol^{-1} in C_3 and 0 to 5 μmol mol^{-1} in C_4 plants (Table 10). They have a weakly developed Kranz anatomy, compared with the true C_4 species, but Rubisco is located both in the mesophyll and the bundle sheath cells (Brown & Bouton 1993).

Two main types of intermediates are distinguished. In the first type (e.g., *Alternanthera ficoides*, *Alternanthera enella*, *Moricandia arvensis*, and *Panicum milioides*) the activity of key enzymes of the C_4 pathway is very low, and they do not have a functional C_4 acid cycle. Their low CO_2-compensation point is due to the light-dependent recapture by mesophyll cells of CO_2 released in photorespiration in the bundle sheath cells, which contain a large fraction of the organelles involved in photorespiration, compared with that in C_3 species (Table 10). In these C_3–C_4 intermediates a system has evolved to salvage CO_2 escaping from the bundle sheath cells, but they do not have the CO_2-concentrating mechanism of true C_4 species (Ehleringer & Monson 1993). In the leaves of this type of intermediate species, **glycine decarboxylase**, a key enzyme in photorespiration that releases the photorespiratory CO_2, occurs exclusively in the cells surrounding the vascular bundle sheath (Morgan et al. 1992). Products of the oxygenation reaction, including glycine, probably move to the bundle sheath cells. Presumably, the products are metabolized in the bundle sheath, so that serine can move back to the mesophyll (Fig. 41). Due to the exclusive location of glycine decarboxylase in the bundle sheath cells, the release of CO_2 in photorespiration occurs close to the vascular tissue, with chloroplasts occurring between these mitochondria and the intercellular spaces.

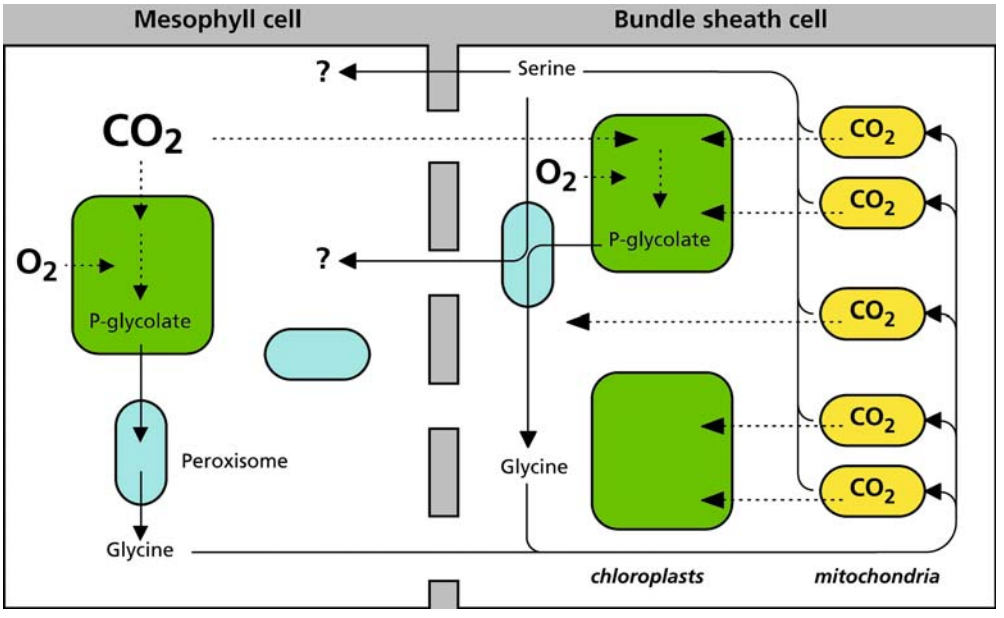

FIGURE 41. A model of the photorespiratory metabolism in leaves of the C_3–C_4 intermediate *Moricandia arvensis*, showing the recapture of CO_2 released by glycine decarboxylase. The model accounts for the low CO_2-compensation point and the low apparent rate of photorespiration in this type of intermediate (Morgan et al. 1992). Copyright SPB Academic Publishing.

Glycine decarboxylase is only found in the enlarged mitochondria arranged along the cell walls adjacent to the vascular tissue and overlain by chloroplasts. This location of glycine decarboxylase increases the diffusion path for CO_2 between the site of release and the atmosphere and allows the recapture of a large fraction of the photorespiratory CO_2, released by glycine decarboxylase, by Rubisco located in the bundle sheath. The location of glycine decarboxylase in the bundle sheath allows some build-up of CO_2, but not to the same extent as in the true C_4 plants. Since the oxygenation reaction of Rubisco is only suppressed in the bundle sheath, and there probably only partly, whereas oxygenation in the mesophyll cells occurs to the same extent as in C_3 plants, the advantage in terms of the net rate of CO_2 assimilation is rather small, compared with that in a true C_4 plant (Von Caemmerer 1989).

In the second type of intermediate species (e.g., *Flaveria anomala* and *Neurachne minor*), the activity of key enzymes of the C_4 pathway is considerable. Rapid fixation of $^{14}CO_2$ into C_4 acids, followed by transfer of the label to Calvin-cycle intermediates, has been demonstrated. These species have a limited capacity for C_4 photosynthesis, but lower quantum yields than either C_3 or C_4, presumably because the operation of the C_4 cycle in these plants does not really lead to a concentration of CO_2 to the extent it does in true C_4 species.

In addition to the C_3–C_4 intermediate species, there are some species [e.g., *Eleocharis vivipara* (sprouting spikerush) and *Nicotiana tabacum* (tobacco)] that are capable of either C_3 or C_4 photosynthesis in different tissues (Ueno et al. 1988, Ueno 2001). Tobacco, a typical C_3 plant, shows characteristics of C_4 photosynthesis in cells of stems and petioles that surround the xylem and phloem; these cells are supplied with carbon for photosynthesis from the vascular system, and not from stomata. These photosynthetic cells possess high activities of enzymes characteristic of C_4 photosynthesis which allows the decarboxylation of four-carbon organic acids from the xylem and phloem, thus releasing CO_2 for photosynthesis (Hibberd & Quick 2002).

C_4 plants that can shift to a CAM mode occur in the genus *Portulaca* (Sect. 10.4).

9.6 Evolution and Distribution of C_4 Species

C_4 species represent approximately 5% of all higher plant species, C_3 species accounting for about 85% and CAM species (Sect. 10) for 10%. C_4 photosynthesis first arose in grasses, 24–35 million years ago, and in dicots 15–21 million years ago (Sage 2004). However, it took several millions of years before the C_4 pathway spread on several continents and became dominant over large areas, between 8 and 6 million years ago, as indicated by changes in the carbon-isotope ratios of fossil tooth enamel in Asia, Africa, North America, and South America (Cerling et al. 1997). A decreasing **atmospheric CO_2 concentration**, as a result of the photosynthetic activity of plants and possibly much more so due to tectonic and subsequent geochemical events, has been a significant factor contributing to C_4 evolution. Briefly, the collision of the Indian subcontinent caused the uplift of the Tibetan Plateau. With this, Earth crust consuming CO_2 became exposed over a vast area. The reaction $CaSiO_3 + CO_2 <---> CaCO_3 + SiO_2$ is responsible for the dramatic decline in atmospheric CO_2 concentration (Raymo & Ruddiman 1992, Ehleringer & Monson 1993). Since CO_2 levels were already low when the first C_4 plants evolved, other factors must have been responsible for the rapid spread of C_4 plants many millions of years after they first arose.

The universal carboxylating enzyme Rubisco does not operate efficiently at the present low CO_2 and high O_2 atmospheric conditions. Low atmospheric CO_2 concentrations would increase photorespiration and thus favor the **CO_2-concentrating mechanisms** and **lack of photorespiration** that characterize C_4 species. Considering the three subtypes of C_4 species and their occurrence in at least 19 different families of widely different taxonomic groups, C_4 plants must have evolved from C_3 ancestors independently about 48 times on different continents (**convergent evolution**) (Table 7). Morphological and eco-geographical information combined with molecular evidence suggests that C_4 photosynthesis has evolved twice in different lineages within the genus *Flaveria* (Sage 2004). The physiology of C_3–C_4 intermediates suggests that the mechanism to recapture CO_2 evolved before the CO_2-concentrating mechanism (Sect. 9.5). The phylogeny of *Flaveria* species, as deduced from an analysis of the nucleotide sequences encoding a subunit of glycine decarboxylase, suggests that C_4 species originated from C_3–C_4 intermediates, and that C_4 in this genus developed relatively recently (Sage 2004).

C_4 photosynthesis originated in **arid regions** of low latitude, where **high temperatures** in combination with **drought** and/or **salinity**, due to a globally drying climate and increased **fire frequency**, promoted the spread of C_4 plants (Keeley & Rundel 2005, Beerling & Osborne 2006). A major role for climatic factors as the driving force for C_4 evolution is also indicated by C_4 distributions in

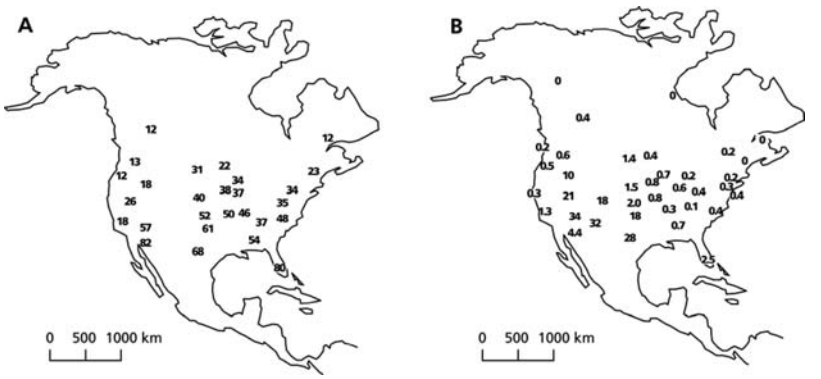

FIGURE 42. Geographic distribution of C_4 species in North America. *Left*: percentage of grass taxa that are C_4 plants. *Right*: percentage of dicotyledon taxa that are C_4 plants in regional floras of North America (Teeri & Stowe 1976, and Stowe & Teeri 1978, as cited in Osmond et al. 1982).

Mesoamerican sites that have experienced contrasting moisture variations since the last glacial maximum. Analyses of the carbon-isotope composition of leaf wax components indicate that regional climate exerts a strong control over the relative abundance of C_3 and C_4 species, and that in the absence of favorable moisture and temperature conditions a low atmospheric CO_2 concentration alone does not favor C_4 expansion (Huang et al. 2001).

Low altitudes in tropical areas continue to be centers of distribution of C_4 species. Tropical and temperate lowland grasslands, with abundant warm-season precipitation, are dominated by C_4 species. At higher elevations in these regions C_3 species are dominant, both in cover and in composition, for example on the summits of the Drakenberg in South Africa (Vogel et al. 1978) and on highland plains in a temperate arid region of Argentinia (Cavagnaro 1988).

The high concentration of CO_2 at the site of Rubisco, allows net CO_2 assimilation at relatively high temperatures, where photorespiration results in low net photosynthesis of C_3 species due to the increased oxygenating activity of Rubisco. This explains why C_4 species naturally occur in warm, open ecosystems, where C_3 species are less successful (Figs. 42 and 43). There is no a priori reason, however, why C_4 photosynthesis could not function in cooler climates. The lower quantum yield of C_4 species at low temperature would be important in dense canopies where light limits photosynthesis (and where **quantum yield** is therefore important). Quantum yield, however, is less important at higher levels of irradiance, and there is quite a wide tem-

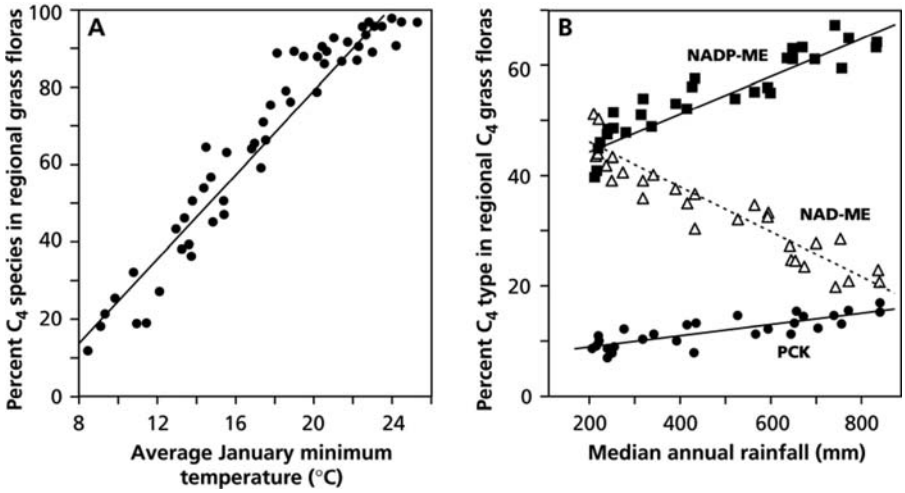

FIGURE 43. *Left*: The percentage occurrence of C_4 metabolism in grass floras of Australia in relation to temperature in the growing season (January). *Right*: The percentage occurrence of C_4 grass species of the three metabolic types in regional floras in Australia in relation to median annual rainfall (Henderson et al. 1995).

perature range where the quantum yield is still high compared with that of C_3 plants (Fig. 39). The high sensitivity to low temperature of pyruvate P_i-dikinase, a key enzyme in the C_4 pathway may be the main reason why C_4 species have rarely expanded to cooler places (Sect. 7.2). Compatible solutes can decrease the low-temperature sensitivity of this enzyme and this could allow the expansion of C_4 species into more temperate regions in the future. Alternatively, rising atmospheric CO_2 concentration may offset the advantages of the CO_2-concentrating mechanism of C_4 photosynthesis (Sect. 12).

9.7 Carbon-Isotope Composition of C_4 Species

Although Rubisco of C_4 plants discriminates between $^{12}CO_2$ and $^{13}CO_2$, just like that of C_3 plants, the fractionation in C_4 species is considerably less than that in C_3 plants. This is explained by the small extent to which inorganic carbon **diffuses back** from the vascular bundle to the mesophyll (Sect. 9.2). Moreover, the inorganic carbon that does diffuse back to the mesophyll cells will be **refixed** by PEP carboxylase, which has a very high affinity for bicarbonate (Box 2A.2). Most of the $^{13}CO_2$ that accumulates in the bundle sheath is ultimately assimilated; hence the isotope fractionation of CO_2 is very small in C_4 species (Fig. 44).

The isotopic differences between C_3 and C_4 plants (Fig. 44) are large compared with isotopic changes occurring during digestion by herbivores or decomposition by soil microbes. This makes it possible to determine the relative abundance of C_3 and C_4 species in the diets of animals by analyzing tissue samples of animals ("You are what you eat") or as sources of soil organic matter in paleosols (old soils). These studies have shown that many generalist herbivores show a preference for C_3 rather than C_4 plants (Ehleringer & Monson 1993). C_3 species, however, also tend to have more toxic secondary metabolites, which cause other herbivores to show exactly the opposite preference.

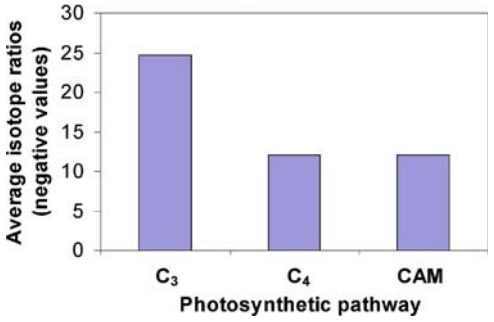

FIGURE 44. The carbon-isotope composition of C_3, C_4, and CAM plants (Sternberg et al. 1984).

10. CAM Plants

10.1 Introduction

In addition to C_3 and C_4 species, there are many succulent plants with another photosynthetic pathway: **Crassulacean Acid Metabolism** (CAM). This pathway is named after the Crassulaceae, a family in which many species show this type of metabolism. CAM, however, also occurs commonly in other families, such as the Cactaceae, Euphorbiaceae, Orchidaceae, and Bromeliaceae [e.g., *Ananas comosus* (pineapple)]. There are about 10000 CAM species from 25 to 30 families (Table 11), all angiosperms, with the exception of a few fern species that also have CAM characteristics.

The unusual capacity of CAM plants to fix CO_2 into organic acids in the dark, causing **nocturnal acidification**, with de-acidification during the day, has been known for almost two centuries. A full appreciation of CAM as a photosynthetic process was greatly stimulated by analogies with C_4 species.

The productivity of most CAM plants is fairly low. This is not an inherent trait of CAM species, however, because some cultivated CAM plants (e.g., *Agave mapisaga* and *Agave salmiana*) may achieve an average above-ground productivity of 4 kg dry mass $m^{-2}yr^{-1}$. An even higher productivity has been observed for irrigated, fertilized, and carefully pruned *Opuntia amyclea* and *Opuntia ficus-indica*

TABLE 11. Taxonomic survey of flowering plant families known to have species showing crassulacean acid metabolism (CAM) in different taxa.

Agavaceae	Geraniaceae
Aizoaceae	Gesneriaceae
Asclepidiaceae	Labiatae
Asteraceae	Liliaceae
Bromeliaceae	Oxalidaceae
Cactaceae	Orchidaceae
Clusiaceae	Piperaceae
Crassulaceae	Polypodiaceae
Cucurbitaceae	Portulacaceae
Didieraceae	Rubiaceae
Euphorbiaceae	Vitaceae

Source: Kluge & Ting (1978) and Medina (1996).

(prickly pears) (4.6 kg m^{-2} yr^{-1}; Nobel et al. 1992). These are among the highest productivities reported for any species. In a comparison of two succulent species with similar growth forms, *Cotyledon orbiculata* (pig's ear) (CAM) and *Othonna optima* (C_3), during the transition from the rainy season to subsequent drought, the daily net rate of CO_2 assimilation is similar for the two species. This shows that rates of photosynthesis of CAM plants may be as high as those of C_3 plants, if morphologically similar plants adapted to the similar habitats are compared (Eller & Ferrari 1997).

As with C_4 plants, none of the enzymes or metabolic reactions of CAM are really unique to these species. The reactions proceed at different times of the day, however, quite distinct from C_3 and C_4 species. Based on differences in the major decarboxylating enzyme, two subtypes of CAM species are discerned (Sect. 10.2). In addition, there are intermediate forms between C_3 and CAM, as well as facultative CAM plants (Sect. 10.4).

10.2 Physiological, Biochemical, and Anatomical Aspects

CAM plants are characterized by their **succulence** (but this is not pronounced in epiphytic CAM plants; Sect. 10.5), the capacity to fix CO_2 at night via **PEP carboxylase**, the accumulation of **malic acid** in the vacuole, and subsequent de-acidification during the day, when CO_2 is released from malic acid and fixed in the Calvin cycle, using Rubisco.

CAM plants show a strong fluctuation in pH of the cell sap, due to the synthesis and breakdown of malic acid. The concentration of this acid may increase to 100 mM. By isolating vacuoles of the CAM plant *Kalanchoe daigremontiana* (devil's backbone), it was shown that at least 90% of all the acid in the cells is in the vacuole. The kinetics of malic acid efflux from the leaves of *Kalanchoe daigremontiana* provides further evidence for the predominant location of malic acid in the vacuole.

At night, CO_2 is fixed in the cytosol, catalyzed by **PEP carboxylase**, producing oxaloacetate (Fig. 45). PEP originates from the breakdown of glucose in glycolysis; glucose is formed from starch. Oxaloacetate is immediately reduced to malate, catalyzed by malate dehydrogenase. Malate is transported to the large vacuoles in an energy-dependent manner. A H^+-ATPase and a pyrophosphatase pump H^+ into the vacuole, so that malate can move down an electrochemical potential gradient (Sect. 2.2.2 of Chapter 6 on mineral nutrition). In the vacuole it will be present as malic acid.

The release of malic acid from the vacuole during the day is supposedly passive. Upon release it is decarboxylated, catalyzed by **malic enzyme** (NAD- or NADP-dependent), or by **PEP carboxykinase** (PEPCK). Like C_4 species, CAM species are subdivided depending on the decarboxylating enzyme. The malic enzyme subtypes (ME-CAM) have a cytosolic NADP-malic enzyme, as well as a mitochondrial NAD-malic enzyme; they use a chloroplastic pyruvate P_i-dikinase to convert the C_3 fragment originating from the decarboxylation reaction into carbohydrate via PEP. PEPCK-type CAM plants have very low malic enzyme activities (as opposed to PEPCK-C_4 plants) and no pyruvate P_i-dikinase activity, but high activities of PEP carboxykinase.

The C_3 fragment (pyruvate or PEP) that is formed during the decarboxylation, is converted into starch and the CO_2 that is released is fixed by **Rubisco**, much the same as in C_3 plants. During the decarboxylation of malic acid and the fixation of CO_2 by Rubisco in the Calvin cycle, the stomata are closed. They are open during the nocturnal fixation of CO_2.

The CAM traits can be summarized as follows:

1. Fluctuation of organic acids, mainly of malic acid, during a diurnal cycle;
2. Fluctuation of the concentration of sugars and starch, opposite to the fluctuation of malic acid;
3. A high activity of PEP carboxylase (at night) and of a decarboxylase (during the day);
4. Large vacuoles in cells containing chloroplasts;
5. Some degree of succulence;
6. The CO_2 assimilation by the leaves occurs predominantly at night.

Four "phases" in the diurnal pattern of CAM are discerned (Fig. 46). **Phase I**, the carboxylation phase, starts at the beginning of the night. Toward the end of the night, the rate of carboxylation declines and the malic acid concentration reaches its maximum. The stomatal conductance and the CO_2 fixation change more or less in parallel. During phase I, carbohydrates are broken down. **Phase II**, at the beginning of the day, is characterized by a high rate of CO_2 fixation, generally coinciding with an increased stomatal conductance. CO_2 fixation by PEP carboxylase and malic acid formation coincide with the fixation of CO_2 by Rubisco. Gradually, fixation by PEP carboxylase is taken over by fixation by Rubisco. In the last part of phase II, C_3 photosynthesis predominates, using exogenous CO_2 as the substrate. Phase II typically occurs

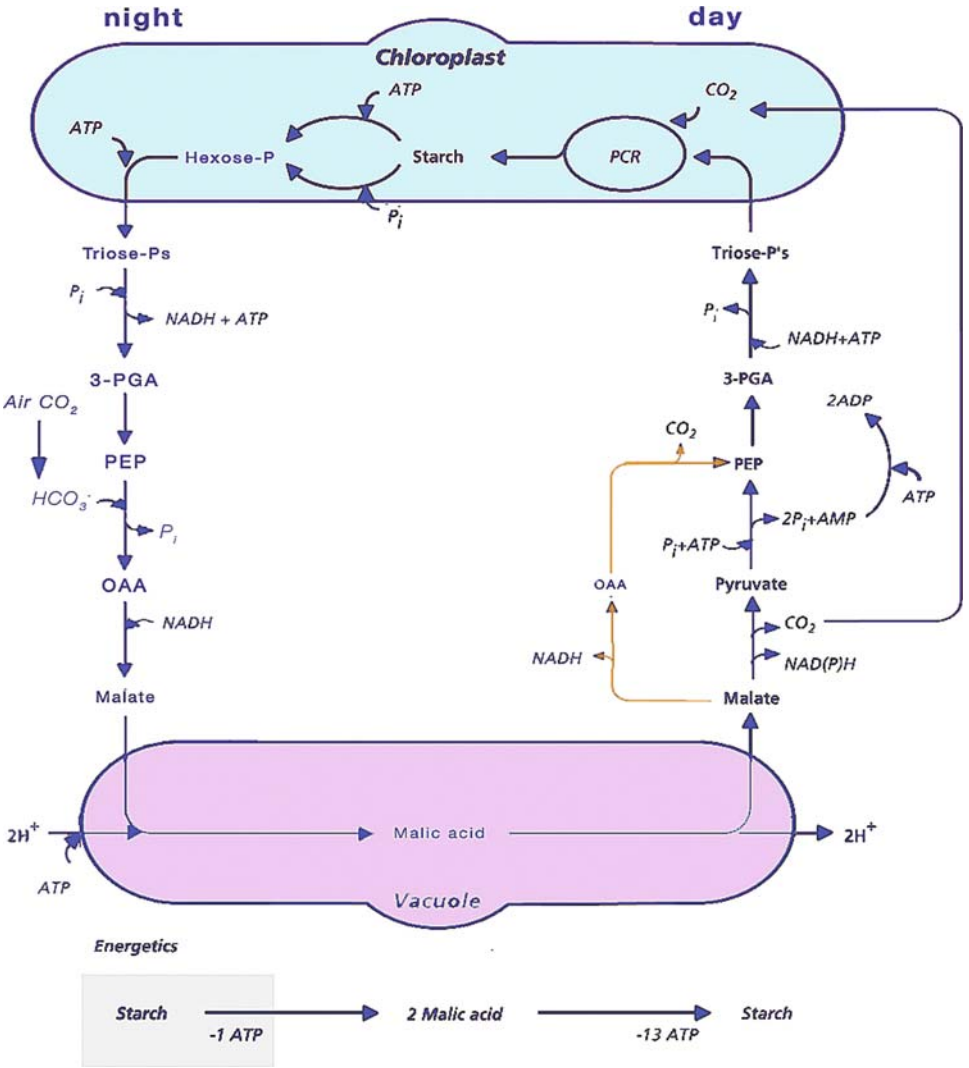

FIGURE 45. Metabolic pathway and cellular compartmentation of Crassulacean Acid Metabolism (CAM), showing the separation in night and day of carboxylation and decarboxylation. The steps specific for PEPCK-CAM plants are depicted in red.

under laboratory conditions, following an abrupt dark-to-light transition, but is not apparent under natural conditions. In **phase III** the stomata are fully closed and malic acid is decarboxylated. The C_i may then increase to values above 10000 µmol mol^{-1}. This is when normal C_3 photosynthesis takes place and when sugars and starch accumulate. When malic acid is depleted, the stomata open again, possibly because C_i drops to a low level; this is the beginning of **phase IV**. Gradually more exogenous and less endogenous CO_2 is being fixed by Rubisco. In this last phase, CO_2 may be fixed by PEP carboxylase again, as indicated by the photosynthetic quotient (PQ), i.e., the ratio of O_2 release and CO_2 uptake. Over an entire day the PQ is about 1 (Table 12), but deviations from this value occur, depending on the carboxylation process (Fig. 47).

In phase III, when the stomata are fully closed, malic acid is decarboxylated, and the C_i is very high, **photorespiration** is suppressed, as indicated by the relatively slow rate of O_2 uptake (as measured using $^{18}O_2$; Fig. 47). In phase IV, when malic acid is depleted and the stomata open again, photorespiration does occur, as demonstrated by increased uptake of $^{18}O_2$.

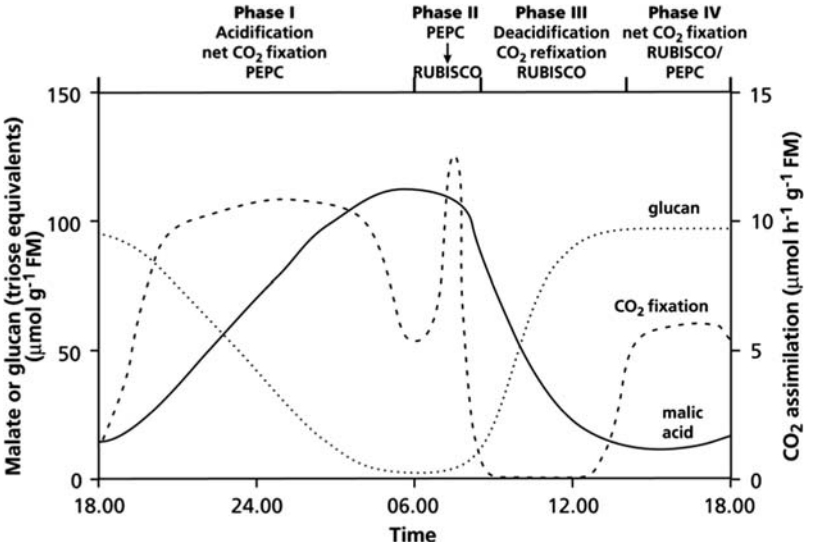

FIGURE 46. CO_2 fixation in CAM plants, showing diurnal patterns for net CO_2 assimilation, malic acid concentration and carbohydrate concentrations (PEPC is PEP carboxylase). Four phases are distinguished, as described in Sect. 10.2 (after Osmond & Holtum 1981).

How do CAM plants regulate the activity of the two carboxylating enzymes and decarboxylating enzymes in a coordinated way to avoid futile cycles? Rubisco is inactive at night for the same reason as in C_3 plants: this enzyme is part of the Calvin cycle that depends on the light reactions and is inactivated in the dark (Sect. 3.4.2). In addition, the kinetic properties of PEP carboxylase are modulated. In *Mesembryanthemum crystallinum* (ice plant) and in *Crassula argentea* (jade plant), PEP carboxylase occurs in two configurations: a "day-configuration" and a "night-configuration". The night-configuration is relatively insensitive to malate (the K_i for malate is 0.06–0.9 mM, depending on pH) and has a high affinity for PEP (the K_m for PEP is 0.1–0.3 mM). The day-configuration is strongly inhibited by malate (the K_i for malate is 0.004–0.07 mM, again depending on the pH) and has a low affinity for PEP (the K_m for PEP is 0.7–1.25 mM). Therefore, when malate is rapidly exported to the vacuole at night in phase I, the carboxylation of PEP readily takes place, whereas it is suppressed during the day in phase III. The modification of the kinetic properties involves the **phosphorylation** and **de-phosphorylation** of PEP carboxylase (Nimmo et al. 2001).

Through modification of its kinetic properties, the inhibition of PEP carboxylase prevents a futile cycle of carboxylation and concomitant decarboxylation reactions. Further evidence that such a futile cycle does not occur comes from studies on the labeling with ^{13}C of the first or fourth carbon atom in malate. If a futile cycle were to occur, doubly labeled malate should appear, as fumarase in the mitochondria would randomize the label in the malate molecule. Such randomization only occurs during the acidification phase, indicating rapid exchange of the malate pools of the cytosol and the mitochondria, before malate enters the vacuole.

TABLE 12. Cumulative daily net CO_2 and O_2 exchange in the dark and in the light periods (12 hours each) and the daily Photosynthetic Quotient for the entire 24 hours period of a shoot of *Ananas comosus* (pineapple).*

	Cumulative daily net CO_2 and O_2 exchange (mmol shoot^{-1}]				
	Dark		Light		
	CO_2 assimilation	O_2 consumption	CO_2 assimilation	O_2 release	Daily Photosynthetic Quotient
Day 1	10.6	6.4	10.4	27.1	0.99
Day 2	11.1	6.3	10.7	27.5	0.98

***Source*: Coté et al. (1989).**

*** Photosynthetic quotient is the ratio of the total net amount of O_2 evolved to the net CO_2 fixed in 24 hours (i.e., the total amount of O_2 evolved in the light period minus the total amount of O_2 consumed in the dark period) to the total amount of CO_2 fixed in the light plus dark period. Measurements were done over two consecutive days.**

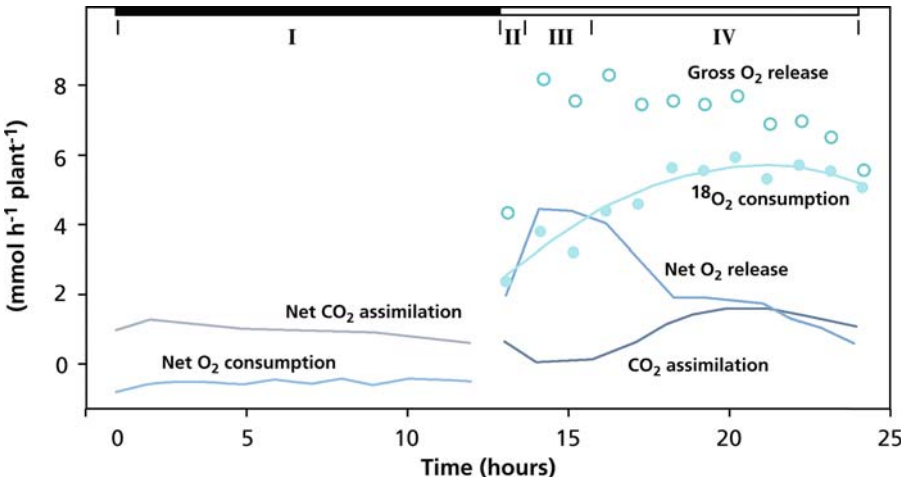

FIGURE 47. Gas exchange of *Ananas comosus* (pineapple) during the dark and light period. O_2 consumption during the day is measured using the stable isotope $^{18}O_2$. Gross O_2 release is the sum of net O_2 production and $^{18}O_2$ consumption. The phases are the same as those shown in Fig. 45 (after Coté et al. 1989). Copyright American Society of Plant Biologists.

TABLE 13. Effects of malate and glucose-6-phosphate (G6P) on the kinetic parameters of PEP carboxylase.*

	V_{max} mmol mg^{-1} (Chl) min^{-1}	Ratio	K_m mM	Ratio
Control	0.42	1.0	0.13	1.0
+ 1 mM G6P	0.45	1.07	0.08	0.61
+ 2 mM G6P	0.47	1.12	0.05	0.39
+ 5 mM malate	0.31	0.74	0.21	1.60
+ 5 mM malate and 2 mM G6P	0.34	0.81	0.05	0.39

Next to malate, glucose 6-phosphate is also an effector of PEP carboxylase (Table 13). The physiological significance of this effect is that glucose 6-phosphate, which is produced from glucose, during its conversion into PEP thus stimulates the carboxylation of PEP.

Temperature has exactly the opposite effect on the kinetic properties of PEP carboxylase from a CAM plant and that from a C_4 plant (Fig. 48). These temperature effects help to explain why a low temperature at night enhances acidification.

10.3 Water-Use Efficiency

Since CAM plants keep their stomata closed during the day when the vapor pressure difference (w_i–w_a) between the leaves and the surrounding air is highest, and open at night when w_i–w_a, is lowest, they have a very high **water-use efficiency**. As long as they are not severely stressed which leads to complete closure of their stomata, the WUE of CAM plants tends to be considerably higher than that of both C_3 and C_4 plants (Table 8 in Chapter 3 on plant water relations).

Populations of the leaf-succulent *Sedum wrightii* (Crassulaceae) differ greatly in their leaf thickness, $\delta^{13}C$ values (ranging from –13.8 to –22.9‰), the proportion of day *vs.* night CO_2 uptake, and growth. The largest plants exhibit the greatest proportion of day *vs.* night CO_2 uptake and hence the lowest WUE, suggesting an inverse relation between the plants' ability to conserve water and their ability to gain carbon (Kalisz & Teeri 1986).

10.4 Incomplete and Facultative CAM Plants

When exposed to severe desiccation, some CAM plants may not even open their stomata during the

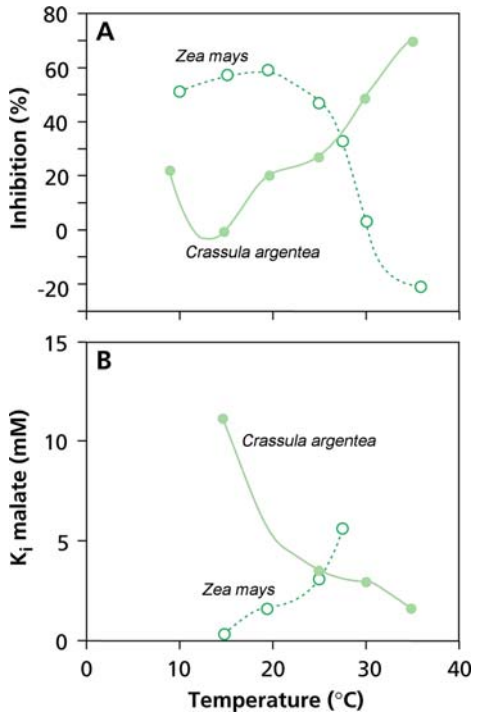

FIGURE 48. The effect of temperature on kinetic properties of PEP carboxylase from leaves of a *Crassula argenta* (jade plant, a CAM plant) and *Zea mays* (corn, a C_4 plant). (A) Effect on percent inhibition by 5 mM malate. (B) Effect on the inhibition constant (K_i) for malate (Wu & Wedding 1987). Copyright American Society of Plant Biologists.

night (Bastide et al. 1993), but they may continue to show a diurnal fluctuation in malic acid concentration, as first found in *Opuntia basilaris* (prickly pear). The CO_2 they use to produce malic acid at night does not come from the air, but is derived from respiration. It is released again during the day, allowing some Rubisco activity. This metabolism is termed **CAM idling**. Fluorescence measurements have indicated that the photosystems remain intact during severe drought. CAM idling can be considered as a modification of normal CAM. The plants remain "ready to move" as soon as the environmental conditions improve, but keep their stomata closed during severe drought.

Some plants show a diurnal fluctuation in the concentration of malic acid without a net CO_2 uptake at night, but with normal rates of CO_2 assimilation during the day. These plants are capable of **recapturing** most of the CO_2 derived from dark respiration at night, and to use this as a substrate for PEP carboxylase. This is termed **CAM cycling** (Patel & Ting 1987). In *Peperomia camptotricha*, 50% of the CO_2 released in respiration during the night is fixed by PEP carboxylase. At the beginning of the day, some of the CO_2 that is fixed at night becomes available for photosynthesis, even when the stomatal conductance is very low. In *Talinum calycinum* (fame flower), naturally occurring on dry rocks, CAM cycling may reduce water loss by 44%. CAM cycling enhances a plant's water-use efficiency (Harris & Martin 1991).

CAM idling typically occurs in ordinary CAM plants that are exposed to severe water stress and have a very low stomatal conductance throughout the day and night. CAM cycling occurs in plants that have a high stomatal conductance and normal C_3 photosynthesis during the day, but refix the CO_2 produced in dark respiration at night which ordinary C_3 plants lose to the atmosphere.

In a limited number of species, CAM only occurs upon exposure to drought stress: **facultative CAM plants**. For example, in plants of *Agave deserti*, *Clusia uvitana, Mesembryanthemum crystallinum* (ice plant), and *Portulacaria afra* (elephant's foot), irrigation with saline water or drought can change from a virtually normal C_3 photosynthesis to the CAM mode (Fig. 49; Winter et al. 1992). We know of one genus containing C_4 species that can shift from a normal C_4 mode under irrigated conditions, to a CAM mode under water stress: *Portulaca grandiflora* (moss rose), *Portulaca mundula* (hairy purslane), and *Portulaca oleracea* (common purslane) (Koch & Kennedy 1982, Mazen 1996). The transition from the C_3 or C_4 to the CAM mode coincides with an enhanced PEP carboxylase activity and of the mRNA encoding this enzyme. Upon removal of NaCl from the root environment of *Mesembryanthemum crystallinum* (ice plant), the level of mRNA encoding PEP carboxylase declines in 2 to 3 hours by 77%. The amount of the PEP carboxylase enzyme itself declines more slowly: after 2 to 3 days the activity is half its original level (Vernon et al. 1988).

10.5 Distribution and Habitat of CAM Species

CAM is undoubtedly an adaptation to drought, since CAM plants close their stomata during most of the day. This is illustrated in a survey of epiphytic bromeliads in Trinidad (Fig. 50). There are two major ecological groupings of CAM plants: **succulents** from arid and semi-arid regions and **epiphytes** from tropical and subtropical regions (Ehleringer & Monson 1993). In addition, there are some submerged aquatic plants exhibiting CAM (Sect. 11.5). Although CAM plants are uncommon

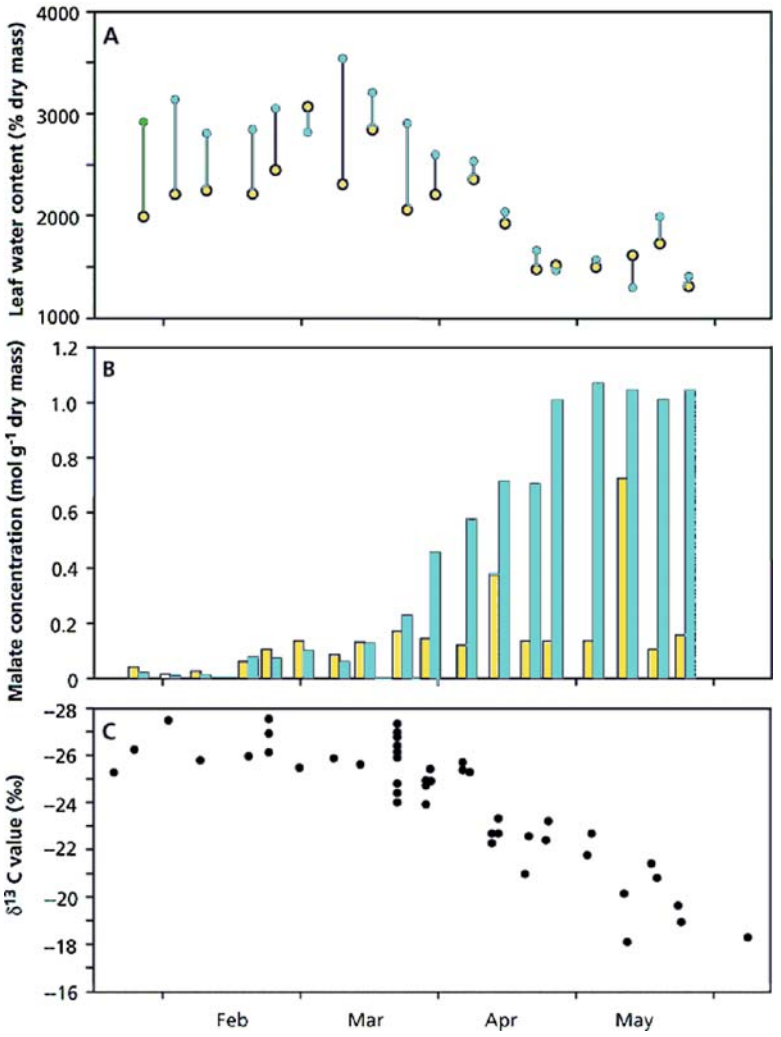

FIGURE 49. Induction of CAM in the facultative CAM species *Mesembryanthemum crystallinum* (ice plant), growing in its natural habitat on rocky coastal cliffs of the Mediterranean Sea. Upon prolonged exposure to drought, the leaf water content (A) declines, and the nocturnal malate concentration (B) increases (yellow symbols and bars, day; turquoise symbols and bars, night). There is a shift from the C_3 mode to CAM, coinciding with less carbon-isotope fractionation (C) (Osmond et al. 1982).

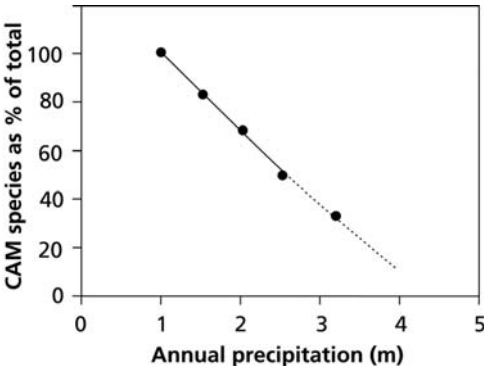

FIGURE 50. The relationship between percentage of epiphytic bromeliad species with CAM in a tropical forest and mean annual rainfall across the north-south precipitation gradient in Trinidad (Winter & Smith 1996).

in cold environments, this may reflect their evolutionary origin in warm climates rather than a temperature sensitivity of the CAM pathway (Nobel & Hartsock 1990). Roots of some orchids which lack stomata also show CAM.

In temperate regions and alpine habitats worldwide, CAM plants, or species showing incomplete or facultative CAM, occur on shallow soils and rock outcrops, niches that are rather dry in moist climates.

10.6 Carbon-Isotope Composition of CAM Species

Like Rubisco from C_3 and C_4 plants, the enzyme from CAM plants discriminate against $^{13}CO_2$, but,

the fractionation at the leaf level is considerably less than that of C_3 plants and similar to that of C_4 species (Fig. 44). This is expected, as the stomata are closed during malate decarboxylation and fixation of CO_2 by Rubisco. Hence, only a small amount of CO_2 diffuses back from the leaves to the atmosphere, and Rubisco processes the accumulated $^{13}CO_2$ (Sects. 9.3 and 9.4).

Upon a shift from C_3 to CAM photosynthesis in **facultative CAM plants**, the stomata are closed during most of the day and open at night, and the **carbon-isotope fractionation** decreases (Fig. 49). Hence, the carbon-isotope composition of CAM plants can be used as an estimate of the employment of the CAM pathway during past growth.

11. Specialized Mechanisms Associated with Photosynthetic Carbon Acquisition in Aquatic Plants

11.1 Introduction

Contrary to the situation in terrestrial plants, in submerged aquatic plants chloroplasts are frequently located in the **epidermis**. In terrestrial plants, CO_2 diffuses from the air through the stomata to the mesophyll cells. In aquatic plants, where diffusion is directly through the outer epidermal cell walls, the rate of this process is often limiting for photosynthesis. A thick boundary layer around the leaves, and slow diffusion of CO_2 in water limit the rate of CO_2 uptake. How do aquatic plants cope with these problems? To achieve a reasonable rate of photosynthesis and avoid excessive photorespiration, special mechanisms are required to allow sufficient diffusion of CO_2 to match the requirement for photosynthesis. Several specialized mechanisms have evolved in different species adapted to specific environmental conditions. Another feature of the habitat of many submerged aquatics is the low irradiance. Leaves of many aquatics have the traits typical of shade leaves (Sect. 3.2).

11.2 The CO_2 Supply in Water

In fresh water, molecular CO_2 is readily available. Between 10 and 20°C, the partitioning coefficient (that is, the ratio between the molar concentration of CO_2 in air and that in water) is about 1. The equilibrium concentration in water at an atmospheric CO_2 concentration of 380 μmol mol^{-1} is 12 μM (at 25°C, but rapidly decreasing with increasing temperature). Under these conditions, leaves of submerged aquatic macrophytes experience about the same CO_2 concentration as those in air. The **diffusion** of dissolved gasses in water, however, occurs approximately 10^4 times more slowly than in air, leading to rapid depletion of CO_2 inside the leaf during CO_2 assimilation. In addition, the O_2 concentration inside photosynthesizing leaves may increase. Decreasing CO_2 concentrations, especially in combination with increasing O_2, inexorably lead to conditions that restrict the **carboxylating** activity and favor the **oxygenating** activity of Rubisco (Mommer et al. 2005).

The transport of CO_2 through the unstirred **boundary layer** is only by diffusion. The thickness of the boundary layer is proportional to the square root of the leaf dimension, measured in the direction of the streaming water, and inversely proportional to the flow of the streaming water (Sect. 2.4 of Chapter 4A on the plant's energy balance). It ranges from 10 μm in well stirred media, to 500 μm in nonstirred media. The slow diffusion in the boundary layer is often a major factor limiting an aquatic macrophyte's rate of photosynthesis.

CO_2 dissolved in water interacts as follows:

$$H_2O + CO_2 \Leftrightarrow H_2CO_3 \Leftrightarrow H^+ + HCO_3^- \Leftrightarrow 2H^+ + CO_3^{2-} \quad (10)$$

$$HCO_3^- \Leftrightarrow OH^- + CO_2 \quad (11)$$

Since the concentration of H_2CO_3 is very low in comparison with that of CO_2, the two are commonly combined and indicated as $[CO_2]$.

The interconversion between CO_2 and HCO_3^- is slow, at least in the absence of **carbonic anhydrase**. The presence of the dissolved inorganic carbon compounds strongly depends on the pH of the water (Fig. 51). In ocean water, as pH increases from 7.4 to 8.3, the contribution of dissolved inorganic carbon species shifts as follows: CO_2 as a fraction of the total inorganic carbon pool decreases from 4 to 1%, that of HCO_3^- from 96 to 89%, and that of CO_3^{2-} increases from 0.2 to 11%.

During darkness, the CO_2 concentration in ponds and streams is generally high, exceeding the concentration that is in equilibrium with air, due to respiration of aquatic organisms and the slow exchange of CO_2 between water and the air above it. The high CO_2 concentration coincides with a relatively low pH. During the day the CO_2 concentration may decline rapidly due to photosynthetic activity, and the pH rises accordingly. The rise in pH, especially in the boundary layer, represents a crucial problem for

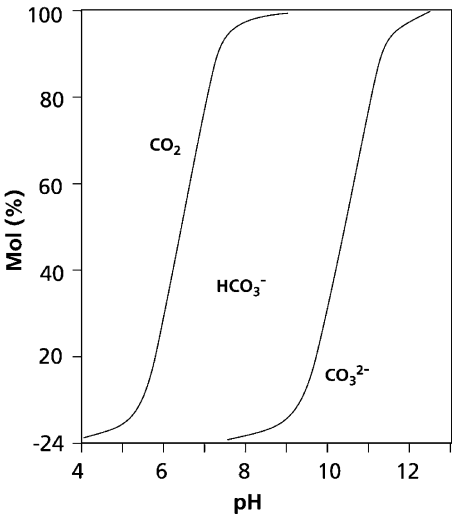

FIGURE 51. The contribution of the different inorganic carbon species as dependent on the pH of the water (Osmond et al. 1982).

CO_2 availability in water at a neutral pH. While the concentration of all dissolved inorganic carbon (i.e., CO_2, HCO_3^-, and CO_3^{2-}) may decline by a few percent only, the CO_2 concentration declines much more, since the high pH shifts the equilibrium from CO_2 to HCO_3^- (Fig. 51). This adds to the diffusion problem and further aggravates the limitation by supply of inorganic carbon for assimilation in submerged leaves that only use CO_2 and not HCO_3^-.

11.3 The Use of Bicarbonate by Aquatic Macrophytes

Many aquatic macrophytes, cyanobacteria, and algae can use HCO_3^-, in addition to CO_2, as a carbon source for photosynthesis (Maberly & Madsen 2002). This might!be achieved either by **active uptake** of HCO_3^- itself, or by **proton extrusion**, commonly at the abaxial side of the leaf, thus lowering the pH in the extracellular space and shifting the equilibrium towards CO_2 (Elzenga & Prins 1988). In some species [e.g., *Elodea canadensis* (waterweed)] the conversion of HCO_3^- into CO_2 is also catalyzed by an extracellular **carbonic anhydrase**. In *Ranunculus penicillatus* spp. *pseudofluitans* (a stream water crowfoot), the enzyme is closely associated with the epidermal cell wall (Newman & Raven 1993). Active uptake of HCO_3^- also requires proton extrusion, to provide a driving force.

Aquatic plants that use HCO_3^- in addition to CO_2 have a mechanism to concentrate CO_2 in their chloroplasts. Although this **CO_2-concentrating mechanism** differs from that of C_4 plants (Sect. 9.2), its effect is similar: it suppresses the oxygenating activity of Rubisco and lowers the CO_2-compensation point. In *Elodea canadensis* (common waterweed), *Potamogeton lucens* (ribbonweed), and other aquatic macrophytes, the capacity to acidify the lower side of the leaves, and thus to use HCO_3^-, is expressed most at high irradiance and low dissolved inorganic carbon concentration in the water (Elzenga & Prins 1989). The capacity of the carbon-concentrating mechanism also depends on the N supply: the higher the supply, the greater the capacity of the photosynthetic apparatus as well as that of the carbon- concentrating mechanism (Madsen & Baattrup- Pedersen 1995). Acidification of the lower side of the leaves is accompanied by an increase in extracellular pH at the upper side of the leaves. The leaves become "polar" when the carbon supply from the water is less than the CO_2-assimilating capacity (Prins & Elzenga 1989). There are also anatomical differences between the upper and lower side of "polar" leaves: the lower epidermal cells are often **transfer cells**, characterized by ingrowths of cell-wall material which increases the surface area of the plasma membrane. They contain numerous mitochondria and chloroplasts. At the upper side of the leaves, the pH increase leads to precipitation of calcium carbonates. This process plays a major role in the geological sedimentation of calcium carbonate (Sect. 11.7).

Due to the use of HCO_3^-, the internal CO_2 concentration may become much higher than it is in terrestrial C_3 plants. This implies that they do not need a Rubisco enzyme with a high affinity for CO_2. Interestingly, just like C_4 plants (Sect. 9.4), they have a Rubisco with a relatively high K_m for CO_2. The values are approximately twice as high as those of terrestrial C_3 plants (Yeoh et al. 1981). This high K_m is associated with a high maximum catalytic activity (k_{cat}) of Rubisco, as in the HCO_3^--using green alga, *Chlamydomonas reinhardtii*, and in C_4 species. For the Rubisco of the cyanobacterium *Synechococcus* that also has a carbon-concentrating mechanism, even higher $K_m(CO_2)$ and k_{cat} values are reported. (Table 9).

Hydrilla verticillata (waterthyme) has an inducible CO_2-concentrating mechanism, even when the pH of the medium is so low that there is no HCO_3^- available. This monocotyledonous species predates modern terrestrial C_4 monocots and may represent an ancient form of C_4 photosynthesis (Magnin et al. 1997). The species has an inducible single-cell

C_4-type photosynthetic cycle (Table 7; Sect. 9.5). This mechanism is induced at high temperatures and when the plants are growing in water that contains low concentrations of dissolved inorganic carbon (Reiskind et al. 1997). There appears to be a clear ecological benefit to this CO_2-concentrating mechanism when the canopy becomes dense, the dissolved O_2 concentration is high, and the CO_2 supply is low. Under these conditions photorespiration decreases photosynthesis of a C_3-type plant by at least 35%, whereas in *Hydrilla verticillata* this decrease is only about 4% (Bowes & Salvucci 1989). A carbon-concentrating mechanism in the form of a single-cell C_4-like pathway has also been identified in a marine diatom of common occurrence in the oceans (Reinfelder et al. 2000), indicating that this pathway is more common than thought previously (Sage 2004).

11.4 The Use of CO_2 from the Sediment

Macrophytes like water lilies that have an internal ventilation system assimilate CO_2 arriving from the roots due to pressurized flow (Sect. 4.1.4 of Chapter 2B on plant respiration). The use of CO_2 from the sediment is only minor for most emergent wetland species such as *Scirpus lacustris* (bull rush) and *Cyperus papyrus* (papyrus), where it approximates 0.25% of the total CO_2 uptake in photosynthesis (Farmer 1996). For *Stratiotes aloides* (water soldier), the sediment is a major source of CO_2, although only after diffusion into the water column (Prins & de Guia 1986). *Stylites andicola* is a vascular land plant without stomata that derives nearly all its carbon through its roots (Keeley et al. 1984).

Submerged macrophytes of the isoetid life form (quillworts) receive a very large portion of their carbon for photosynthesis directly from the sediment via their roots: 60 to 100% (Table 14). This capability is considered an adaptation to growth in low-pH, carbon-poor ("soft-water") lakes, where these plants are common. None of the investigated species from "hard-water" lakes or marine systems show significant CO_2 uptake via their roots (Farmer 1996). In the quillworts, CO_2 diffuses from the sediment, via the lacunal air system to the submerged leaves. These leaves are thick with thick cuticles, have no functional stomata when growing submerged, but large air spaces inside, so that gas exchange with the atmosphere is hampered, but internal exchange is facilitated. Emergent leaves have very few stomata at the leaf base, and normal densities at the leaf tips (Fig. 52). The chloroplasts in isoetid leaves are concentrated around the lacunal system. The air spaces in the leaves are connected with those in stems and roots, thus facilitating the transport of CO_2 from the sediment to the leaves where it is assimilated. At night, only part of the CO_2 coming up from the sediment via the roots through the lacunal system is fixed (Sect. 11.5), the rest being lost to the atmosphere.

Table 14. Assimilation of $^{14}CO_2$ derived from the air or from the rhizosphere by leaves and roots of *Littorella uniflora* (quillwort).*

	$^{14}CO_2$ assimilation[μg C g^{-1} (leaf or root DM) h^{-1}]			
	Leaves		Roots	
Source:	Air	Rhizosphere	Air	Rhizosphere
CO_2 concentration around the roots (mM)				
0.1	300	340	10	60
	(10)	(50)	(0.3)	(70)
0.5	350	1330	10	170
	(5)	(120)	(0.3)	(140)
2.5	370	8340	10	570
	(4)	(1430)	(0.3)	(300)

***Source*: Nielsen et al. (1991).**

*** $^{14}CO_2$ was added to the air around the leaves or to the water around the roots (rhizosphere). Measurements were made in the light and in the dark; values of the dark measurements are given in brackets.**

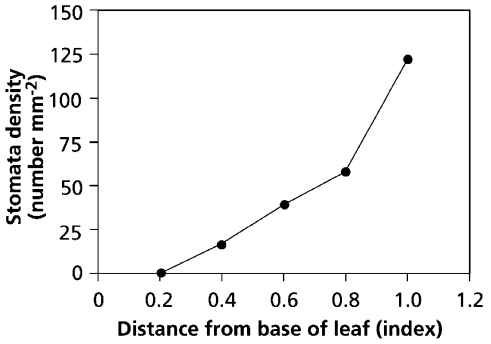

FIGURE 52. The stomatal density along mature leaves of *Littorella uniflora* (shoreweed) from the base to the tip (Nielsen et al. 1991).

11.5 Crassulacean Acid Metabolism (CAM) in Aquatic Plants

Though aquatic plants by no means face the same problems connected with water shortage as desert plants, some of them [*Isoetes* (quillwort) species] have a similar photosynthetic metabolism: Crassulacean Acid Metabolism (CAM) (Keeley 1990). They accumulate **malic acid** during the night and have rates of CO_2 fixation during the night that are similar in magnitude as those during the day, when the CO_2 supply from the water is very low (Fig. 53). The aerial leaves of *Isoetes howellii*, in contrast to the submerged leaves of the same plants, do not show a diurnal fluctuation in the concentration of malic acid.

Why would an aquatic plant have a similar photosynthetic pathway as is common in species from arid habitats? CAM in *Isoetes* is considered an adaptation to very low levels of CO_2 in the water, especially during the day (Fig. 53), and allows the plants to assimilate additional CO_2 at night. This nocturnal CO_2 fixation gives them access to a carbon source that is unavailable to other species. Though some of the carbon fixed in malic acid comes from the surrounding water, where it accumulates due to the respiration of aquatic organisms, some is also derived from the plant's own respiration during the night. A CAM pathway has also been discovered in other genera of aquatic vascular plants (Maberly & Madsen 2002).

11.6 Carbon-Isotope Composition of Aquatic Plants

There is a wide variation in carbon-isotope composition among different aquatic plants, as well as a large difference between aquatic and terrestrial plants (Fig. 54). A low carbon-isotope fractionation might reflect the employment of the C_4 pathway of photosynthesis, although the typical Kranz anatomy is usually lacking. Only about a dozen aquatic C_4 species have been identified, and very few have submersed leaves with a well developed Kranz anatomy (Bowes et al. 2002). A low carbon-isotope fractionation in aquatic plants might also reflect the CAM pathway of photosynthesis. Isoetids often have rather negative $\delta^{13}C$ values, due to the isotope composition of the substrate (Table 15). Four factors account for the observed variation in isotope composition of freshwater aquatics (Keeley & Sandquist 1992):

1. The isotope composition of the carbon source varies substantially. It ranges from a $\delta^{13}C$ value of +1‰, for HCO_3^- derived from limestone, to –30‰, for CO_2 derived from respiration. The average $\delta^{13}C$ value of CO_2 in air is –8‰. The isotope composition also changes with the water depth (Table 16).
2. The species of inorganic carbon fixed by the plant; HCO_3^- has a $\delta^{13}C$ that is 7–11‰ less negative than that of CO_2.
3. Resistance for diffusion across the unstirred boundary layer is generally important (except in rapidly streaming water), thus decreasing carbon-isotope fractionation (Box 2).
4. The photosynthetic pathway (C_3, C_4, and CAM) that represent different degrees of fractionation.

The isotope composition of plant carbon is dominated by that of the source (see 1 and 2 above), because diffusional barriers are strong (see 3). This accounts for most of the variation as described in Fig. 54, rather than biochemical differences in the photosynthetic pathway (Osmond et al. 1982).

11.7 The Role of Aquatic Macrophytes in Carbonate Sedimentation

The capacity of photosynthetic organisms [e.g., *Chara* (musk-grass), *Potamogeton* (pondweed), and *Elodea* (waterweed)] to acidify part of the apoplast and use HCO_3^- (Sect. 11.3) plays a major role in the formation of calcium precipitates in fresh water, on both an annual and a geological time scale. Many calcium-rich lake sediments contain plant-induced carbonates, according to:

$$Ca^{2+} + 2HCO_3^- \rightarrow CO_2 + CaCO_3 \qquad (12)$$

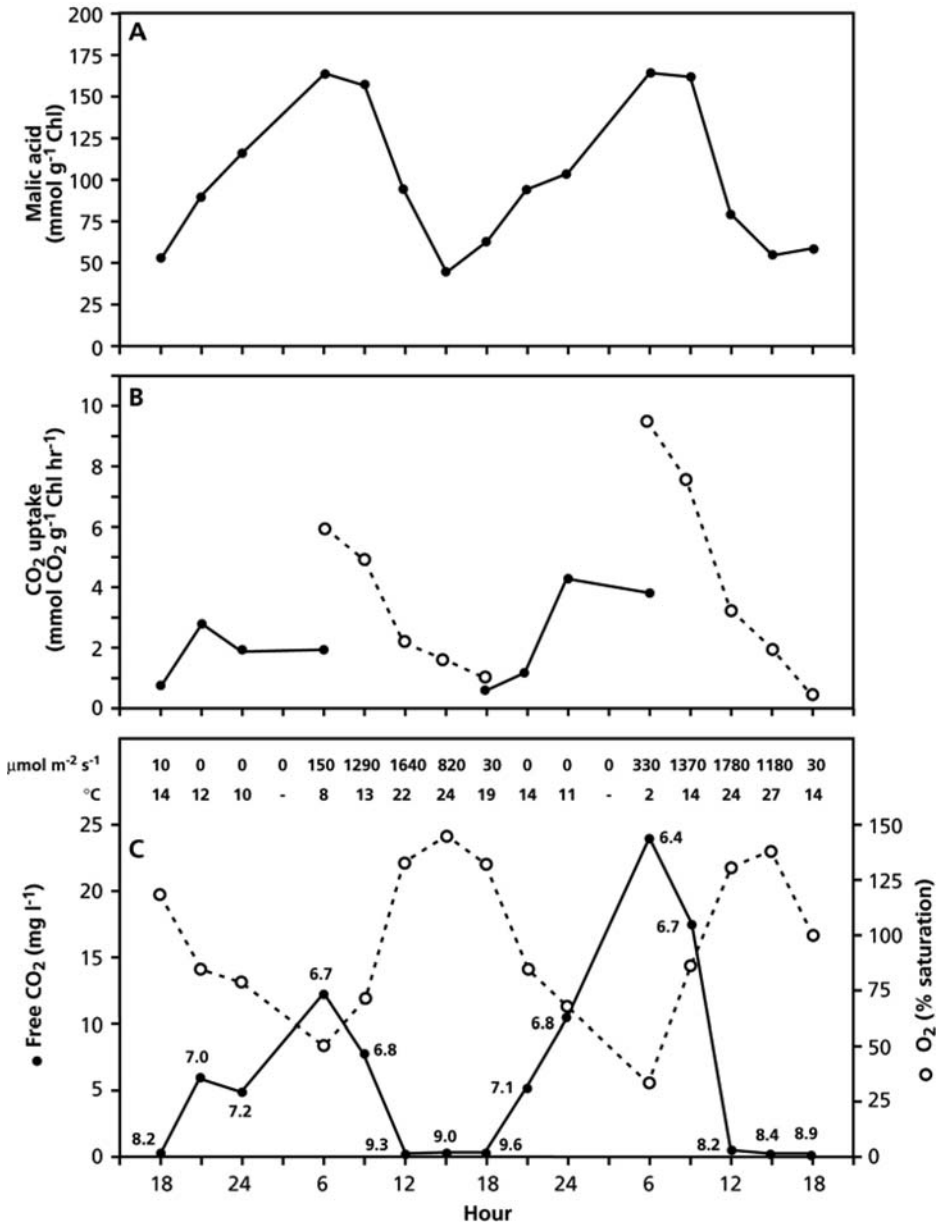

FIGURE 53. CAM photosynthesis in submerged leaves of *Isoetes howellii* (quillwort) in a pool. (A) Malic acid levels, (B) rates of CO_2 uptake, and (C) irradiance at the water surface, water temperatures, and concentrations of CO_2 and O_2; the numbers near the symbols give the pH values. Open and filled symbols refer to the light and dark period, respectively (after Keeley & Busch 1984). Copyright American Society of Plant Biologists.

This reaction occurs in the alkaline compartment that is provided at the upper side of the polar leaves of aquatic macrophyytes (Sect. 11.3). Similar amounts of carbon are assimilated in photosynthesis and precipitated as carbonate. If only part of the CO_2 released in this process is assimilated by the macrophyte, as may occur under nutrient-deficient conditions, CO_2 is released to the atmosphere. On the other hand, if the alkalinity of the compartment is relatively low, there is a net transfer of atmospheric CO_2 to the water (McConnaughey et al. 1994).

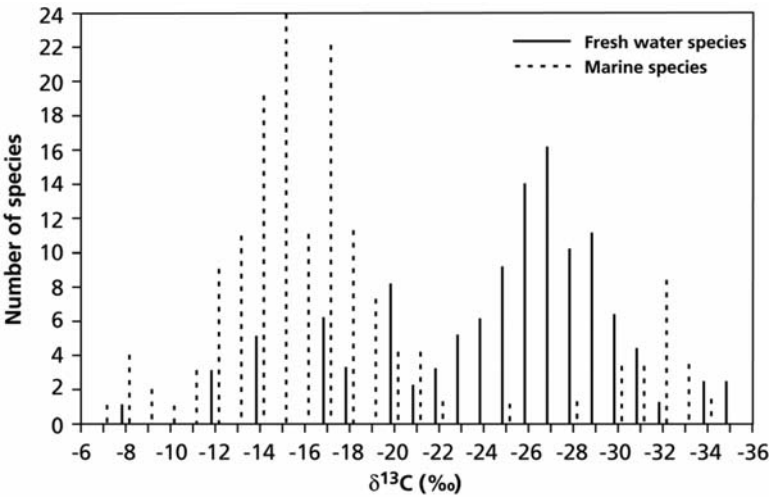

FIGURE 54. Variation in the carbon-isotope composition ($\delta^{13}C$) of freshwater and marine aquatic species. The observed variation is due to variation in $\delta^{13}C$ values of the substrate and in the extent of diffusional limitation (Osmond et al. 1982).

TABLE 15. Carbon-isotope composition ($\delta^{13}C$ in ‰) of submerged and emergent *Isoetes howellii* plants.*

Pondwater carbonate	–15.5 to –18.6
Submerged	
Leaves	–27.9 to –29.4
Roots	–25.8 to –28.8
Emergent	
Leaves	–29.4 to –30.1
Roots	–29.0 to –29.8

***Source*: Keeley & Busch (1984).**
*** Values are given for both leaves and roots and also for the pondwater carbonate.**

TABLE 16. Changes in the dissolved carbon isotope composition with depth as reflected in the composition of the organic matter at that depth.

Water depth (m)	$\delta^{13}C$ (‰)
1	–20.80
2	–20.75
5	–23.40
7	–24.72
9	–26.79
11	–29.91

***Source*: Osmond et al. (1982).**

Equation (12) shows how aquatic photosynthetic organisms play a major role in the global carbon cycle, even on a geological time scale. On the other hand, rising atmospheric CO_2 concentrations have an acidifying effect and dissolve part of the calcium carbonate precipitates in sediments, and thus contribute to a further rise in atmospheric [CO_2] (Sect. 12).

12. Effects of the Rising CO_2 Concentration in the Atmosphere

Vast amounts of carbon are present in carbonates in the Earth's crust. Also stored in the Earth's crust is another major carbon pool: the organic carbon derived form past photosynthesis; a key factor in the development of the present low CO_2/high O_2 atmosphere. Some CO_2 enters the atmosphere when carbonates are used for making cement, but apart from that, carbonates are only biologically important on a geological time scale. Far more important for the carbon balance of the atmosphere is the burning of fossil fuels (coal, oil, and natural gas) and changes in land-use that represent a CO_2 input into the atmosphere of 8.10^{15} g of carbon per year (10^{15} g equals 1 petagram, Pg). Compared with the total amount of carbon present in the atmosphere, 720 Pg, such inputs are substantial and inevitably affect the CO_2 concentration in the Earth's atmosphere (Falkowski et al. 2000). CO_2 is, by far, the largest contributor to the anthropogenically enhanced **greenhouse effect** (Houghton 2007).

Since the beginning of the industrial revolution in the late 18th century, the atmospheric CO_2 concentration has increased from about 290 μmol mol^{-1} to the current level of over 385 μmol mol^{-1} (Tans 2007). The concentration continues to rise by about

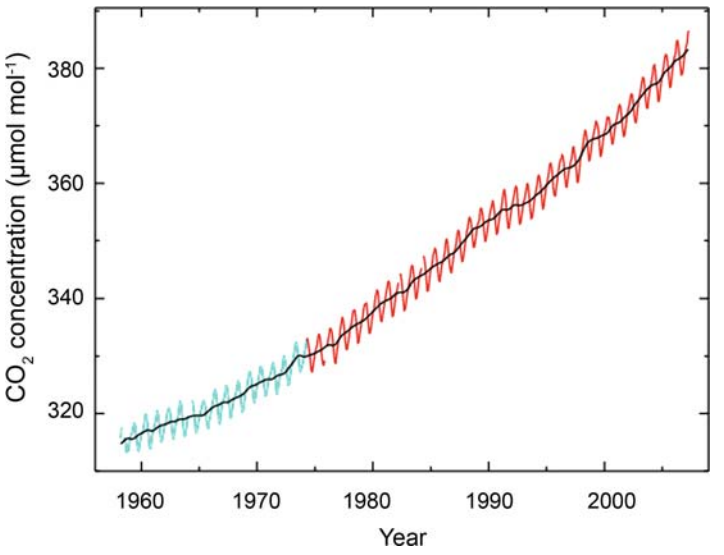

FIGURE 55. The rise in atmospheric CO_2 concentration, as measured at Mauna Loa (Hawaii), accelerated from about 0.7 µmol mol^{-1} yr^{-1} in the early years to about 2.0 µmol mol^{-1} yr^{-1} today. The blue line refers to data collected during 1958–1974 at the Scripps Institute of Oceanography; the red line refers to data collected since 1974 by the National Oceanic and Atmospheric Administration, US Department of Commerce (Tans 2007). Reproduced with the author's permission.

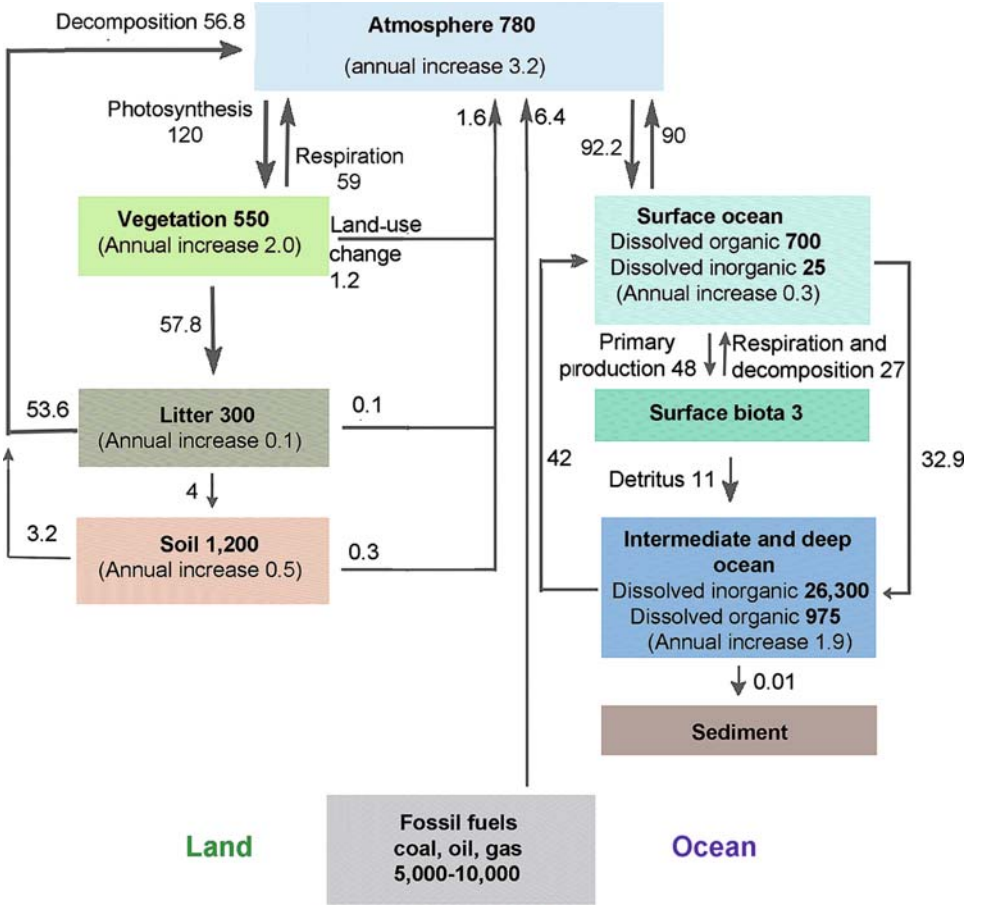

FIGURE 56. The global carbon cycle and global carbon reservoirs. Units are Pg C or Pg C yr^{-1}; 1 petagram = 10^{15} g = 10^9 metric tones (updated following Houghton 2007). Courtesy R.A. Houghton, The Woods Hole Research Center, Falmouth, Massachusetts, USA.

1.5 μmol mol^{-1} per year (Fig. 55). Measurements of CO_2 concentrations in **ice cores** indicate a pre-industrial value of about 280 μmol mol^{-1} during the past 10000 years, and about 205 μmol mol^{-1} some 20000 years ago during the last ice age. Considerable quantities of CO_2 have also been released into the atmosphere as a result of **deforestation**, **ploughing of prairies, drainage of peats**, and other land-use changes that cause oxidation of organic compounds in soil and, to a lesser extent, biomass. **Combustion of fossil fuel** adds far greater amounts of carbon per year (Fig. 56). Combined anthropogenic fluxes to the atmosphere amount to 8 Pg of carbon per year (Falkowski et al. 2000). Yet, the increase in the atmosphere is only 4.2 Pg of carbon per year (2000–2005). About 2.2 Pg of the "missing" carbon is taken up in the oceans and a similar amount (2.3 Pg) is fixed by terrestrial ecosystems (Grace 2004, Houghton 2007). Analysis of atmospheric CO_2 concentrations and its isotopic composition shows that north-temperate and boreal forests are the most likely sinks for the missing carbon. There is also strong uptake by tropical forests, but this is offset by CO_2 release from deforestation in the tropics. This increased terrestrial uptake of CO_2 has many causes, including stimulation of photosynthesis by elevated [CO_2] (about half of the increased terrestrial uptake) or by N deposition in N-limited ecosystems and regrowth of northern and mid-latitude forests (Houghton 2007).

Since the rate of net CO_2 assimilation is not CO_2-saturated in C_3 plants at 385 μmol mol^{-1} CO_2, the rise in CO_2 concentration is more likely to enhance photosynthesis in C_3 than in C_4 plants, where the rate of CO_2 assimilation is virtually saturated at a CO_2 concentration of 385 μmol mol^{-1} (Bunce 2004). The consequences of an enhanced rate of photosynthesis for plant growth are discussed in Sect. 5.8 of Chapter 7 on growth and allocation.

12.1 Acclimation of Photosynthesis to Elevated CO_2 Concentrations

Upon long-term exposure to 700 μmol mol^{-1}, about twice the present atmospheric CO_2 concentration, there may be a reduction of the photosynthetic capacity, associated with reduced levels of Rubisco and organic N per unit leaf area. This **down-regulation** of photosynthesis increases with increasing duration of the exposure to elevated [CO_2] and is most pronounced in plants grown at low N supplies. By contrast, water-stressed plants tend to increase net photosynthesis in response to elevated [CO_2] (Wullschleger et al. 2002). Herbaceous plants consistently reduce **stomatal conductance** in response to elevated [CO_2], so that C_i does not increase as much as would be expected from the increase in C_a, but their intrinsic **WUE** tends to be increased (Long et al. 2004). Tree photosynthesis continues to be enhanced by elevated [CO_2], except when seedlings are grown in small pots, inducing nutrient limitation (Norby et al. 1999). The decrease in stomatal conductance of C_3 plants often indirectly stimulates photosynthesis in dry environments by reducing the rate of soil drying and therefore the water limitation of photosynthesis (Hungate et al. 2002). C_3 and C_4 plants, however, benefit equally from increased water-use efficiency and water availability, reducing the relative advantage that C_3 plants gain from their greater CO_2 responsiveness of photosynthesis (Wand et al. 1999, Sage & Kubien 2003).

Why would acclimation of photosynthesis to elevated [CO_2] be more pronounced when N supply is poor? This could be a direct effect of N or an indirect effect by limiting the development of sinks for photoassimilates. This question can be tested by growing *Lolium perenne* (perennial ryegrass) in the field under elevated and current atmospheric CO_2concentrations at both low and high N supply. Cutting of this herbage crop at regular intervals removes a major part of the canopy, decreasing the ratio of photosynthetic area to **sinks for photoassimilates**. Just before the cut, when the canopy is relatively large, growth at elevated [CO_2] and low N supply decreases in carboxylation capacity and the amount of Rubisco protein. At a high N supply there are no significant decreases in carboxylation capacity or proteins. Elevated [CO_2] results in a marked increase in leaf carbohydrate concentration at low N supply, but not at high N supply. This acclimation at low N supply is absent after a harvest, when the canopy size is small. Acclimation under low N is therefore most likely caused by limitation of sink development rather than being a direct effect of N supply on photosynthesis (Rogers et al. 1998).

How do herbaceous plants sense that they are growing at an elevated CO_2 concentration and then down-regulate their photosynthetic capacity? Acclimation is not due to sensing the CO_2 concentration itself, but sensing the concentration of sugars in the leaf cells, more precisely the soluble hexose sugars (Sect. 4.2), mediated by a specific **hexokinase** (Sect. 4.3). In transgenic plants in which the level of hexokinase is greatly reduced, down-regulation of photosynthesis upon prolonged exposure to high [CO_2] is considerably

TABLE 17. Light-saturated rate of photosynthesis (A_{max}, measured at the CO_2 concentrations at which the plants were grown), in vitro Rubisco activity, chlorophyll concentration and the concentration of hexose sugars in the fifth leaf of *Solanum lycopersicum* (tomato) at various stages of development.*

		A_{max} (μmol m^{-2} s^{-1})		Rubisco activity (μmol m^{-2} s^{-1})mg m^{-2}		Chlorophyll (mg m^{-2})		Glucose (mg m^{-2})		Fructose	
Leaf expansion (% of full expansion)	Exposure time (days)	Control	High	Control	High	Control	High	Control	High	Control	High
2	0	16.3	21.3	22.6	–	270	–	750	–	500	–
60	11	18.9	28.7	20.5	25.1	480	520	1000	1200	1400	1400
95	22	15.0	25.1	15.7	12.7	540	500	1100	1250	1800	2100
100	31	9.3	18.0	9.5	4.9	450	310	1100	2100	1800	4200

Source: Van Oosten & Besford (1995), Van Oosten et al. (1995).
* Plants were grown at different atmospheric CO_2 concentrations: control, 350 μmol CO_2 mol^{-1}; high, 700 μmol CO_2 mol^{-1}.

less. Via a signal-transduction pathway, which also involves phytohormones, the **sugar-sensing mechanism** regulates the transcription of nuclear encoded photosynthesis-associated genes (Rolland et al. 2006). Among the first photosynthetic proteins that are affected are the small subunit of Rubisco and Rubisco activase. Upon longer exposure, the level of thylakoid proteins and chlorophyll is also reduced (Table 17).

The down-regulation of photosynthesis at elevated CO_2 has led to the discovery of sugar-sensing in plants, but it has recently become clear that the signaling pathway is intricately involved in a network regulating acclimation to other environmental factors, including light and nutrient availability as well as biotic and abiotic stress (Rolland et al. 2002). Down-regulation of photosynthesis in response to long-term exposure to elevated CO_2 has important global implications. The capacity of terrestrial ecosystems to **sequester carbon** appears to be saturating, leaving a larger proportion of human carbon emissions in the atmosphere, and accelerating the rate of global warming (Canadell et al. 2007).

12.2 Effects of Elevated CO_2 on Transpiration—Differential Effects on C_3, C_4, and CAM Plants

Different types of plants respond to varying degrees to elevated CO_2. For example, C_4 plants, whose rate of photosynthesis is virtually saturated at 385 μmol mol^{-1}, generally respond less to elevated CO_2 than do C_3 plants.

Also *Opuntia ficus-indica* (prickly pear), a CAM species cultivated worldwide for its fruits and cladodes, responds to the increase in CO_2 concentration in the atmosphere. The rate of CO_2 assimilation is initially enhanced, both at night and during the day, but this disappears upon prolonged exposure to elevated CO_2 (Cui & Nobel 1994). CAM species show, on average, a 35% increase in net daily CO_2 uptake which reflects increases in both Rubisco-mediated CO_2 uptake during the day and PEP carboxylase-mediated CO_2 uptake at night (Drennan & Nobel 2000).

13. Summary: What Can We Gain from Basic Principles and Rates of Single-Leaf Photosynthesis?

Numerous examples have been given on how differences in photosynthetic traits enhance a genotype's survival in a specific environment. These include specific biochemical pathways (C_3, C_4, and CAM) as well as more intricate differences between sun and shade plants, aquatic and terrestrial plants, and plants differing in their photosynthetic N-use efficiency and water-use efficiency. Information on photosynthetic traits is also highly relevant when trying to understand effects of global environmental changes in temperature and atmospheric CO_2concentrations. For a physiological ecologist, a full appreciation of the process of leaf photosynthesis is quintessential.

What we *cannot* derive from measurements on photosynthesis of **single leaves** is what the rate of photosynthesis of an **entire canopy** will be. To

work out these rates, we need to take the approach discussed in Chapter 5, dealing with scaling-up principles. It is also quite clear that short-term measurements on the effect of atmospheric CO_2concentrations are not going to tell us what will happen in the long term. Acclimation of the photosynthetic apparatus ("down-regulation") may occur, reducing the initial stimulatory effect. Most importantly, we *cannot* derive plant growth rates or crop yields from rates of photosynthesis of a single leaf. Growth rates are not simply determined by rates of single-leaf photosynthesis per unit leaf area, but also by the total leaf area per plant and by the fraction of daily produced photosynthates required for plant respiration, issues that are dealt with in later chapters.

References

Adams III, W.W., Demmig-Adams, B., Logan, B.A., Barker, D.H., & Osmond, C.B. 1999. Rapid changes in xanthophyll cycle-dependent energy dissipation and photosystem II efficiency in two vines, *Stephania japonica* and *Smilax australis*, growing in the understory of an open *Eucalyptus* forest. *Plant Cell Environ.* **22**: 125–136.

Allen, M.T. & Pearcy, R.W. 2000. Stomatal behavior and photosynthetic performance under dynamic light regimes in a seasonally dry tropical rain forest. *Oecologia* **122:** 470–478.

Atkin, O.K., Scheurwater, I., & Pons, T.L. 2006. High thermal acclimation potential of both photosynthesis and respiration in two lowland *Plantago* species in contrast to an alpine congeneric. *Global Change Biol.* **12:** 500–515.

Bailey, S., Walters, R.G., Jansson, S., & Horton, P. 2001. Acclimation of *Arabidopsis thaliana* to the light environment: the existence of separate low light and high light responses. *Planta* **213:** 794–801.

Bastide, B., Sipes, D., Hann, J., & Ting, I.P. 1993. Effect of severe water stress on aspects of crassulacean acid metabolism in *Xerosicyos*. *Plant Physiol.* **103:** 1089–1096.

Beerling, D.J. & Osborne, C.P. 2006. The origin of the savanna biome. *Global Change Biol.* **12:** 2023–2031.

Bernacchi, C.J., Pimentel, C., & Long, S.P. 2003. In vivo temperature response functions of parameters required to model RuBP-limited photosynthesis. *Plant Cell Environ.* **26:** 1419–1430.

Bernacchi, C.J., Singsaas, E.L., Pimentel, C., Portis Jr., A.R., & Long, S.P. 2001. Improved temperature response functions for models of Rubisco-limited photosynthesis. *Plant Cell Environ.* **24:** 253–259.

Bernacchi, C.J., Portis, A.R., Nakano, H., Von Caemmerer, S., & Long, S.P. 2002. Temperature response of mesophyll conductance. Implications for the determination of Rubisco enzyme kinetics and for limitations to photosynthesis *in vivo*. *Plant Physiol.* **130:** 1992–1998.

Berry, J.A. & Björkman, O. 1980. Photosynthetic response and adaptation to temperature in higher plants. *Annu. Rev. Plant Physiol.* **31:** 491–543.

Berry, J.A. & Raison, J.K. 1981. Responses of macrophytes to temperature. In: Encyclopedia of plant physiology, Vol 12A, O.L. Lange, P.S. Nobel, C.B. Osmond, & H. Ziegler (eds.). Springer-Verlag, Berlin, pp. 277–338.

Björkman, O. 1981. Responses to different quantum flux densities. In: Encyclopedia of plant physiology, N.S., Vol. 12A, O.L. Lange, P.S. Nobel, C.B. Osmond, & H. Ziegler (eds.). Springer-Verlag, Berlin, pp. 57–107.

Bolhàr-Nordenkampf, H.R. & Öquist, G. 1993. Chlorophyll fluorescence as a tool in photosynthesis research. In: Photosynthesis and production in a changing environment, D.O. Hall, J.M.O. Scurlock, H.R. Bolhàr-Nordenkampf, R.C. Leegood, & S.P. Long (eds.). Chapman & Hall, London, pp. 193–206.

Boonman, A., Prinsen, E., Gilmer, F., Schurr, U., Peeters, A.J.M., Voesenek, L.A.C.J., & Pons, T.L. 2007. Cytokinin import rate as a signal for photosynthetic acclimation to canopy light gradients. *Plant Physiol.* **143:** 1841–1852.

Bowes, G. & Salvucci, M.E. 1989. Plasticity in the photosynthetic carbon metabolism of submersed aquatic macrophytes. *Aquat. Bot.* **34:** 233–286.

Bowes, G., Rao, S.K., Estavillo, G.M., & Reiskind, J.B. 2002. C_4 mechanisms in aquatic angiosperms: comparisons with terrestrial C_4 systems. *Funct. Plant Biol.* **29:** 379–392.

Brown, R. & Bouton, J.H. 1993. Physiology and genetics of interspecific hybrids between photosynthetic types. *Annu. Rev. Plant Physiol. Plant Mol. Biol.* **44:** 435–456.

Brown, R.H. & Hattersley, P.W. 1989. Leaf anatomy of C_3–C_4 species as related to evolution of C_4 photosynthesis. *Plant Physiol.* **91:** 1543–1550.

Brugnoli, E. & Björkman, O. 1992. Chloroplast movements in leaves: influence on chlorophyll fluorescence and measurements of light-induced absorbance changes related to ΔpH and zeaxanthin formation. *Photosynth. Res.* **32:** 23–35.

Buchmann, N., Guehl, J.M., Barigah, T.S., & Ehleringer, J.R. 1997. Interseasonal comparison of CO_2 concentrations, isotopic composition, and carbon dynamics in an amazonian rain forest (French Guiana). *Oecologia* **110:** 120–131.

Bunce, J.A. 2004. Carbon dioxide effects on stomatal responses to the environment and water use by crops under field conditions. *Oecologia* **140:** 1–10.

Canadell, J.G., Pataki, D.E., Gifford, R., Houghton, R.A., Luo, Y., Raupach, M.R., Smith, P., & Steffen. W. 2007. Saturation of the terrestrial carbon sink. In: Terrestrial ecosystems in a changing world, J.G. Canadell, D. Pataki, & L. Pitelka (eds.). Springer, Berlin, pp. 59–78.

Cavagnaro, J.B. 1988. Distribution of C_3 and C_4 grasses at different altitudes in a temperate arid region of Argentina. *Oecologia* **76:** 273–277.

Cen, Y.-P. & Sage, R.F. 2005. The regulation of ribulose-1,5-bisphosphate carboxylase activity in response to variation in temperature and atmospheric CO_2 partial pressure in sweet potato. *Plant Physiol.* **139:** 1–12.

Cerling, T.E., Harris, J.H., MacFadden, B.J., Leakey, M.G., Quade, J., Eisenmann, V., & Ehleringer, J.R. 1997. Global

vegetation change through the Miocene/Pliocene boundary. *Nature* **389:** 153–158.

Chazdon, R.L. & Pearcy, R.W. 1986. Photosynthetic responses to light variation in rainforest species. I. Induction under constant and fluctuating light conditions. *Oecologia* **69:** 517–523.

Chazdon, R.L. & Pearcy, R.W. 1991. The importance of sunflecks for forest understory plants.*BioSciences* **41:** 760–766.

Chow, W.S. 2003. Photosynthesis: from natural towards artificial. *J. Biol. Phys.* **29:** 447–459.

Chow, W.S., Hope, A.B., & Anderson, J.M. 1989. Oxygen per flash from leaf disks quantifies photosystem II. *Biochim. Biophys. Acta* **973:** 105–108.

Christie, E.K. & Detling, J.K. 1982. Analysis of interference between C_3 and C_4 grasses in relation to temperature and soil nitrogen supply. *Ecology* **63:** 1277–1284.

Christmann, A., Hoffmann, T., Teplova, I., Grill, E., & Müller, A. 2005. Generation of active pools of abscisic acid revealed by in vivo imaging of water-stressed *Arabidopsis*. *Plant Physiol.* **137:** 209–219.

Coté, F.X., André, M., Folliot, M., Massimino, D., & Daguenet, A. 1989. CO_2 and O_2 exchanges in the CAM plant *Ananas comosus* (L.) Merr. determination or total and malate-decarboxylation-dependent CO_2-assimilation rates; study of light O_2-uptake. *Plant Physiol.* **89:** 61–68.

Coupe, S.A., Palmer, B.G., Lake, J.A., Overy, S.A., Oxborough, K., Woodward, F.I., Gray, J.E., & Quick, W.P. 2006 Systemic signalling of environmental cues in *Arabidopsis* leaves. *J. Exp. Bot.* **57:** 329–341.

Cui, M. & Nobel, P.S. 1994. Gas exchange and growth responses to elevated CO_2 and light levels in the CAM species *Opuntia ficus-indica*. *Plant Cell Environ.* **17:** 935–944.

DeLucia, E.H., Nelson, K., Vogelmann, T.C., & Smith, W.K. 1996. Contribution of intercellular reflectance to photosynthesis in shade leaves. *Plant Cell Environ.* **19:** 159–170.

Demmig-Adams, B. & Adams III, W.W. 1996. The role of xanthophyll cycle carotenoids in the protection of photosynthesis. *Trends Plant Sci.* **1:** 21–26.

Demmig-Adams, B. & Adams III, W.W. 2006. Photoprotection in an ecological context: the remarkable complexity of thermal energy dissipation. *New Phytol.* **172**: 11–21.

DeRidder, B.P. & Salvucci, M.E. 2007. Modulation of Rubisco activase gene expression during heat stress in cotton (*Gossypium hirsutum* L.) involves post-transcriptional mechanisms. *Plant Sci.* **172:** 246–254.

Downton, W.J.S., Loveys, B.R., & Grant, W.J.R. 1988. Stomatal closure fully accounts for the inhibition of photosynthesis by abscisic acid. *New Phytol.* **108:** 263–266.

Drennan, P.M. & Nobel, P.S. 2000. Responses of CAM species to increasing atmospheric CO_2 concentrations. *Plant Cell Environ.* **23:** 767–781.

Eckstein, J., Beyschlag, W., Mott, K.A., & Ryell, R.J. 1996. Changes in photon flux can induce stomatal patchiness. *Plant Cell. Environ.* **19:** 1066–1074.

Ehleringer, J., & Björkman, O. 1977. Quantum yields for CO_2 uptake in C_3 and C_4 plants. Dependence on temperature, CO_2, and O_2concentration. *Plant Physiol.* **59:** 86–90.

Ehleringer, J.R. & Monson, R. K. 1993. Evolutionary and ecological aspects of photosynthetic pathway variation. *Annu. Rev. Ecol. Syst.* **24:** 411–439.

Ehleringer, J., Björkman, O., & Mooney, H.A. 1976. Leaf pubescence: effects on absorptance and photosynthesis in a desert shrub. *Science* **192:** 376–377.

Ehleringer, J.R., Schulze, E.-D., Ziegler, H., Lange, O.L., Farquhar, G.D., & Cowan, I.R. 1985. Xylem-tapping mistletoes: water or nutrient parasites? *Science* **227:** 1479–1481.

Eller, B.M. & Ferrari, S. 1997. Water use efficiency of two succulents with contrasting CO_2 fixation pathways. *Plant Cell Environ.* **20:** 93–100.

Ellis, R.P. 1977. Distribution of the Kranz syndrome in the Southern African Eragrostoideae and the Panicoideae according to bundle sheath anatomy and cytology. *Agroplantae* **9:** 73–110.

Ellis, R.P., Vogel, J.C., & Fuls, A. 1980. Photosynthetic pathways and the geographical distribution of grasses in south west Africa/Namibia. *S. Afr. J. Sci.* **76:** 307–314.

Elzenga, J.T.M. & Prins, H.B.A. 1988. Adaptation of *Elodea* and *Potamogeton* to different inorganic carbon levels and the mechanism for photosynthetic bicarbonate utilisation. *Aust. J. Plant Physiol.* **15:** 727–735.

Elzenga, J.T.M. & Prins, H.B.A. 1989. Light-induced polar pH changes in leaves of *Elodea canadensis*. I. Effects of carbon concentration and light intensity. *Plant Physiol.* **91:** 62–67.

Evans, J.R. 1988. Acclimation by the thylakoid membranes to growth irradiance and the partitioning of nitrogen between soluble and thylakoid proteins. *Aust. J. Plant Physiol.* **15:** 93–106.

Evans, J.R. 1989. Photosynthesis and nitrogen relationships in leaves of C_3 plants. *Oecologia* **78:** 9–19.

Evans, J.R. & Loreto, F. 2000. Acquisition and diffusion of CO_2 in higher plant leaves. *In:* Photosynthesis: physiology and metabolism, R.C. Leegood, T.D. Sharkey, & S. Von Caemmerer (eds.). Kluwer Academic Publishers, Dordrecht, pp. 321–351.

Evans, J.R. & Seemann, J.R. 1989. The allocation of protein nitrogen in the photosynthetic apparatus: costs, consequences, and control. In: Photosynthesis, W.R. Briggs (ed.). Alan Liss, New York, pp. 183–205.

Evans, J.R. & Vogelmann, T.C. 2003. Profiles of ^{14}C fixation through spinach leaves in relation to light absorption and photosynthetic capacity. *Plant Cell Environ.* **26:** 547–560.

Evans, J.R., Sharkey, T.D., Berry, J.A., & Farquhar, G.D. 1986. Carbon isotope discrimination measured with gas exchange to investigate CO_2 diffusion in leaves of higher plants. *Aust. J. Plant Physiol.* **13:** 281–292.

Falkowski, P., Scholes, R.J., Boyle, E., Canadell, J., Canfield, D., Elser, J., Gruber, N., Hibbard, K., Högberg, P., Linder, S., Mackenzie, F.T., Moore III, B., Pedersen, T., Rosenthal, Y., Seitzinger, S., Smetacek, V., & Steffen, W. 2000. The global carbon cycle: a test of our knowledge of Earth as a system. *Science* **290:** 291–296.

Farmer, A.M. 1996. Carbon uptake by roots. In: Plant roots: the hidden half, Y. Waisel, A. Eshel, & U. Kafkaki (eds.). Marcel Dekker, Inc., New York, pp. 679–687.

Farquhar, G.D. & Richards, R.A. 1984. Isotopic composition of plant carbon correlates with water-use efficiency of wheat genotypes. *Aust. J. Plant Physiol.* **11:** 539–552.

Farquhar, G.D., Von Caemmerer, S., & Berry, J.A. 1980. A biochemical model of photosynthetic CO_2 assimilation in leaves of C_3 species. *Planta* **149:** 78–90.

Farquhar, G.D., O'Leary, M.H., & Berry, J.A. 1982. On the relationship between carbon isotope discrimination and the intercellular carbon dioxide concentration in leaves. *Aust. J. Plant Physiol.* **9:** 131–137.

Field, C.B., Ball, T., & Berry, J.A. 1989. Photosynthesis: principles and field techniques. In: Plant physiological ecology; field methods and instrumentation, R.W. Pearcy, J.R. Ehleringer, H.A. Mooney, & P.W. Rundel (eds.). Chapman and Hall, London, pp. 209–253.

Feild, T.S., Lee, D.W., & Holbrook, N.M. 2001. Why leaves turn red in autumn. The role of anthocyanins in senescing leaves of red-osier dogwood. *Plant Physiol.* **127:** 566–574.

Flexas, J. & Medrano, H. 2002. Drought-inhibition of photosynthesis in C_3 plants: stomatal and non-stomatal limitations revisited. *Ann. Bot.* **89:** 183–189.

Flexas, J., Bota, J., Loreto, F., Cornic, G., & Sharkey T.D. 2004. Diffusive and metabolic limitations to photosynthesis under drought and salinity in C_3 plants. *Plant Biol.***6:** 269–279.

Flexas, J., Ribas-Carbó, M., Hanson, D.T., Bota J., Otto, B., Cifre, J., McDowell, N., Medrano, H., & Kaldenhoff, R. 2006a. Tobacco aquaporin NtAQP1 is involved in mesophyll conductance to CO_2 *in vivo*. *Plant J.* **48:** 427–439.

Flexas, J., Bota, J., Galmés, J., Medrano, H., & Ribas-Carbó, M. 2006b. Keeping a positive carbon balance under adverse conditions: responses of photosynthesis and respiration to water stress. *Physiol. Plant.* **127:** 343–352.

Flexas, J., Diaz-Espejo, Galmés, J., Kaldenhoff, R., Medrano, H. & Ribas-Carbó, M. 2007a. Rapid variations of mesophyll conductance in response to changes in CO_2 concentration around leaves. *Plant Cell Environ.* **30:** 1284–1298.

Flexas, J., Diaz-Espejo, A., Berry, J.A., Cifre, J., Galmés, J., Kaidenhoff, R., Medrano, H. & Ribas-Carbo, M. 2007b. Analysis of leakage in IRGA's leaf chambers of open gas exchange systems: quantification and its effects in photosynthesis parameterization. *J. Exp. Bot.* **58:** 1533–1543.

Flexas, J., Ribas-Carbó, M., Diaz-Espejo, A., Galmés, J., & Medrano, H. 2008. Mesophyll conductance to CO_2: current knowledge and future prospects. *Plant Cell Environ.* **31:** 602–621.

Flügge, U.I., Stitt, M., & Heldt, H.W. 1985. Light-driven uptake or pyruvate into mesophyll chloroplasts from maize. *FEBS Lett.* **183:** 335–339.

Fredeen, A.L., Gamon, J.A., & Field, C.B. 1991. Responses of photosynthesis and carbohydrate partitioning to limitations in nitrogen and water availability in field grown sunflower. *Plant Cell Environ.* **14:** 969–970.

Galmés, J., Flexas, J., Keys, A.J., Cifre, J., Mitchell, R.A.C., Madgwick, P.J., Haslam R.P., Medrano, H., & Parry, M.A.J. 2005. Rubisco specificity factor tends to be larger in plant species from drier habitats and in species with persistent leaves. *Plant Cell Environ.* **28:** 571–579.

Galmés, J., Medrano, H., & Flexas, J. 2007. Photosynthetic limitations in response to water stress and recovery in Mediterranean plants with different growth forms. *New Phytol.* **175:** 81–93.

Genty, B., Briantais, J.-M., & Baker, N.R. 1989. The relationship between the quantum yield of photosynthetic electron transport and quenching of chlorophyll fluorescence. *Biochim. Biophys. Acta* **990:** 87–92.

Ghannoum, O., Evans, J.R., Chow, W.S., Andrews, T.J., Conroy, J.P., & Von Caemmerer, S. 2005. Faster Rubisco is the key to superior nitrogen-use efficiency in NADP-malic enzyme relative to NAD-Malic enzyme C_4 grasses. *Plant Physiol.* **137:** 638–650.

Gillon, J.S. & Yakir, D. 2000. Internal conductance to CO_2 diffusion and $C^{18}OO$ discrimination in C_3 leaves. *Plant Physiol.* **123:** 201–214.

Gilmore, A.M. 1997. Mechanistic aspects of xanthophyll cycle-dependent photoprotection in higher plant chloroplasts and leaves. *Physiol. Plant* **99:** 197–209.

Goldschmidt, E.E. & Huber, S.C. 1992. Regulation of photosynthesis by end-product accumulation in leaves of plants storing starch, sucrose, and hexose sugars. *Plant Physiol.* **99:** 1443–1448.

Grace, J. 2004. Understanding and managing the global carbon cycle. *J. Ecol.* **92:** 189–202.

Grams, E.E., Koziolek, C., Lautner, S., Matyssek, R., & Fromm, J. 2007. Distinct roles of electric and hydraulic signals on the reaction of leaf gas exchange upon re-irrigation in *Zea mays* L. *Plant Cell Environ.* **30:** 79–84.

Grassi, G. & Magnani, F. 2005. Stomatal, mesophyll conductance and biochemical limitations to photosynthesis as affected by drought and leaf ontogeny in ash and oak trees. *Plant Cell Environ.* **28:** 834–849.

Gunasekera, D. & Berkowitz, G.A. 1992. Heterogenous stomatal closure in response to leaf water deficits is not a universal phenomenon. *Plant Physiol.* **98:** 660–665.

Guy, R.D., Fogel, M.L., & Berry, J.A. 1993. Photosynthetic fractionation of the stable isotopes of oxygen and carbon. *Plant Physiol.* **101:** 37–47.

Hanson, H.C. 1917. Leaf structure as related to environment. *Am. J. Bot.* **4**: 533–560.

Harris, F.S. & Martin, C.E. 1991. Correlation between CAM-cycling and photosynthetic gas exchange in five species of (*Talinum*) (Portulacaceae) *Plant Physiol.* **96:** 1118–1124.

Hatch, M.D. & Carnal, N.W. 1992. The role of mitochondria in C_4 photosynthesis. In: Molecular, biochemical and physiological aspects of plant respiration, H. Lambers & L.H.W. Van der Plas (eds.). SPB Academic Publishing, The Hague, pp. 135–148.

Hatch, M.D. & Slack, C.R. 1966. Photosynthesis by sugar cane leaves A new carboxylation reaction and

the pathway of sugar formation. *Biochem. J.* **101:** 103–111.

Hatch, M.D. & Slack, C.R. 1998. C_4 photosynthesis: discovery, resolution, recognition, and significance. In: Discoveries in plant biology, S.-Y. Yang & S.-D. Kung (eds.). World Scientific Publishing, Hong Kong, pp. 175–196.

Henderson, S.A., Von Caemmerer, S., & Farquhar, G.D. 1992. Short-term measurements of carbon isotope discrimination in several C_4 species. *Aust. J. Plant Physiol.* **19:** 263–285.

Henderson, S, Hattersley, P., Von Caemmerer, S & Osmond, C.B. 1995. Are C_4 pathway plants threatened by global climatic change? In: Ecophysiology of photosynthesis, E.-D. Schulze & M.M. Caldwell (eds.). Springer-Verlag, Berlin, pp. 529–549.

Hibberd, J.M. & Quick, W.P. 2002. Xharacteristics of C_4 photosynthesis in stms and ptioes of C_3 flowering plants. *Nature* **415:** 451–454.

Hikosaka, K., Ishikawa, K., Borjigidai, A., Muller, O., & Onoda, Y. 2006. Temperature acclimation of photosynthesis: mechanisms involved in the changes in temperature dependence of photosynthetic rate. *J. Exp. Bot.* **57:** 291–302.

Holbrook, N.M., Shashidhar, V.R., James, R.A., & Munns, R. 2002. Stomatal control in tomato with ABA-deficient roots: response of grafted plants to soil drying. *J. Exp. Bot.* **53:** 1503–1514.

Houghton, R.A. 2007. Balancing the global carbon budget. *Annu. Rev. Earth Planet. Sci.* **35:** 313–347.

Huang, Y., Street-Perrott, F.A., Metcalfe, S.E., Brenner, M., Moreland, M., Freeman, K.H. 2001. Climate change as the dominant control on glacial-interglacial variations in C_3 and C_4 plant abundance. *Science* **293**: 1647–1651.

Hubick, K. 1990. Effects of nitrogen source and water limitation on growth, transpiration efficiency and carbon-isotope discrimination in peanut cultivars. *Aust. J. Plant Physiol.* **17:** 413–430.

Hubick, K. & Farquhar, G.D. 1989. Carbon isotope discrimination and the ratio of carbon gained to water lost in barley cultivars. *Plant Cell Environ.* **12:** 795–804.

Huner, N.P.A., Öquist, G., & Sarhan, F. 1998. Energy balance and acclimation to light and cold. *Trends Plant Sci.* **3:** 224–230.

Hungate, B.A., Reichstein, M., Dijkstra, P., Johnson, D., Hymus, G., Tenhunen, J. D., Hinkle, C.R., & Drake, B.G. 2002. Evapotranspiration and soil water content in a scrub-oak woodland under carbon dioxide enrichment. *Global Change Biol.* **8:** 289–298.

Jahnke, S. & Pieruschka, R. 2006. Air pressure in clamp-on leaf chambers: a neglected issue in gas exchange measurements. *J. Exp. Bot.* **57:** 2553–2561.

Jones, P.G., Lloyd, J.C., & Raines, C.A. 1996. Glucose feeding of intact wheat plants represses the expression of a number of Calvin cycle genes. *Plant Cell Environ.* **19:** 231–236.

Jordan, D.B. & Ogren, W.L. 1981. The CO_2/O_2 specificity of ribulose 1,5-bisphosphate carboxylase/oxygenase. *Planta* **161:** 308–313.

Kalisz, S. & Teeri, J.A. 1986. Population-level variation in photosynthetic metabolism and growth in *Sedum wrightii*. *Ecology* **67:** 20–26.

Kao, W.-Y. & Forseth, I.N. 1992. Diurnal leaf movement, chlorophyll fluorescence and carbon assimilation in soybean grown under different nitrogen and water availabilities. *Plant Cell Environ.* **15:** 703–710.

Keeley, J.E. 1990. Photosynthetic pathways in freshwater aquatic plants. *Trends Ecol. Evol.* **5:** 330–333.

Keeley, J.E. & Busch, G. 1984. Carbon assimilation characteristics of the aquatic CAM plant, *Isoetes howellii*. *Plant Physiol.* **76:** 525–530.

Keeley, J.E. & Rundel, P.W. 2005. Fire and the Miocene expansion of C_4 grasslands. *Ecol. Lett.* **8:** 683–690.

Keeley, J.E. & Sandquist, D.R. 1992. Carbon: freshwater aquatics. *Plant Cell Environ.* **15:** 1021–1035.

Keeley, J.E., Osmond, C.B., & Raven, J.A. 1984. *Stylites*, a vascular land plant without stomata absorbs CO_2 via its roots. *Nature* **310**: 694–695.

Kirschbaum, M.U.F. & Pearcy, R.W. 1988. Gas exchange analysis of the relative importance of stomatal and biochemical factors in photosynthetic induction in *Alocasia macrorrhiza*. *Plant Physiol.* **86:** 782–785.

Kluge, M. & Ting, I.P 1978. Crassulacean acid metabolism. Analysis of an ecological adaptation. Springer-Verlag, Berlin.

Koch, K.E. & Kennedy, R.A. 1982. Crassulacean acid metabolism in the succulent C_4 dicot, *Portulaca oleracea* L. under natural environmental conditions. *Plant Physiol.* **69:** 757–761.

Körner, C. & Larcher, W. 1988. Plant life in cold climates. *Symp. Soc. Exp. Biol.* **42:** 25–57.

Krall, J.P. & Edwards, G.E. 1992. Relationship between photosystem II activity and CO_2 fixation. *Physiol. Plant* **86:** 180–187.

Krall, J.P., Edwards, G.E. and Andrea, C.S. 1989. Protection of pyruvate, P_i dikinase from maize against cold lability by compatible solutes. *Plant Physiol.* **89:** 280–285.

Krause, G.H. & Weis, E. 1991. Chlorophyll fluorescence and photosynthesis: The basics. *Annu Rev. Plant Physiol. Plant Mol. Biol.* **42:** 313–349.

Kropf, M. 1989. Quantification of SO_2 effects on physiological processes, plant growth and crop production. PhD Thesis, Wageningen Agricultural University, The Netherlands.

Külheim, C., Agren, J., & Jansson, S. 2002. Rapid regulation of light harvesting and plant fitness in the field. *Science* **297**: 91–93.

Lake, J.A., Quick, W.P., Beerling, D.J., & Woodward, F.I. 2001. Plant development. Signals from mature to new leaves. *Nature* **411:** 154.

Lawlor, D.W. 1993. Photosynthesis; molecular, physiological and environmental processes. Longman, London.

Leverenz, J.W. 1987. Chlorophyll content and the light response curve of shade adapted conifer needles. *Physiol. Plant* **71:** 20–29.

Li, X.-P., Phippard, A., Pasari, J., & Niyogi, K.K. 2002. Structure-function analysis of photosystem II subunit S (PsbS) *in vivo*. *Funct. Plant Biol.* **29**: 1131–1139.

Lichtenthaler, H.K. 2007. Biosynthesis, accumulation and emission of carotenoids, α-tocopherol, plastoquinone, and isoprene in leaves under high photosynthetic irradiance. *Photosynth. Res.* **92:** 163–179.

Lichtenthaler, H.K. & Babani, F. 2004. Light adaptation and senescence of the photosynthetic apparatus. Changes in pigment composition, chlorophyll fluorescence parameters and photosynthetic activity. In: Chlorophyll fluorescence: a signature of photosynthesis, G.C. Papageorgiou & Govindjee (eds.). Springer, Dordrecht, pp. 713–736.

Logan, B.A., Barker, D.H., Demmig-Adams, B., & Adams III, W.W. 1996. Acclimation of leaf carotenoid composition and ascorbate levels to gradients in the light environment within an Australian rainforest. *Plant Cell Environ.* **19:** 1083–1090.

Long, S.P. & Bernacchi, C.J. 2003. Gas exchange measurements, what can they tell us about the underlying limitations to photosynthesis? Procedures and sources of error. *J. Exp. Bot.* **54:** 2393–2401.

Long, S.P. & Hällgren, J.E. 1993. Measurement of CO_2 assimilation by plants in the field and the laboratory. In: Photosynthesis and production in a changing environment, D.O. Hall, J.M.O. Scurlock, H.R. Bolhàr-Nordenkampf, R.C. Leegood, & S.P. Long (eds.). Chapman and Hall, London, pp. 129–167.

Long, S.P., Humphries, S., & Falkowski, P.G. 1994. Photoinhibition of photosynthesis in nature. *Annu. Rev. Plant Physiol. Plant Mol. Biol.* **45:** 633–662.

Long, S.P., Ainsworth, E.A., Rogers, A., & Ort, D.R. 2004. Rising atmospheric carbon dioxide: plants FACE the future. *Annu. Rev. Plant Biol.* **55:** 591–628.

Maberly, S.C. & Madsen, T.V. 2002. Freshwater angiosperm carbon concentrating mechanisms: processes and patterns. *Funct. Plant Biol.* **29:** 393–405.

Madsen, T.V. & Baattrup-Pedersen, A. 1995. Regulation of growth and photosynthetic performance in *Elodea canadensis* in response to inorganic nitrogen. *Funct. Ecol.* **9:** 239–247.

Magnin, N.C., Cooley, B.A., Reiskind, J.B., & Bowes, G. 1997. Regulation and localization of key enzymes during the induction of Kranz-less, C_4-type in *Hydrilla verticillata*. *Plant Physiol.* **115:** 1681–1689.

Martin, B., Tauer, C.G., Lin, R.K. 1999. Carbon isotope discrimination as a tool to improve water-use efficiency in tomato. *Crop Sci.* **39:** 1775–1783.

Mazen, A.M.A. 1996. Changes in levels of phospho*enol*pyruvate carboxylase with induction of Crassulacean acid metabolism (CAM)-like behavior in the C_4 plant *Portulaca oleracea*. *Physiol. Plant.* **98:** 111–116.

McConnaughey, T.A., LaBaugh, J.W., Rosenberry, D.O., Striegl, R.G., Reddy, M.M., & Schuster, P.F. 1994. Carbon budget for a groundwater-fed lake: calcification supports summer photosynthesis. *Limnol. Oceanogr.* **39:** 1319–1332.

Medina, E. 1996. CAM and C_4 plants in the humid tropics. In: Tropical forest plant ecophysiology, S.D. Mulkey, R. L. Chazdon, & A.P. Smith (eds.). Chapman & Hall, New York, pp. 56–88.

Mommer, L., Pons, T.L., Wolters-Arts, M., Venema, J.H., & Visser, E.J.W. 2005. Submergence-induced morphological, anatomical, and biochemical responses in a terrestrial species affect gas diffusion resistance and photosynthetic performance. *Plant Physiol.* **139:** 497–508.

Monsi, M. & Saeki T. 1953. Über den Lichtfaktor in den Pflanzengesellschaften und sein Bedeutung für die Stoffproduktion. *Jap. J. Bot.* **14:** 22–52.

Monsi, M. & Saeki T. 2005. On the factor light in plant communities and its importance for matter production. *Ann. Bot.* **95:** 549–567.

Mooney, H.A. 1986. Photosynthesis. In: Plant ecology, M.J. Crawley (ed.). Blackwell Scientific Publications, Oxford. pp. 345–373.

Morgan, C.L., Turner, S.R., & Rawsthorne, S. 1992. Cell-specific distribution of glycine decarboxylase in leaves of C_3, C_4 and C_3–C_4 intermediate species. In: Molecular, biochemical and physiological aspects of plant respiration, H. Lambers & L.H.W. Van der Plas (eds.). SPB Academic Publishing, The Hague, pp. 339–343.

Morgan, P.B., Ainsworth, E.A., & Long, S.P. 2003. How does elevated ozone impact soybean? A meta-analysis of photosynthesis, growth and yield. *Plant Cell Environ.* **26:** 1317–1328.

Mott, K.A. & Buckley, T.N. 2000. Patchy stomatal conductance: emergent collective behaviour of stomata. *Trends Plant Sci.* **5:** 1380–1385.

Murchie, E.H. & Horton, P. 1997. Acclimation of photosynthesis to irradiance and spectral quality in British plant species: chlorophyll content, photosynthetic capacity and habitat preference. *Plant Cell Environ.* **20:** 438–448.

Newman, J.R. & Raven, J.R. 1993. Carbonic anhydrase in *Ranunculus penicillatus* spp. *pseudofluitans*: activity, location and implications for carbon assimilation. *Plant Cell Environ.* **16:** 491–500.

Nielsen, S.L., Gacia, E., & Sand-Jensen, K. 1991. Land plants or amphibious *Littorella uniflora* (L.) Aschers. maintain utilization of CO_2 from sediment. *Oecologia* **88:** 258–262.

Niinemets, Ü. 2007. Photosynthesis and resource distribution through plant canopies. *Plant Cell. Environ.* **30:** 1052–1071.

Nimmo, H.G., Fontaine, V., Hartwell, J., Jenkins, G.I., Nimmo, G.A., & Wilkins, M.B. 2001. PEP carboxylase kinase is a novel protein kinase controlled at the level of expression. *New Phytol.* **151:** 91–97.

Nishiyama, Y., Allakhverdiev, S.I., & Murata, N. 2006. A new paradigm for the action of reactive oxygen species in the photoinhibition of photosystem II. *Biochim. Biophys. Acta* **1757:** 742–749.

Nishio, J.N., Sun, J., & Vogelmann, T.C. 1993. Carbon fixation gradients across spinach leaves do not follow internal light gradients. *Plant Cell* **5:** 953–961.

Niyogi, K., Grossman, A.R., & Björkman, O. 1998. *Arabidopsis* mutants define a central role for the xanthophyll cycle in the regulation of photosynthetic energy conversion. *Plant Cell* **10:** 1121–1134.

Nobel, P.S. & Hartsock, T.L. 1990. Diel patterns of CO_2 exchange for epiphytic cacti differing in succulence. *Physiol. Plant* **78:** 628–634.

Nobel, P.S., Garcia-Moya, E., & Quero, E. 1992. High annual productivity of certain agaves and cacti under cultivation. *Plant Cell Environ.* **15:** 329–335.

Norby, R.J., Wullschleger, S.D., Gunderson, C.A., Johnson, D.W., & Ceulemans, R. 1999. Tree responses to rising CO_2 in field experiments: implications for the future forest. *Plant Cell Environ.* **22:** 683–714.

Ögren, E. 1993. Convexity of the photosynthetic light-response curve in relation to intensity and direction of light during growth. *Plant Physiol.* **101:** 1013–1019.

Ogren, W.L. 1984. Photorespiration: pathways, regulation, and modification. *Annu. Rev. Plant Physiol.* **35:** 415–442.

Oguchi, R., Hikosaka, K., & Hirose, T. 2005. Leaf anatomy as a constraint for photosynthetic acclimation: differential responses in leaf anatomy to increasing growth irradiance among three deciduous trees. *Plant Cell Environ.* **28:** 916–927.

O'Leary M.H. 1993. Biochemical basis of carbon isotope fractionation. In: Stable isotopes and plant carbon-water relations, J.R. Ehleringer, A.E. Hall, & G.D. Farquhar (eds.). Academic Press, San Diego, pp. 19–28.

Öquist, G., Brunes, L., & Hällgren, J.E. 1982. Photosynthetic efficiency of *Betula pendula* acclimated to different quantum flux densities. *Plant Cell Environ.* **5:** 9–15.

Osmond, C.B. 1994. What is photoinhibition? Some insights from comparisons of shade and sun plants. In: Photoinhibition of photosynthesis from molecular mechanisms to the field, N.R. Baker & J.R. Bowyer (eds.). Bios Scientific Publishers, Oxford, pp. 1–24.

Osmond, C.B. & Holtum, J.A.M. 1981. Crassulacean acid metabolism. In: The biochemistry of plants. A comprehensive treatise, Vol 8, P.K. Stumpf & E.E. Conn (eds.). Academic Press, New York, pp. 283–328.

Osmond, C.B., Winter, K., & Ziegler, H. 1982. Functional significance of different pathways or CO_2 fixation in photosynthesis. In: Encyclopedia or plant physiology, Vol. 12B, O.L. Lange, P.S. Nobel, C.B. Osmond, & H. Ziegler (eds.). Springer-Verlag, Berlin, pp. 479–548.

Pascal, A.A., Liu, Z.F., Broess, K., Van Oort, B., Van Amerongen, H., Wang, C., Horton, P., Robert, B., Chang, W.R., & Ruban, A. 2005. Molecular basis of photoprotection and control of photosynthetic light-harvesting. *Nature* **436:** 134–137.

Patel, A. & Ting, I.P. 1987. Relationship between respiration and CAM-cycling in *Peperomia camptotricha*. *Plant Physiol.* **84:** 640–642.

Paul, M.J. & Foyer, C.H. 2001. Sink regulation of photosynthesis. *J. Exp. Bot.* **52:** 1383–1400.

Pearcy, R.W. 1977. Acclimation of photosynthetic and respiratory carbon dioxide exchange to growth temperature in *Atriplex lentiformis* (Torr.) Wats. *Plant Physiol.* **59:** 795–799.

Pearcy, R.W. 1988. Photosynthetic utilisation of lightflecks by understorey plants. *Aust. J. Plant Physiol.* 15: 223–238.

Pearcy, R.W. 1990. Sunflecks and photosynthesis in plant canopies. *Annu. Rev. Plant Physiol. Plant Mol. Biol.* **41:** 421–453.

Plaut, Z., Mayoral, M.L., & Reinhold, L. 1987. Effect of altered sink:source ratio on photosynthetic metabolism of source leaves. *Plant Physiol.* **85:** 786–791.

Pons, T.L. & Pearcy, R.W. 1992. Photosynthesis in flashing light in soybean leaves grown in different conditions. II. Lightfleck utilization efficiency. *Plant Cell Environ.* **15:** 577–584.

Pons, T.L. & Pearcy, R.W. 1994. Nitrogen reallocation and photosynthetic acclimation in response to partial shading in soybean plants. *Physiol. Plant.* **92:** 636–644.

Pons, T.L. & Welschen, R.A.M. 2002. Overestimation of respiration rates in commercially available clamp-on leaf chambers. Complications with measurement of net photosynthesis. *Plant Cell Environ.* **25:** 1367–1372.

Pons, T.L., Van der Werf, A., & Lambers, H. 1994. Photosynthetic nitrogen use efficiency of inherently slow and fast-growing species: possible explanations for observed differences. In: A whole-plant perspective of carbon-nitrogen interactions, J. Roy & E. Garnier (eds.). SPB Academic Publishing, The Hague, pp. 61–77.

Poot, P., Pilon, J., & Pons, T.L. 1996. Photosynthetic characteristics of leaves of male sterile and hermaphroditic sex types of *Plantago lanceolata* grown under conditions of contrasting nitrogen and light availabilities. *Physiol. Plant.* **98:** 780–790.

Portis, A. 2003. Rubisco activase – Rubisco's catalytic chaperone. *Photosynth. Res.* **75:** 11–27.

Portis, A.R., Salvucci, M.E., & Ogren, W.L. 1986. Activation of ribulosebisphosphate carboxylase/oxygenase at physiological CO_2 and ribulosebisphosphate concentrations by Rubisco activase. *Plant Physiol.* **82:** 967–971.

Prins, H.B.A. & Elzenga, J.T.M. 1989. Bicarbonate utilization: function and mechanism. *Aquat. Bot.* **34:** 59–83.

Pyankov, V.I. & Kondratchuk, A.V. 1995. Specific features of structural organization of photosynthetic apparatus of the East Pamirs plants. *Proc. Russ. Acad. Sci.* **344:** 712–716.

Pyankov, V.I. & Kondratchuk, A.V. 1998. Structure of the photosynthetic apparatus in woody plants from different ecological and altitudinal in Eastern Pamir. *Russ. J. Plant Physiol.* **45:** 567–578.

Prins, H.B.A. & de Guia, M.B. 1986. Carbon source of the water soldier, *Stratiotes aloides* L. *Aquat. Bot.* **26:** 225–234.

Raymo, M.E. & Ruddiman, W.F. 1992. Tectonic forcing of late Cenozoic climate. *Nature* **359:** 117–122.

Reich, P.B. & Schoettle, A.W. 1988. Role of phosphorus and nitrogen in photosynthetic and whole plant carbon gain and nutrient use efficiency in eastern white pine. *Oecologia* **77:** 25–33.

Reich, P.B., Walters, M.B., & Ellsworth, D.S. 1997. From tropics to tundra: Global convergence in plant functioning. *Proc. Natl. Acad. Sci. USA* **94:** 13730–13734.

Reinfelder, J.R., Kraepiel, A.M.L., & Morel, F.M.M. 2000. Unicellular C-4 photosynthesis in a marine diatom. *Nature* **407:** 996–999.

Reiskind, J.B., Madsen, T.V., Van Ginkel, L.C., & Bowes, G. 1997. Evidence that inducible C_4-type photosynthesis is a chloroplastic CO_2-concentrating mechanism in *Hydrilla*, a submersed monocot. *Plant Cell Environ.* **20:** 211–220.

Rodeghiero, M., Niinemets, Ü. & Cescatti, A. 2007. Major diffusion leaks of clamp-on leaf cuvettes still unaccounted: how erroneous are the estimates of Farquhar

et al. model parameters? *Plant Cell Environ.* **30:** 1006–1022.

Rogers, A., Fischer, B.U., Bryant, J., Frehner, M., Blum, H., Raines, C.A., & Long, S.P. 1998. Acclimation of photosynthesis to elevated CO_2 under low-nitrogen nutrition is affected by the capacity for assimilate utilization. Perennial ryegrass under free-air CO_2enrichment. *Plant Physiol.* **118:** 683–689.

Rolland, F., Moore, B., & Sheen, J. 2002. Sugar sensing and signaling in plants. *Plant Cell* **14:** S185–S205.

Rolland, F., Baena-Gonzalez, E., & Sheen, J. 2006. Sugar sensing and signaling in plants: Conserved and novel mechanisms. *Annu. Rev. Plant Biol.* **57:** 675–709.

Rühle, W. & Wild, A. 1979. Measurements of cytochrome f and P-700 in intact leaves of *Sinapis alba* grown under high-light and low-light conditions. *Planta* **146:** 377–385.

Rundel, P.W. & Sharifi, M.R. 1993. Carbon isotope discrimination and resource availability in the desert shrub *Larrea tridentata*. In: Stable isotopes and plant carbon-water relations, J.R. Ehleringer, A.E. Hall, & G.D. Farquhar (eds.). Academic Press, San Diego, pp. 173–185.

Sage, R.F. 2002. C-4 photosynthesis in terrestrial plants does not require Kranz anatomy. *Trends Plant Sci.* **7:** 283–285.

Sage, R.F. 2004. The evolution of C_4 photosynthesis. *New Phytol.* **161:** 341–370.

Sage, R.F. & Kubien, D. 2003. Quo vadis C_4? An ecophysiological perspective on global change and the future of C_4 plants. *Photosynth. Res.***77:** 209–225.

Sage, R.F. & Sharkey, T.D. 1987. The effect of temperature on the occurrence of O_2 and CO_2 insensitive photosynthesis in field grown plants. *Plant Physiol.* **84:** 658–664.

Sage, R.F. & Pearcy, R.W. 1987a. The nitrogen use efficiency or C_3 and C_4 plants. I. Leaf nitrogen, growth, and biomass partitioning in *Chenopodium album* (L.) and *Amaranthus retroflexus*. *Plant Physiol.* **84:** 954–958.

Sage, R.F. & Pearcy, R.W. 1987b. The nitrogen use efficiency or C_3 and C_4 plants. II. Leaf nitrogen effects on the gas exchange characteristics or *Chenopodium album* (L.) and *Amaranthus retroflexus*. *Plant Physiol.* **84:** 959–963.

Salvucci, M.E. 1989. Regulation of Rubisco activity *in vivo*. *Physiol. Plant.* **77:** 164–171.

Salvucci, M.E. & Crafts-Brandner, S.J. 2004a. Mechanism for deactivation of Rubisco under moderate heat stress. *Physiol. Plant.* **122:** 513–519.

Salvucci, M.E. & Crafts-Brandner, S.J. 2004b. Relationship between the heat tolerance of photosynthesis and the thermal stability of Rubisco activase in plants from contrasting thermal environments. *Plant Physiol.* **134:** 1460–1470.

Sassenrath-Cole, G.F., Pearcy, R.W., & Steinmaus, S. 1994. The role of enzyme activation state in limiting carbon assimilation under variable light conditions. *Photosynth. Res.* **41:** 295–302.

Schreiber, U, Bilger, W., & Neubauer, C. 1995. Chlorophyll fluorescence as a non-intrusive indicator for rapid assessment of *in vivo* photosynthesis. In: Ecophysiology of photosynthesis, E.-D. Schulze & M.M. Caldwell (eds.). Springer-Verlag, Berlin, pp. 49–70.

Schulze, E.-D., Kelliher, F.M., Körner, C., Lloyd, J., & Leuning, R. 1994. Relationships among maximum stomatal conductance, ecosystem surface conductance, carbon assimilation rate, and plant nitrogen nutrition: A global ecology scaling exercise. *Annu. Rev. Ecol. Syst.* **25:** 629–660.

Sharkey, T.D. 2005. Effects of moderate heat stress on photosynthesis: importance of thylakoid reactions, Rubisco deactivation, reactive oxygen species, and thermotolerance provided by isoprene. *Plant Cell Environ.* **28:** 269–277.

Sharkey, T.D., Seemann, J.R., & Pearcy, R.W. 1986a. Contribution of metabolites of photosynthesis to postillumination CO_2 assimilation in response to lightflecks. *Plant Physiol.* **82:** 1063–1068.

Sharkey, T.D., Stitt, M., Heineke, D., Gerhardt, R., Raschke, K., & Heldt, H.W. 1986b. Limitation of photosynthesis by carbon metabolism. II. CO_2-insensitive CO_2 uptake results from limitation of triose phosphate utilization. *Plant Physiol.* **81:** 1123–1129.

Sharkey, T.D., Bernacchi, C.J., Farquhar, G.D., & Singsaas, E.L. 2007. Fitting photosynthetic carbon dioxide response curves for C_3 leaves. *Plant Cell Environ.* **30:** 1035–1040.

Sims, D.A. & Pearcy, R.W. 1989. Photosynthetic characteristics of a tropical forest understorey herb, *Alocasia macrorrhiza*, and a related crop species, *Colocasia esculenta*, grown in contrasting light environments. *Oecologia* **79:** 53–59.

Smedley, M.P., Dawson, T.E., Comstock, J.P., Donovan, L.A., Sherrill, D.E., Cook, C.S., & Ehleringer, J.R. 1991. Seasonal carbon isotope discrimination in a grassland community. *Oecologia* **85:** 314–320.

Smeekens, S. 2000. Sugar induced signal transduction in plants. *Annu. Rev. Plant Physiol. Plant Mol. Biol.* **51:** 49–81.

Smeekens, S. & Rook, F. 1998. Sugar sensing and sugar-mediated signal transduction in plants. *Plant Physiol.* **115:** 7–13.

Smith, H., Samson, G., & Fork, D.C. 1993. Photosynthetic acclimation to shade: Probing the role of phytochromes using photomorphogenetic mutants of tomato. *Plant Cell Environ.* **16:** 929–937.

Staiger, C.J., Gibbon, B.C., Kovar, D.R., & Zonia, L.E. 1997. Profilin and actin-depolymerizing facor: Modulators of actin organization in plants. *Trends Plant Sci.* **2:** 275–281.

Sternberg, L.O., DeNiro, M.J., & Johnson, H.B. 1984. Isotope ratios of cellulose from plants having different photosynthetic pathways. *Plant Physiol.* **74:** 557–561.

Stitt, M. & Hurry, V. 2002. A plant for all seasons: alterations in photosynthetic carbon metabolism during cold acclimation in *Arabidopsis*. *Curr. Opin. Plant Biol.* **5:** 199–206.

Surridge, C. 2002. Agricultural biotech: the rice squad. *Nature* **416:** 576–578.

Tans, P. 2007. NOAA/ESRL (www.esrl.noaa.gov/gmd/ccgg/trends).

Terashima, I. & Hikosaka, K. 1995. Comparative ecophysiology of leaf and canopy photosynthesis. *Plant Cell Environ.* **18:** 1111–1128.

Terashima, I., Wong, S.C., Osmond, C.B., & Farquhar, G.D. 1988. Characterisation of non-uniform photosynthesis

induced by abscisic acid in leaves having different mesophyll anatomies. *Plant Cell Physiol.* **29:** 385–394.

Terashima, I., Miyazawa, S.-I., & Hanba, Y.T. 2001. Why are sun leaves thicker than shade leaves? – Consideration based on analyses of CO_2 diffusion in the leaf. *J. Plant Res.* **114:** 93–105.

Terashima, I., Hanba, Y.T., Tazoe, Y., Vyas, P., & Yano, S. 2006. Irradiance and phenotype: comparative eco-development of sun and shade leaves in relation to photosynthetic CO_2 diffusion. *J. Exp. Bot.* **57:** 343–354.

Ueno, O. 2001. Environmental regulation of C_3 and C_4 differentiation in the amphibious sedge *Eleocharis vivipara*. *Plant Physiol.* **127:** 1524–1532.

Ueno, O., Samejima, M., Muto, S., Miyachi, S. 1988. Photosynthetic characteristics of an amphibious plant, *Eleocharis vivipara:* expression of C_4 and C_3 modes in contrasting environments. *Proc. Natl. Acad. Sci. USA* **85:** 6733–6737.

Van Oosten, J.-J. & Besford, R.T. 1995. Some relationships between the gas exchange, biochemistry and molecular biology of photosynthesis during leaf development of tomato plants after transfer to different carbon dioxide concentrations. *Plant Cell Environ.* **18:** 1253–1266.

Van Oosten, J.J., Wilkins, D., & Besford, R.T. 1995. Acclimation of tomato to different carbon dioxide concentrations. Relationships between biochemistry and gas exchange during leaf development. *New Phytol.* **130:** 357–367.

Vernon, D.M., Ostrem, J.A., Schmitt, J.M., & Bohnert, H. 1988. PEPCase transcript levels in *Mesembryanthemum crystallinum* decline rapidly upon relief from salt stress. *Plant Physiol.* **86:** 1002–1004.

Vogel, J.C., Fuls, A., & Ellis, R.P. 1978. The geographical distribution of Kranz grasses in South Africa. *S. Afr. J. Sci.* **74:** 209–215.

Vogelmann, T.C. 1993. Plant tissue optics. *Annu. Rev. Plant Physiol. Plant Mol. Biol.* **44:** 231–251.

Vogelmann, T.C. & Evans, J.R. 2002. Profiles of light absorption and chlorophyll within spinach leaves from chlorophyll fluorescence. *Plant Cell Environ.* **25:** 1313–1323.

Vogelmann, T.C., Nishio, J.N., & Smith, W.K. 1996. Leaves and light capture: Light propagation and gradients of carbon fixation within leaves. *Trends Plant Sci.* **1:** 65–70.

Von Caemmerer, S. 1989. A model of photosynthetic CO_2 assimilation and carbon-isotope discrimination in leaves of certain C_3–C_4 intermediates. *Planta* **178:** 463–474.

Von Caemmerer, S. 2000. Biochemical models of leaf photosynthesis. CSIRO Publishing, Collingwood.

Von Caemmerer, S. & Farquhar, G.D. 1981. Some relationships between biochemistry of photosynthesis and gas exchange of leaves. *Planta* **153:** 376–387.

Wakabayashi, K. & Böger, P. 2002. Target sites for herbicides: entering the 21st century. *Pest Manage. Sci.* **58:** 1149–1154.

Walters, R.G. 2005. Towards an understanding of photosynthetic acclimation. *J. Exp. Bot.* **56:** 435–447.

Walters, R.G., Rogers, J.J.M., Shephard, F., & Horton, P. 1999. Acclimation of *Arabidopsis thaliana* to the light environment: the role of photoreceptors. *Planta* **209:** 517–527.

Wand, S.J.E., Midgley, G.F., Jones, M.H., & Curtis, P.S. 1999. Responses of wild C_4 and C_3 grass (Poaceae) species to elevated atmospheric CO_2 concentration: a meta-analytic test of current theories and perceptions. *Global Change Biol.* **5:** 723–741.

Warren, C.R. 2007. Stand aside stomata, another actor deserves centre stage: the forgotten role of the internal conductance to CO_2 transfer. *J. Exp. Bot.* **59:** 1475–1487.

Warren, C.R. & Adams, M.A. 2006. Internal conductance does not scale with photosynthetic capacity: implications for carbon isotope discrimination and the economics of water and nitrogen use in photosynthesis. *Plant Cell Environ.* **29:** 192–201.

Warren, C.R., Low, M., Matysek, R., & Tausz, M. 2007. Internal conductance to CO_2transfer of adult *Fagus sylvatica*: variation between sun and shade leaves and due to free-air ozone fumigation. *Environ. Exp. Bot.* **59:** 130–138.

Weger, H.G., Silim, S.N., & Guy, R.D. 1993. Photosynthetic acclimation to low temperature by western red cedar seedlings. *Plant Cell Environ.* **16:** 711–717.

Weston, D.J., Bauerle, W.L., Swire-Clark, G.A., Moore, Bd., & Baird, W.V. 2007. Characterization of Rubisco activase from thermally contrasting genotypes of *Acer rubrum* (Aceraceae). *Am. J. Bot.* **94:** 926–934.

Winter, K. & Smith, J.A.C. 1996. An introduction to crassulaceaen acid metabolism. Biochemical principles and ecological diversity. In: Crassulacean acid metabolism, biochemistry, ecophysiology and evolution. Ecological studies 114, K. Winter & J.A.C. Smith (eds.). Springer-Verlag, Berlin, pp. 1–13.

Winter, K., Zotz, G., Baur, B., & Dietz, K.-J. 1992. Light and dark CO_2 fixation in *Clusia uvitana* and the effects of plant water status and CO_2 availability. *Oecologia* **91:** 47–51.

Wright, G.C., Hubick,.K.T., & Farquhar, G.D. 1988. Discrimination in carbon isotopes of leaves correlates with water-use efficiency of field-grown peanut cultivars. *Aust. J. Plant Physiol.* **15:** 815–825.

Wright, I.J., Reich, P.B., & Westoby, M. 2001. Strategy shifts in leaf physiology, structure and nutrient content between species of high- and low-rainfall and high- and low-nutrient habitats. *Funct. Ecol.* **15:** 423–434.

Wright, I.J., Reich, P.B., Westoby, M., Ackerly, D.D., Baruch, Z., Bongers, F., Cavender-Bares, J., Chapin, T., Cornelissen, J.H.C., Diemer, M., Flexas, J., Garnier, E., Groom, P. K., Gulias, J., Hikosaka, K., Lamont, B.B., Lee, T., Lee, W., Lusk, C., Midgley, J.J., Navas, M.-L., Niinemets, Ü., Oleksyn, J., Osada, N., Poorter, H., Poot, P., Prior, L., Pyankov, V.I., Roumet, C., Thomas, S.C., Tjoelker, M.G., Veneklaas, E.J., & Villar, R. 2004. The worldwide leaf economics spectrum. *Nature* **428:** 821–827.

Wu, M.-.X & Wedding, R.T. 1987. Temperature effects on phospho*enol*pyruvate carboxylase from a CAM and a C_4 plant: a comparative study. *Plant Physiol.* **85:** 497–501.

Wullschleger, S.D. Tschaplinski, T.J., & Norby, R.J. 2002. Plant water relations at elevated CO_2 – implications for water-limited environments. *Plant Cell Environ.* **25:** 319–331.

Yamori, W., Noguchi, K., & Terashima, I. 2005. Temperature acclimation of photosynthesis in spinach leaves: analyses of photosynthetic components and temperature dependencies of photosynthetic partial reactions. *Plant Cell Environ.* **28:** 536–547.

Yamori, W., Noguchi, K., Hanba, Y.T., & Terashima, I. 2006a. Effects of internal conductance on the temperature dependence of the photosynthetic rate in spinach leaves from contrasting growth temperatures. *Plant Cell Physiol.* **47:** 1069–1080.

Yamori, W., Suzuki, K., Noguchi, K., Nakai, M., & Terashima, I. 2006b. Effects of Rubisco kinetics and Rubisco activation state on the temperature dependence of the photosynthetic rate in spinach leaves from contrasting growth temperatures. *Plant Cell Environ.* **29:** 1659–1670.

Yano, S. & Terashima, I. 2001. Separate localization of light signal perception for sun or shade type chloroplast and palisade tissue differentiation on *Chenopodium album*. *Plant Cell Physiol.* **41:** 1303–1310.

Yeoh, H.-H., Badger, M.R., & Watson, L. 1981. Variations in kinetic properties of ribulose-1,5-bisphosphate carboxylase among plants. *Plant Physiol.* **67:** 1151–1155.